17431

NAME OF AUTHOR..... RANDOLPH PERRY ANGLE ....

TITLE OF THESIS..... AIRFLOW MODIFICATION DUE ....

..... TO A CHANGE IN ....

..... SURFACE -ROUGHNESS ....

UNIVERSITY........ ALBERTA .....

DEGREE FOR WHICH THESIS WAS PRESENTED.. MASTER OF SCIENCE

YEAR THIS DEGREE GRANTED..... FALL, 1973 ....

Permission is hereby granted to THE NATIONAL LIBRARY

OF CANADA to microfilm this thesis and to lend or sell copies

of the film.

The author reserves other publication rights, and

neither the thesis nor extensive extracts from it may be

printed or otherwise reproduced without the author's

written permission.

(Signed)..... Randolph P. Angle.....

PERMANENT ADDRESS:

..... 448-D MICHENER PK.,

..... EDMONTON, ALBERTA.

..... CANADA, T6H 4M5.

DATED... July 4 1973

NL-91 (10-68)

THE UNIVERSITY OF ALBERTA

AIRFLOW MODIFICATION DUE TO A CHANGE IN SURFACE ROUGHNESS

BY

Ⓒ

RANDOLPH PERRY ANGLE

A THESIS

SUBMITTED TO THE FACULTY OF GRADUATE STUDIES AND RESEARCH

IN PARTIAL FULFILMENT OF THE REQUIREMENTS FOR THE DEGREE

OF MASTER OF SCIENCE

IN

METEOROLOGY

DEPARTMENT OF GEOGRAPHY

EDMONTON, ALBERTA

FALL, 1973

THE UNIVERSITY OF ALBERTA

FACULTY OF GRADUATE STUDIES AND RESEARCH

The undersigned certify that they have read, and
recommend to the Faculty of Graduate Studies and Research, for
acceptance, a thesis entitled "Airflow Modification due to a
Change in Surface Roughness", submitted by Randolph Perry
Angle in partial fulfilment of the requirements for the degree
of Master of Science, in Meteorology.

....
Supervisor

....

....

Date ..JUNE 22, 1977......

ABSTRACT

Real terrain is complex and its effects on the atmosphere are not well understood. The two-dimensional change-of-roughness problem is the first step in learning about the interaction. A critical review of relevant literature is presented, various analytical solutions are surveyed, and several numerical models are described. An experimental study of airflow from mustard, roughness length $z_0 = 12$ cm, to fallow, roughness $z_0 = 1$ cm, leads to several conclusions. The zero-plane displacement is found to be an important, yet neglected, parameter. The surface friction velocity overshoots and returns slowly to the equilibrium value. The wind profile in the modified region is more nearly logarithmic than the Peterson model predicts. The Glushko model gives the best overall description of the flow transformation, although the Elliot theory, with the great advantage of simplicity, is in fair agreement with the data. Values for the ratio of the standard deviation of the vertical wind to the friction velocity (σ_w/u_*) reveal no variation with stability and are in good agreement with the value for laboratory flows. Values for the ratio of the standard deviation of the longitudinal wind component to the friction velocity (σ_u/u_*) show a variation with wind direction, due probably to large-scale properties of the terrain. A plausible value is obtained for the constant of proportionality between the kinematic shear stress and the mean turbulent kinetic energy. A brief discussion of attempts to extend the theory to more realistic conditions is given, and some recommendations for future work are made.

ABSTRACT

ACKNOWLEDGEMENTS

TABLE OF CONTENTS

LIST OF TABLES

LIST OF FIGURES

INTRODUCTION

1.1 The Problem of Inhomogeneous Terrain

Micrometeorology has been much devoted to elucidating the fundamental relations which are presumed to exist between vertical fluxes of sensible heat, water vapour, and momentum in the surface boundary layer of the atmosphere, and the gradients of the corresponding variables. To simplify the governing equations, the theory has assumed horizontal homogeneity, thereby employing essentially a one-dimensional model of the atmosphere near the ground. Implicit in the idealization is the existence of equilibrium between the vertical profiles and the underlying uniform surface.

Natural terrain, however, is far from uniform. Apart from flat grassland, desert plains, or frozen lakes, few areas qualify as approximations to 'infinite planes'. Experimental sites suitable for testing the theory can be located only after extensive search. Most of the earth's surface is characterized by spatial changes in roughness, temperature, and moisture, as plainly evidenced by the chequered pattern of agricultural lands. The effects of this 'patchiness' on the vertical profiles and fluxes is yet to be determined, despite the obvious importance of ascertaining the extent of deviations from the simple theoretical model.

Because the fluid particles in the turbulent boundary layer possess a higher velocity parallel to the earth's surface than normal to it, the boundary layer is often said to have a 'memory'. Once equilibrium is established with a particular surface, the flow characteristics will tend to persist even after a new surface is encountered. Intuitively, it is expected that adjustment to the new surface will grow very much like a boundary layer on a flat plate. If point observations, taken from a tower for instance, are to be representative of these new surroundings, then clearly they must be made within the new equilibrium layer. Thus, it is of considerable practical concern to learn something of the response of the flow

properties to typical surface irregularities. In the field a rule of thumb in the form of a height to fetch ratio would be most valuable. Observation sites could then be placed far enough downwind from the beginning of any particular type of land cover to ensure that measurements up to any chosen height would be representative of that cover. For areas of very limited extent the maximum height of instrumentation could be calculated provided that the distance downwind from the start of the cover was known.

Representation of the effect of the earth's surface on the atmosphere as a whole has long been an obstacle in numerical forecasting and general circulation modelling. For short-range forecasts it appears not to be important, but for medium and long-range forecasts it is vital. The surface is an important link in the energy exchange process; induced vertical velocities and the convective transfer of heat and moisture couple the boundary layer with the atmosphere above. While it is not expected that small crop to crop variations will be significant, the overall difference between land and sea, or mountain and plain, should exert some influence on large scale properties. Air mass modification is one familiar manifestation. The formation of ideas about the effects of surface inhomogeneity is thus of some consequence on the synoptic scale as well.

1.2 The Black Box Analogy

While much of the interest in the problem of inhomogeneity has been practical, another motive of the investigation has been to gain a better understanding of the structure of turbulent boundary layers. Clauser (1956) has suggested that the turbulent boundary layer is a complex non-linear system resembling Maxwell's problem of a complicated machine in a closed room, connected to the exterior only by means of a number of ropes. By pulling the ropes and correlating the responses in an intelligent fashion, can the complete behaviour of the machine be predicted, say when a stranger pulls the ropes in any manner whatsoever? Like the machine in the closed room the actual mechanism of turbulence is inaccessible, the only connection to the outside being a number of measurable parameters.

In modern terminology, Maxwell's room is called the 'black-box' problem. The black box has a number of inputs such that varying functions can arbitrarily be fed to the unknown mechanism inside. A series of outputs from the box indicate the behaviour of the mechanism inside. The objective is to establish what the output function will be for any given input.

The turbulent boundary layer has as inputs various external influences such as pressure gradient, roughness, and heat flux, to which it is subjected in travelling along a surface. Typical response variables are the mean velocity profile, shear stress, heat transer, and turbulent energy. Recent investigation into the problem of inhomogeneous terrain is thus a search for a better understanding of the nature of turbulent flow by submitting it to a sudden change in one of its inputs and examining closely its response.

Figure 2-1. Schematic diagram of internal boundary layer development for smooth to rough flow.

the shear stress distribution, the horizontal velocity profile, and the vertical velocity distribution, in the developing internal boundary layer. At large x distances the lower atmosphere (few tens of metres) should be completely in equilibrium with the new surface, and behave as if it had developed over an infinite uniform plane.

The equations of mean motion for a two-dimensional, incompressible flow, in neutral stratification and steady-state conditions, neglecting the viscous and Coriolis terms, are:

$$u \frac{\partial u}{\partial x} + w \frac{\partial u}{\partial z} = -\frac{\partial}{\partial x}\left(\frac{p}{\rho}\right) - \frac{\partial}{\partial x}\left(\overline{u'^2}\right) + \frac{\partial}{\partial z}\left(-\overline{u'w'}\right)$$

$$u \frac{\partial w}{\partial x} + w \frac{\partial w}{\partial z} = -\frac{\partial}{\partial z}\left(\frac{p}{\rho}\right) - \frac{\partial}{\partial z}\left(\overline{w'^2}\right) + \frac{\partial}{\partial x}\left(-\overline{u'w'}\right)$$

where p is the pressure, ρ is the density, u' is the fluctuating or turbulent part of the horizontal wind, w' is the fluctuating or turbulent part of the vertical wind. In addition there is the equation of continuity,

$$\frac{\partial u}{\partial x} + \frac{\partial w}{\partial z} = 0$$

which provides a system of three equations in six unknowns. To simplify the problem further the following assumptions are made:

(1) The contribution to the momentum balance of the normal stress components $\overline{u'^2}$ and $\overline{w'^2}$ is small compared with other terms in the equations. Observations on the whole have confirmed this.

(2) The pressure is constant throughout the region of the roughness change. The atmosphere is, of course, always subject to at least a small synoptic pressure gradient, but over distances of micrometeorological interest, it will be negligible. Near the discontinuity local pressure fields are expected, but provided attention is restricted to distances somewhat downstream the error should not be too great. This assumption will be re-examined later.

(3) Initially w = 0 everywhere, so the left side of the vertical momentum equation is zero. Because of uniformity and equilibrium upwind, the shear stress is not changing in the x direction so $\frac{\partial(-\overline{u'w'})}{\partial x} = 0$. Hence the pressure term is also zero and the equation as a whole can be dropped from the system. Near the discontinuity, however, w is definitely non-zero and is changing rapidly in both the x and z directions. So too is the shear stress. Downstream from the step it is expected that the

usual boundary layer conditions will prevail, that is, all the terms in the equation will be small. At large distances the return to equilibrium will again set the whole equation to zero. Thus, except close to the discontinuity, the vertical momentum equation can be neglected. This assumption will also be re-examined later.

Alternatively, the normal turbulent stress terms can be retained so that away from the roughness change the vertical equation of motion simplifies, after integration, to

$$P + \rho \overline{w'^2} = \text{constant} = P_s$$

where the constant P_s can be identified as the static pressure at the ground (Plate, 1971, p. 141). The pressure and normal stress terms in the horizontal equation of motion become

$$-\frac{\partial}{\partial x}\left(\frac{P}{\rho}\right) - \frac{\partial}{\partial x}\overline{u'^2} = -\frac{1}{\rho}\frac{\partial P_s}{\partial x} - \frac{\partial}{\partial x}(\overline{u'^2} - \overline{w'^2})$$

The assumption of isotropy, $\overline{u'^2} = \overline{w'^2}$, would reduce the right side to a single term expressing the fact that the pressure gradient is impressed by the conditions that determine P_s. In shear flow it is impossible to have isotropy (Stewart, 1956), but away from the discontinuity changes in $\overline{u'^2} - \overline{w'^2}$ with x will be small. Therefore the second term can be neglected, again revealing that the pressure gradient is controlled by conditions outside the boundary layer, namely, the synoptic gradient.

With these assumptions the governing equations reduce to

$$u\frac{\partial u}{\partial x} + w\frac{\partial u}{\partial z} = \frac{\partial \tau}{\partial z}$$

$$\frac{\partial u}{\partial x} + \frac{\partial w}{\partial z} = 0$$

a system of two equations in three unknowns. Solution of the set requires a third equation plus boundary conditions.

2.2 Qualitative Features of the Flow Modification

When air passes from a smooth surface to a rough surface, a series of reactions are set up. A pressure field is produced and the air will be affected before it reaches the transition. The pressure will probably be felt only a few roughness lengths upstream, but, in addition to causing an initial deflection of the streamlines away from the roughness elements, it may cause local distortion of the velocity field. One example observed by Meroney (1968) is that near the edge of a crop or forest the velocities near the ground are greater than those higher up or farther inside the canopy. Plate (1971, p. 144) claimed that the pressure acts as a smoothing function to make the profile changes less abrupt, and that it is restricted to a fairly narrow region near the discontinuity. He suggested that the overall effect may be to shift the origin of the internal boundary layer, much as occurs in jets and wakes where the boundary layer assumptions are not satisfied at the physical origin, and a 'virtual' origin appears.

As the air rises to pass over the roughness elements there may be a slight tendency for the fluid particles in the lower layers to accelerate. The increased roughness would quickly counteract this, the higher drag removing momentum. The velocity gradient would increase and cause an increase in the turbulent energy. In other words, some of the energy of the mean wind is converted into turbulence to satisfy the increase in momentum flux at the surface. The increased turbulence helps bring down, from successively deeper layers of air, the momentum required to overcome surface drag. The region near the discontinuity is one of intense turbulence production where a strong stress field is present. Meroney (1968) also observed that at the edge of a canopy the surface drag and turbulent intensities were increased considerably over the values farther inside.

2.3 Boundary Conditions

The complete situation is shown in Fig. 2-1. The streamline displacement is represented by δ and the height to which the flow is affected by the new surface is denoted by h. Above $z = h$ the flow is still characteristic of the upwind conditions. Near the ground, starting perhaps a little downwind from the discontinuity, a thin layer exists where the profiles are governed entirely by the local surface conditions. This equilibrium layer is denoted by h'. Between h' and h there exists a blending region in which:

(1) the velocity distribution changes gradually from the logarithmic one characteristic of the second roughness to that characteristic of the first roughness;

(2) the stress changes from u_{*2}^2 to u_{*1}^2;

(3) the vertical wind velocity is non-zero.

Accounting for the streamline displacement, continuity of velocity at $z = h$ requires that

$$u_2(h) = u_1(h - \delta)$$

$$= (u_{*1}/k) \ln (h - \delta)/z_{01}$$

Below $z = h$ the velocity distribution can be represented by a profile of the form

$$u_2/u_{*2} = (1/k) \ln z/z_{02} + f_1(z/h)$$

where u_{*2} is the friction velocity at the second surface, and f_1 is a function of the parameter z/h, the height divided by the new length scale. This 'blending' function must be such that:

(1) for $z \leq h'$ $f_1 = 0$

Below h' the profile is simply the logarithmic one characteristic of the second roughness;

(2) at $z = h$, $f_1(1)$ must fulfill the continuity condition

$$u_2(h) = (u_{*2}/k) \ln z/z_{02} + u_{*2} f_1(1) = u_1(h - \delta)$$

Similarly, the stress and vertical wind distributions can be written as:

$$\tau_a = u_{*2}^2 + (u_{*1}^2 - u_{*2}^2) f_2(z/h)$$

$$w_a = f_3(z/h)$$

where the functions f_2 and f_3 must satisfy the conditions:

(a) for $z \leq h'$ $f_2 = 0$ $\tau_a = u_{*2}^2$

The shear stress is constant with height and equal to the square of the friction velocity at the second surface.

for $z \leq h'$ $f_3 = 0$ $w_2 = 0$

There is no vertical wind in the equilibrium layer.

(b) at $z = h$ $f_2(1) = 1$ $\tau_a = u_{*1}^2$

The shear stress equals the upstream value.

at $z = h$ $f_3(1) = 0$ • $w_2 = 0$

There is no vertical wind in the upstream flow.

Finally, at the ground, $z = z_{o2}$,

$$\tau_a = \tau_{oa} = u_{*2}^2$$

$$u_2 = 0$$

$$w_2 = 0$$

A complete solution of the internal boundary layer problem will provide the distributions of $u_2(z)$, $w_2(z)$, and $\tau_a(z)$ as functions of x. This will determine the growth of h and h' with x and specify the functions f_1, f_2, and f_3.

CHAPTER III

ANALYTICAL SOLUTIONS

3.1 A Semi-Empirical Approach

. The earliest investigation of flow over a change in roughness
was carried out by Jacobs (1939) in a rectangular channel. Measure-
ments of the mean velocity profile were made at various distances down-
stream from a roughness discontinuity both for the smooth-to-rough and
for the rough-to-smooth transitions. The shear stress distribution was
then computed from these profiles by graphical integration of the
combined equations of motion and continuity in the form:

$$-u \frac{\partial w}{\partial z} + w \frac{\partial u}{\partial z} = \frac{\partial \tau}{\partial z} = Q(z) \quad \text{at fixed } x$$

(Some references to Jacob's work erroneously assume that he used the
Prandtl mixing length technique, for example, Schlichting , 1968, p.
615. In actual fact, Jacobs rejected this approach when preliminary
mixing length calculations were found to be in serious disagreement with
observations.) Jacobs concluded that the new equilibrium value of the
wall shear stress is attained almost immediately, and that the change
spreads upward with distance according to the exponential transition
function $g(z/x) = a \exp(-bz/x)$, where a and b are empirical constants.
According to his observations, $a = 1$, $b = 11.6$, and the resulting inter-
polation formula for the shear stress distribution across a channel is

$$\tau = \frac{H-z}{H} \left[\tau_1 + (\tau_2 - \tau_1) \exp(-11.6 \, z/x) \right]$$

A similar approach was taken by Lettau and Zebransky (1968)
to interpolate wind profiles between an initial state over land and a
final state over water. They proposed a Gaussian transition function
of the form $\exp -a \, (z/h)^2$, whence

$$u = u_1 + (u_2 - u_1) \exp -a \, (z/h)^2$$

Brooks (1961) interpreted Jacobs' results in terms of per
cent transition and examined some of the implications. The internal
boundary layer does not begin to grow immediately at the transition;
the distance required for 95% establishment of the new surface equil-

ibrium shear stress is almost 100 barrier heights for rough-to-smooth
flow and over 200 barrier heights for smooth-to-rough flow. Hence tree
interference is to be expected for a hundred or so tree heights downwind.
Brooks also compared Jacobs's formula with one by Jensen for the depth
of a turbulent boundary layer developing from the beginning of a clearing

$$h = z_o^{0.2} (0.341) \ x^{0.8}$$

He concluded that for changes in shear stress of a factor of two a
height-to-fetch ratio of 1/50 is sufficient for equilibrium.

There is some question about the distances from the wall
measured by Jacobs (Brooks, 1961) because the smooth surface was 0.3 cm
heigher than the top of the preceding roughness elements to eliminate
a pressure jump at the discontinuity. Also some doubt has been cast on
the two-dimensionality of the flow, since the roughness change was
applied only to the floor of the channel (Tani, 1968). Similar exper-
iments in recent times by Logan and Jones (1963) for pipe flow, by Tani
and Makita (1968) for channel flow, and by Antonia and Luxton (1971,
1972) in a wind tunnel, all indicate that the wall shear stress does not
attain its equilibrium value immediately, but that it overshoots and
subsequently returns slowly to the equilibrium value. The velocity
profile adjusts rapidly, establishing the law of the wall. The log-
arithmic form, however, does not mean that the shear stress or the flow
as a whole is in equilibrium with the underlying surface.

Unfortunately, laboratory studies such as these are not directly
applicable to the atmosphere. There are at least two difficult scaling
problems:

(1) The atmosphere possesses an overall, developed, planetary
boundary layer, much thicker than the internal one formed by the roughness
perturbation. In a wind tunnel, both boundary layers will continue to
grow in the streamwise direction. The internal layer quickly grows to
a considerable fraction of the outer layer; soon thereafter the tops of
the two layers actually intersect.

(2) The atmosphere has a thick frictionless region and no
rigid upper boundary. The wind tunnel has a fixed upper wall and a
rapidly diminishing 'free flow' region. Also the fixed volumetric flow
rate allows only the shape of the profile to change whereas in the
atmosphere the whole flow can accelerate (Brooks, 1961).

3.2 A Momentum Integral Technique

The horizontal momentum equation together with the continuity equation can be integrated across the depth of the internal boundary layer after the manner of von Karman to yield the integral momentum equation

$$\frac{d}{dx} \int_{z_0}^{h} u^2 \, dz \; - \; u_h \frac{d}{dx} \int_{z_0}^{h} U \, dz \; = \; \tau_h - \tau_{o2} \; = \; u_{*1}^2 - u_{*2}^2$$

This expression simply states that the horizontal flux out of a region bounded by the top of the boundary layer, the surface and two vertical lines a distance dx apart is equal to the net gain of momentum due to vertical flux into the region. The latter is given by the difference in shearing stress between the top and bottom of the column considered.

For closure Elliot (1958), in a pioneering paper on the subject, assumed that the velocity profile for z < h immediately takes on the logarithmic form of the new surface roughness,

$$u_2 = (u_{*2}/k) \, \ln \, z/z_{o2}$$

implying that $f_1(z/h) = 0$. The boundary conditions were those previously described except that velocity continuity was imposed in the form $u_2(h) = u_1(h)$ at $z = h$, tacitly assuming that the streamline displacement is negligible compared to h. The formal solution is extremely clumsy but Elliot found that the growth of h with distance is well represented by

$$h/z_{o2} = a \, (x/z_{o2})^{0.8} \qquad \text{for } x/z_{o2} > 10^3$$

Near the origin the method could not be expected to yield accurate results owing to pressure effects. The coefficient a is a slowly varying function of the roughness change parameter $M = \ln(z_{o1}/z_{o2})$ which can be approximated by

$$a \approx 0.75 + 0.03 \, M$$

Hence the height of the internal boundary layer is greater for air flowing from a rough-to-smooth surface than for the reverse. The slope of the interface is about 1/10 for distances of micrometeorological interest.

A surprising feature of this growth equation is that it does not contain either the wind speed or the friction velocity. In

boundary layers growing on a flat plate the height is dependent on some power of the free stream velocity. For turbulent flow over an aero- dynamically smooth plate the growth equation is given by

$$h \propto x^{0.8} (u_h/\nu)^{-0.2} \qquad \text{(Schlichting, 1968, p. 599).}$$

and the velocity profile is $u/u_* \propto \ln (u_* z/\nu)$. For flow over a rough plate the velocity profile takes the form $u/u_* \propto \ln (z/z_0)$. A comparison reveals that the surface characteristics measured by z_0 have replaced the viscosity factor ν/u_* as the relevant parameter. If this can be extended to the growth equation and ν is replaced by $u_* z_0$ then

$$h \propto x^{0.8} (u_h/u_* z_0)^{-0.2}$$

$$\text{and } (u_h/u_*)^{0.2} h/z_0 \propto (x/z_0)^{0.8}$$

$$\text{But } u_h/u_* \propto \ln (h/z_0)$$

$$\text{so } (\ln h/z_0)^{0.2} h/z_0 \propto (x/z_0)^{0.8}$$

The factor $(\ln h/z_0)^{0.2}$ is virtually constant over a large range of h/z_0 varying from 1.47 at $h/z_0 = 10^3$ to 1.79 at $h/z_0 = 10^8$. Therefore

$$h/z_0 \propto (x/z_0)^{0.8}$$

This is the dimensional argument put forward by Elliot in support of his growth equation.

The Elliot theory seems to incorporate the essential features of the flow problem as it gives results in general agreement with observations (Echols, 1972; Panofsky and Petersen, 1972). Also see Fig. 3-2. His basic assumption, the immediate attainment of the logarithmic profile, has been demonstrated experimentally both in the laboratory, as already mentioned, and in the atmosphere, by Bradley (1968). Nevertheless, the solution is not complete because the shear stress distribution in the vertical has not been specified. To do this a relationship between the shear stress and the velocity profile must be assumed. If Jacobs' work is any indication, a mixing length assump- tion will not be adequate. The elegance of Elliot's simple approach becomes most evident as other theories are examined.

In an attempt to improve upon Elliot's model, Plate and Hidy (1967) assumed that the streamline displacement is not zero, but small compared to h. The continuity condition at the interface was then written as

$$u_h / u_{*1} = (1/k)(\ln h/z_{01} - \delta /h)$$

by expanding the logarithm in a series and dropping second and higher order terms. A simplification was obtained by integrating the momentum equation between $x = 0$ and $x = x$; the shear stress being set equal to an average value along x, and the streamline through h(x) assumed to be a straight line. Their results are incorporated into a nomogram (Fig. 3-1) from which h/z_{02} and u_{*2} can be obtained. This modification is limited to short fetches where the blending region is not a significant portion of the internal boundary layer.

3.3 A Simple Diffusion Theory

The experimental findings of Dyer and Pruitt (1962) prompted Dyer (1962) to assess the rate of adjustment of profiles and fluxes using simple diffusion theory. For near neutral stability Philip (1959) found a solution of the diffusion equation

$$u \frac{\partial \Theta}{\partial x} = \frac{\partial \phi}{\partial z} , \qquad \phi = - k \frac{\partial \Theta}{\partial z}$$

where Θ is the concentration of the diffusing entity, ϕ is the corresponding vertical flux, and K is the eddy diffusivity. Assuming that the wind profile is given by the power law

$$u = u_r (z/z_r)^{1/7}$$

where u_r is the velocity at a reference height z_r taken to be 1 cm, and assuming that K is a function of z and not x given by

$$K = K_r (z/z_r)^{6/7}$$

the equation becomes

$$\frac{\partial \phi}{\partial x} = \frac{\partial}{\partial z} \left(\frac{1}{u} \frac{\partial \phi}{\partial z} \right)$$

Solutions were found in terms of the parameter
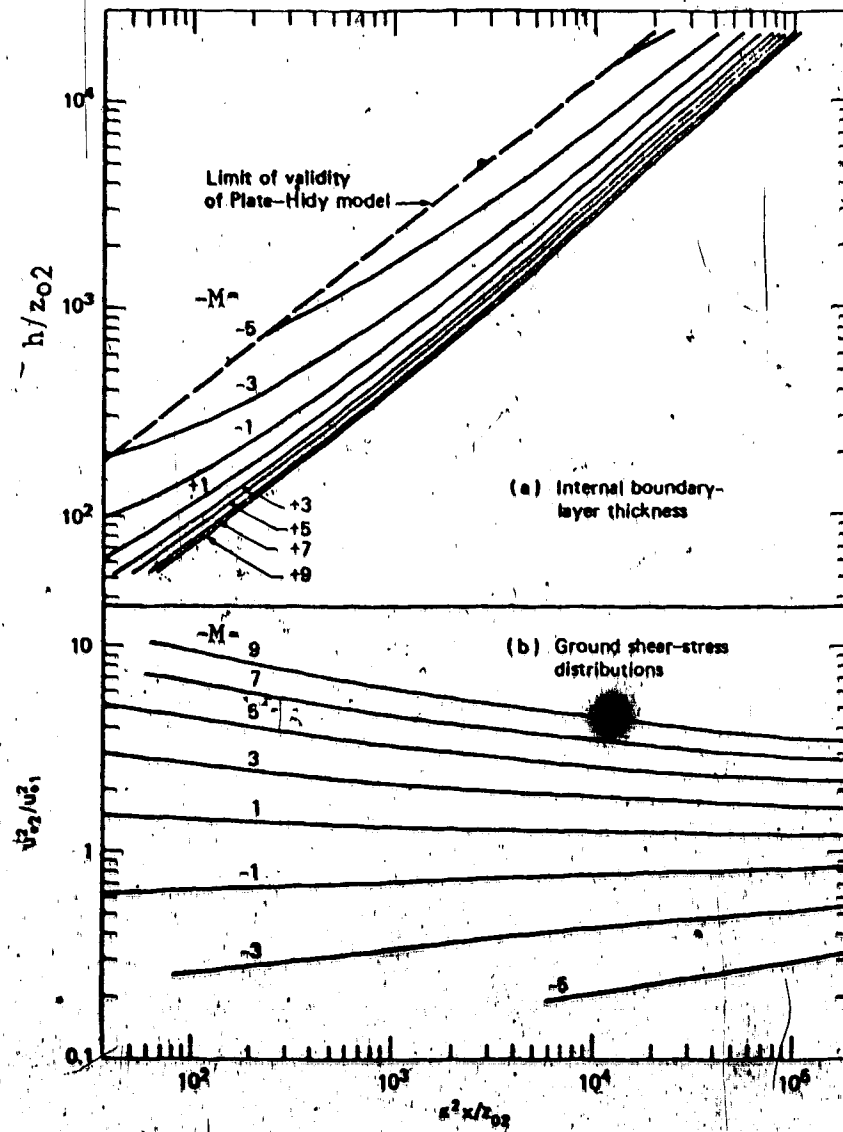
Figure 3-1. Nomogram for calculating internal boundary layers (from Plate and Hidy, 1967).

$$\mathcal{f} = (49/81)(u_r/K_r)(z/x)^{9/7}$$

The rate of adjustment was determined by considering the ratio ϕ/ϕ_∞
where ϕ_∞ is the flux at $x = \infty$, that is, when full equilibrium has been
established. Thus,

$$\phi/\phi_\infty \neq \frac{\partial \Theta}{\partial z} \Big/ \left(\frac{\partial \Theta}{\partial z}\right)_\infty$$

The profiles experience an adjustment rate equal to that of the fluxes,
which follows from assuming that K is independent of x. Philip's
solution gave

$$\phi/\phi_\infty = 1 - I\left(\mathcal{f}, -\frac{1}{9}\right)$$

where $I(\mathcal{f}, -1/9)$ is a form of the incomplete gamma function, the parameter
$-1/9$ arising from the power law assumptions. The solution is a function
of x, z, and u_r/K_r, but Dyer noted that the ratio u_r/K_r is fairly
constant over a wide range of wind speeds. Using Philip's tabulation
for the solution the height to fetch ratio for 90% adjustment ($\phi/\phi_\infty = .9$)
can be computed (Table 3-1).

Dyer's intention was to provide working estimates for research
into heat and moisture transfer, as in the later work of Rider, Philip
and Bradley (1963), and Dyer and Crawford (1965). Although specifically
excluding a change of roughness in the original treatment, Dyer (1965)
considered it to be an approximation to shear stress and wind profile
modification. It is difficult to accept this view because his theory
assumes that K is a function of height only. By definition $K = ku_* z$
and in the change of roughness problem u_* varies with x; it follows that
K must also vary with x. The adequacy of such a simplified diffusion
equation is also questionable.

Table 3-1. Values of fetch and height for 90% adjustment.

Height (m)	Fetch (m)	Height/Fetch
0.5	70	1/140
1.0	170	1/170
2.0	420	1/120
5.0	1,350	1/270
10.0	3,300	1/330
20.0	8,100	1/405
50.0	26,500	1/530
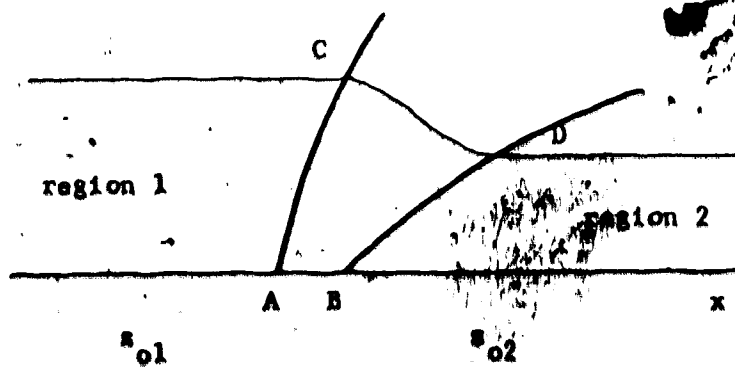
Figure 3-2. Schematic representation of the transition region.

3.4 An Advection Theory

In a dynamical approach R. J. Taylor (1962) identified the region of stress modification with that of streamline displacement as shown in Fig. 3-2. Here AC and BD, both lines of constant stress, mark the boundaries of the transition region, and CD is part of a streamline in the rough-to-smooth change. A streamfunction ψ can be defined so that the horizontal momentum equation becomes

$$\frac{\partial \psi}{\partial z} \frac{\partial u}{\partial x} - \frac{\partial \psi}{\partial x} \frac{\partial u}{\partial z} = \frac{\partial (u_*^2)}{\partial z}$$

Integration over the region ABCD gives

$$\int_0^{\psi_o} (u_2 - u_1)\, d\psi = \oint_{ABCD} u_*^2\, dx$$

where $u_2 - u_1$ is taken along the streamline.

Accepting Jacob's results, Taylor then assumed that the distance between A and B is much less than the distance between C and D, making ABCD approximately triangular. Hence,

$$-\oint_{ABCD} u_*^2\, dx \approx \chi (u_{*1}^2 - u_{*2}^2)$$

where χ is some x-coordinate between C and D (about midway if the shear stress varies regularly along CD), and

$$\int_0^{\psi_o} (u_2 - u_1)\, d\psi = \chi (u_{*1}^2 - u_{*2}^2)$$

For neutral conditions the stream function will be

$$\psi = \frac{u_*}{k}\left(\ln \frac{z}{z_o} - 1\right) \quad \text{if} \quad \psi = 0 \text{ at } z = z_o$$

and

$$\int_0^{\psi_o} u\, d\psi = z u^2 - 2 \psi u_*/k$$

Thus, given u_{*1}, u_{*2}, z_{o1}, and z_{o2} the parameter χ can be evaluated by substitution for the integral.

In practice, however, only three of the four are known and u_{*2} is to be determined. Taylor assumed that

$$u_* \propto z_o^{n} \quad \text{with } n = 0.09$$

and together with the previous equation obtained an expression for χ in terms of the roughness-change ratio $m = \exp M = z_{o1}/z_{o2}$.

If AC is tak̶e̶n̶ ... ̶ ̶a̶n̶d̶ the streamline displacement
is assumed symmetric̶ ... new velocity profile should be
fully established to ... wnwind distance of twice $X(z)$.
For typical values of ... eight/fetch ratios of 1/100 to
1/150.

Taylor's own wind tunnel experiments revealed some variation
in the surface shear stress after the transition, but equilibrium was
quickly reached, in confirmation of Jacobs' results. Also the stream-
lines were observed to drop off at or a little before the transition,
indicating that AC was indeed perpendicular. However, as Panofsky and
Townsend (1964) pointed out, almost all the measurements were made in
a region where the internal boundary layer actually intersected the
tunnel boundary layer.

This solution is not, of course, a complete one; no information
is supplied about the profiles in the blending region. The parameter X
is the scale of the transition and serves only to provide practical
estimates for field work.

3.5 A Parabolic Shear Stress Distribution

Under the mixing length assumption, namely, $\tau = \left(\ell \frac{du}{dz} \right)^2$
the logarithmic profile used by Elliot in the internal boundary layer
implies constant stress u_{*2}^2 up to $z = h$ and then a discontinuous jump
to u_{*1}^2. To remove this unappealing proposition Panofsky and Townsend
(1964) assumed that $\tau^{1/2}$ is a linear function of height such that

$$\tau^{1/2} = u_{*2} + (u_{*1} - u_{*2})(z/d)$$

where d is the depth of the internal boundary layer.
With the mixing length relation

$$\frac{\partial u}{\partial z} = \frac{\tau^{1/2}}{k z}$$

the downstream profile is thus

$$u_2/u_{*2} = (1/k) \ln z/z_{02} + (u_{*1} - u_{*2})/k \ (z/d)$$

the second term on the right being the blending function $f_1(z/d)$.
The conditions of incompressible, steady flow, and velocity continuity
at $z = d$, together with the conservation of momentum, yield an ordinary

differential equation for the growth of d with x. For values of d that are not too small the solution is given by

$$4k^2 \left(\frac{x}{z_{o2}} - \frac{x_c}{z_{oA}} \right) = \frac{d}{z_{o2}} \left\{ \ln \frac{d}{z_{oA}} \quad 5 - \frac{M}{2} + \frac{4 + \frac{7}{4}M - \frac{1}{4}M^2}{\ln \frac{d}{z_{oA}} - 1 - \frac{1}{4}M} \right. $$
$$\left. + \frac{4 - \frac{7}{4}M + \frac{1}{24}M^2 + \frac{1}{16}M^3}{\left(\ln \frac{d}{z_{oA}} - 1 - \frac{1}{4}M \right)^2} \right\} $$

where $x_o/z_{o2} = 0$ for $M \leq 3$, and for $M > 3$

$$4k^2 x_o/z_{o2} = \exp (1+M) (M/18 - 64/27 + 88/27M + 67/9M^2)$$

One consequence of this continuous stress assumption is that the definition of the interface between the two flow regions is changed. In Elliot's theory h is the intersection of the two logarithmic profiles, whereas here d is the top of a transition zone, and so is somewhat higher. Except for short fetches (where neither theory is valid anyway) the theories are in close agreement. Near the top of the internal boundary layer the profile in the Panofsky-Townsend theory begins to deviate from the lower logarithmic profile and enters the upper logarithmic profile smoothly. The height/fetch ratio for 90% adjustment of shear stress is thus somewhat less than in the Elliot theory and is about 1/20 (Townsend, 1965; Dyer, 1965).

In assessing the assumption of the equilibrium relation $\tau^m = kz(du/dz)$ Panofsky and Townsend pointed out that the time necessary for substantial adjustment of the Reynold's stress is of the order of the turbulent energy divided by the rate of energy production. The distance travelled while the adjustment is made is nearly

$$x = Eu/(u_*^2 \, \partial u/\partial z) \quad \text{where} \quad E = 1/2(\overline{u'^2} + \overline{v'^2} + \overline{w'^2})$$

The surface separating adjusted from unadjusted fluid is

$$x/z_o = (E/u_*^2)(d/z_o) \ln d/z_o$$

which has much the same form as the previous solution.

Another line of argument is that of Miyake (Panofsky and Townsend, 1964) who assumed that the vertical rate of spread of the surface change is proportional to the standard deviation of the vertical

wind, $d(d/z_o)/d(x/z_o) = A\sigma_w/u$. With the assumptions $\sigma_w = u_*$
and $u = (u_*/k)\ln d/z_o$ this yields

$$x/z_o = (1/Ak)(d/z_o)(\ln d/z_o - 1)$$

Again the solution has much the same form as that outlined by Panofsky
and Townsend.

Observations by Blackadar, Panofsky, Glass and Boogaard (1967)
of the interface height agreed reasonably well with both the Elliot and
Panofsky-Townsend theories. The extended validity of the relation
$\tau^{1/2} = kz\, \partial u/\partial z$ in near neutral but nonequilibrium conditions was also
investigated. The non-dimensional wind shear $\phi = (kz/\tau^{1/2})\partial u/\partial z$ was
found to deviate from the value 1.0 in a nearly linear fashion with
height, the error at 1/10 the interface height being 5%. Measurements
of the surface shear stress on a beach taken by Hsu (1971) were also in
fair agreement with the predictions of the Panofsky-Townsend theory.

A series of atmospheric experiments related to the change of
roughness problem has been performed with artificial roughness elements
over the ice of Lake Mendota, Wisconsin. Kutzbach (1961) used a
triangular array of bushel baskets, which may not have simulated a truly
two-dimensional situation. His results were in good agreement with both
the Elliot and Panofsky-Townsend theories (Fig. 3-3). Stearns and
Lettau (1963) and Stearns (1964) used Christmas trees in a circular array,
two-dimensionality again being questionable. These experiments were not
designed for the purpose of testing the internal boundary layer theories,
so it is not surprising that the data are inconclusive.

(a) Fetch of 20 m   (b) Fetch of 43 m
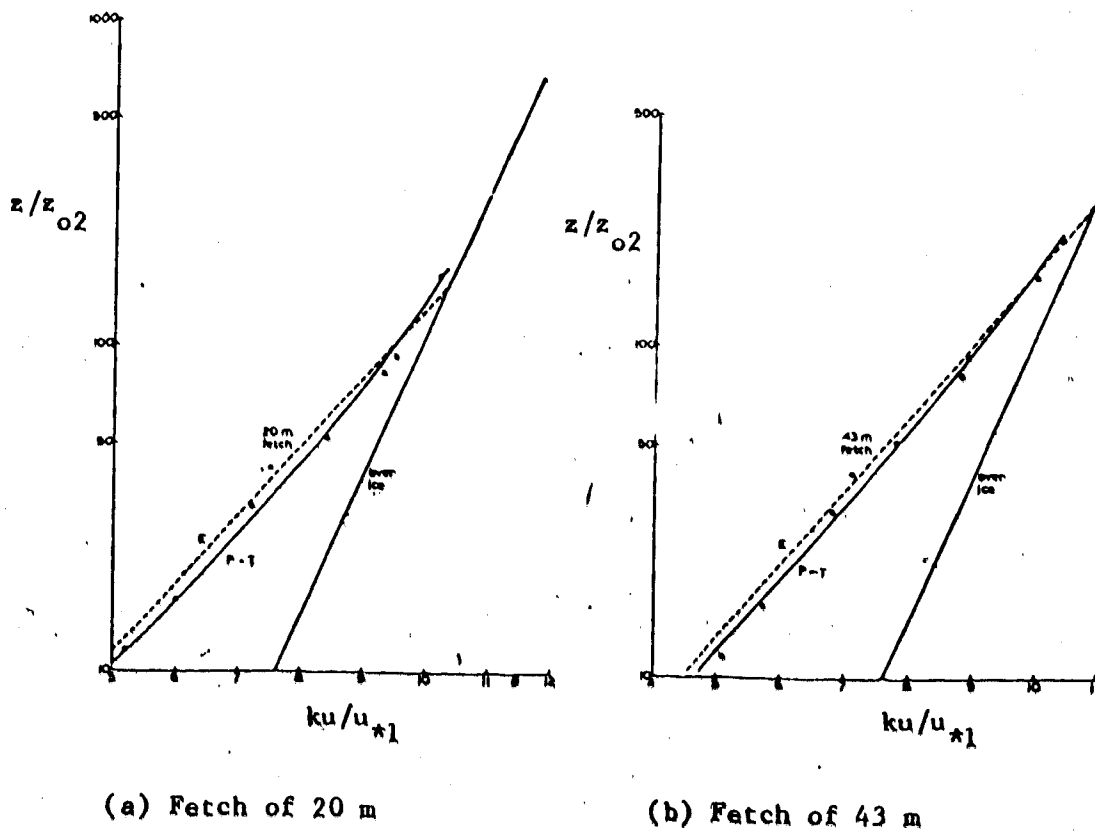
Figure 3-3. Comparison of bushel basket data with the theories of
            Elliot and Panofsky-Townsend (from Panofsky and Townsend,
            1964).

3.6 A Similarity Theory

To improve the estimate of the blending function f_1 Townsend (1965, 1966) investigated the conditions under which it can be assumed to be a similarity profile dependent only on a length scale l_s. He assumed that the velocity downstream of the discontinuity consists of three parts:

(1) the profile u_1 upstream of the discontinuity;

(2) a component Δu that has to be added because of streamline displacement;

(3) the remaining difference u' due to acceleration of the fluid in the internal boundary layer.

For streamline displacement $\delta(z)$ small compared to z, $\Delta u \approx u_{*1} \delta/kz$ from a Taylor series expansion of u_1. Similarity entered through the assumptions

$$u' = (u_s/k)\ f(z/l_s)$$

$$\tau = u_{*1}^2 + (u_{*2}^2 - u_{*1}^2)\ F(z/l_s)$$

where u_s is the velocity scale. The scales l_s and u_s depend only on x. The functions f and F were assumed to depend on z/l_s and not on x. They were related through the mixing length so that, putting $\eta = z/l_s$,

$$\eta \frac{df}{d\eta} = F$$

The equations of motion and continuity were combined to yield

$$- \eta \frac{df}{d\eta} = \frac{dF}{d\eta}$$

so that

$$F = \exp - \eta$$

$$f = Ei(-\eta) = - \int_\eta^\infty e^{-x}/x\, dx$$

The two scales were then found from the conditions that f and F are independent of x (in the sense that they depend only on η), and that the velocity profile near the surface is logarithmic. Townsend's original work contained a small error in not satisfying the latter condition. Blom and Wartena (1969) corrected the derivation to remove this inconsistency. The revised scales are given by

$$l_s/z_{01}(\ln l_s/z_{01} + 1) = 2k^2 x/z_{01}$$

$$u_s = -u_{*1} M/(1+P) \left[\ln l_s/z_{o2} - \gamma + (1+P^{-1})^{-1} \right]^{-1}$$

where $P = (\ln l_s/z_{o1} - 1 - \gamma)^{-1}$ and $\gamma = $ Euler's constant $= 0.577$

The downstream surface shear stress can be calculated from

$$u_{*2} = u_{*1} + u_s(1+P)$$

and the velocity profile is given by

$$u_2 = u_1 + (u_s/k)\left[Ei(-\eta)(1+P) - P(1 - \exp -\eta)\eta^{-1} \right]$$

While l_s is the same order of magnitude as h, the adapted layer according to Blom and Wartena is of order $0.1 \, l_s$. This results in rather long adjustment distances, the height/fetch ratio being about 1/300. Fully developed boundary layers, even to heights of 10 m, will be difficult to find anywhere if this assessment is correct.

3.7 An Exchange Coefficient Theory

Russian work on the problem of inhomogeneous terrain is based on the exchange coefficient $K = ku_{*}z$ (Panchev, Donev, and Godev, 1971). The horizontal momentum equation in the form

$$u \frac{\partial u}{\partial x} + w \frac{\partial u}{\partial z} = \frac{\partial}{\partial z}\left(k \frac{\partial u}{\partial z} \right)$$

is combined with the continuity equation to give

$$u \frac{\partial u}{\partial x} - \frac{\partial u}{\partial z} \int_{z_o}^{z} \frac{\partial u}{\partial x} \, dz = \frac{\partial}{\partial z}\left(k \frac{\partial u}{\partial z} \right)$$

If the perturbation in wind velocity is small compared to the equilibrium velocity over the second surface, linearization is possible, and an approximate solution can be found by the method of Shwetz (described in Panchev, Donev, and Godev, 1971). Gandin did this for the case of a sudden change in surface friction velocity, but not roughness.

Donev was able to solve the non-linear equation of the general case also using the method of Shwetz. The solution for the blending function f_1 is

$$f_1 = \left(\frac{u_{*1}}{u_{*2}} \ln \frac{h}{z_{o1}} - \ln \frac{h}{z_{o2}} \right) \frac{G\left(\ln \frac{z}{z_{o2}}\right)}{G\left(\ln \frac{h}{z_{o2}}\right)}$$

where $G(f) = \exp f \cdot (f-1) + \frac{1}{2}f^2 + 3 + \left(\frac{u_{*1}}{u_{*2}} \ln \frac{h}{z_{o1}} - \ln \frac{h}{z_{o2}} \right)(\exp f - f + 1)$

and the internal boundary layer height can be determined from

$$
k \frac{x}{z_{0A}} = \ln \frac{h}{z_{0A}} - 1 - \frac{b+3}{\kappa \rho b} \left[E_i (\ln \frac{h}{z_{0A}} + b) - E_i(b) \right] + \frac{1}{4} \left(\ln \frac{h}{z_{0A}} \right)^2
$$

$$
+ (2 - \frac{1}{\lambda}) \ln \frac{h}{z_{0A}} + (\frac{1}{\lambda} b^2 - 2b + 3) \ln \left[\frac{\ln(\frac{h}{z_{0A}} + b)}{b} \right]
$$

$$
+ \frac{u_{*1} - u_{*2}}{\lambda u_{*A}} \left[\frac{h}{z_{0A}} - \frac{1}{\lambda} (\ln \frac{h}{z_{0A}})^2 + \ln \frac{h}{z_{0A}} - 1 \right] \quad \text{where} \quad b = \frac{u_{*1}}{u_{*1} - u_{*A}} \ln \frac{z}{z_{01}}
$$

The solution of the linearized equation differs only in the absence of
the last terms in both equations.

3.8 Experimental Evidence

The best atmospheric data presently available are those of
Bradley (1968) who measured simultaneously both velocity profiles and
surface shear stresses. His experiments involved flow over tarmac
($z_o = 0.002$ cm) and an artificial roughness mat made of vertical spikes
($z_o = 0.25$ cm). The surface shear stress was measured with a drag plate.
The results are shown in Figs. 3-4, 3-5, and 3-6.

Several important conclusions can be reached. The velocity
profile is practically unchanged above the point where the lower profile
intersects the upstream profile, implying that the streamline displace-
ment is negligible. Also there is little deviation from the logarithmic
profile over most of the internal boundary layer. Near the top of the
layer the profiles do exhibit a slight curvature. The discontinuity
is rather sharper and the top of the modified region is lower than that
predicted by the Panofsky-Townsend theory. The 4/5 power law is
confirmed and the predicted asymetry between smooth-to-rough and rough-
to-smooth flows is not apparent. When the top of the internal boundary
layer is taken as the upper limit of the linear portion of the profile
the slope of the interface is about 1/20. In fluid mechanics the
'law of the wall' is usually assumed to extend over the lowest 10% of
the boundary layer. With this in mind Bradley recommended that the
height/fetch ratio for the equilibrium layer is 1/200.

Most of the stress change occurs within a short distance of
the transition, more rapidly than either the Elliot or Panofsky-Townsend
theory predicts. The recovery from the initial overshoot is less rapid
in the rough-to-smooth transition. There is a hint of a minimum in the
smooth-to-rough case.
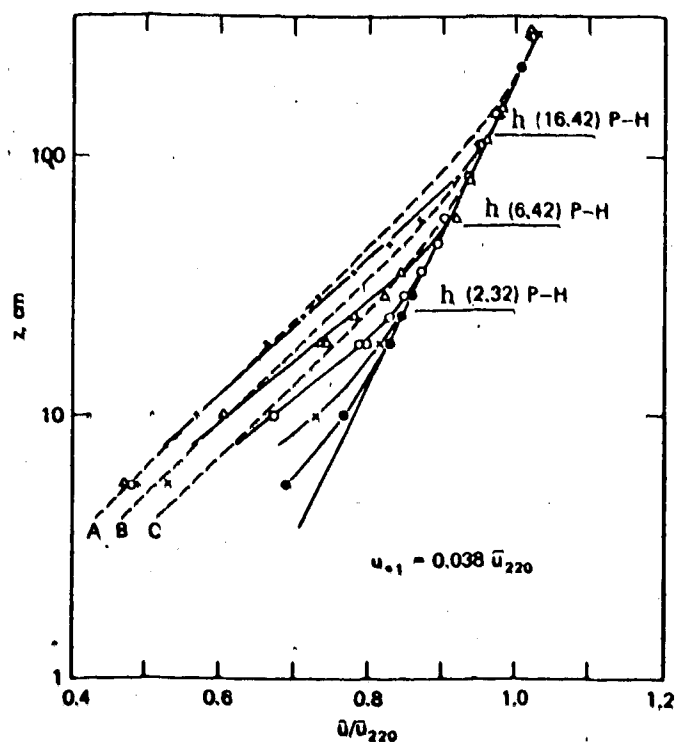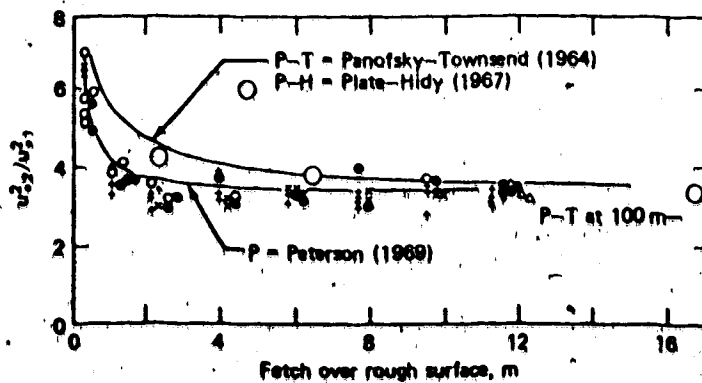
Figure 3-4. Experimental data of Bradley (1968) compared with various
theories for the smooth-to-rough transition (from Plate,
1971, p. 142).
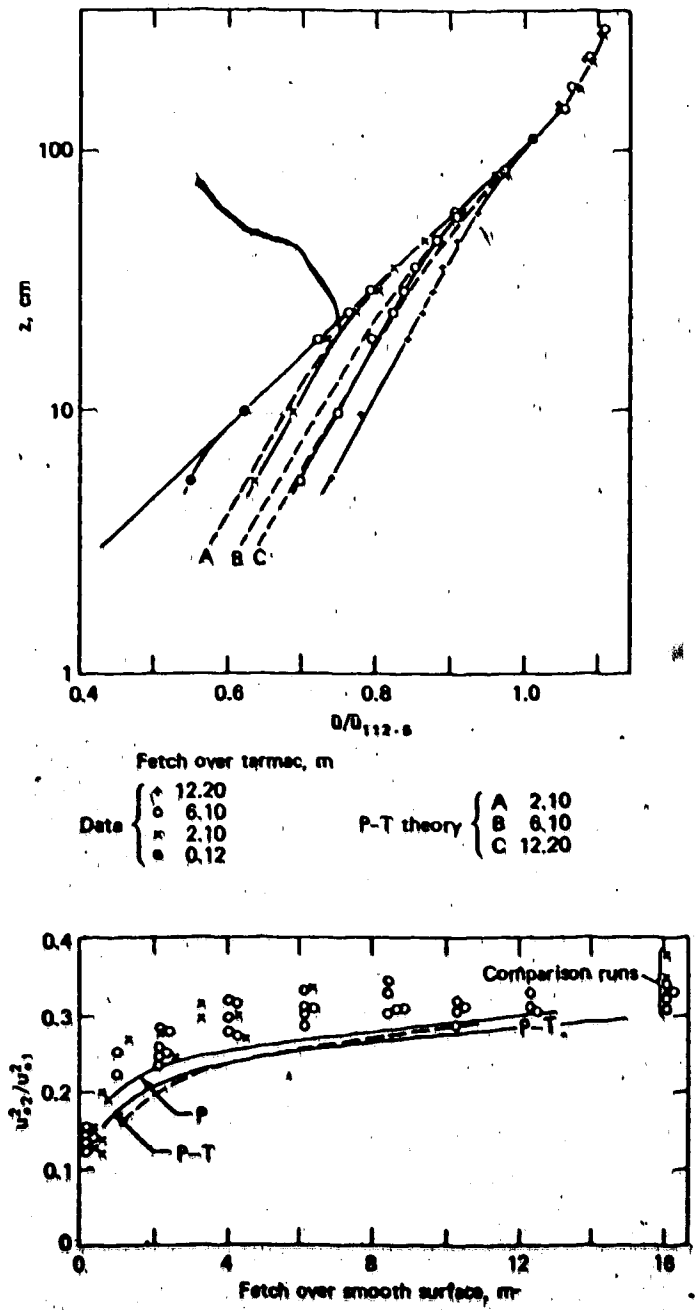
Figure 3-5. Experimental data of Bradley (1968) compared with various theories for the rough-to-smooth transition (from Plate, 1971, p. 143).
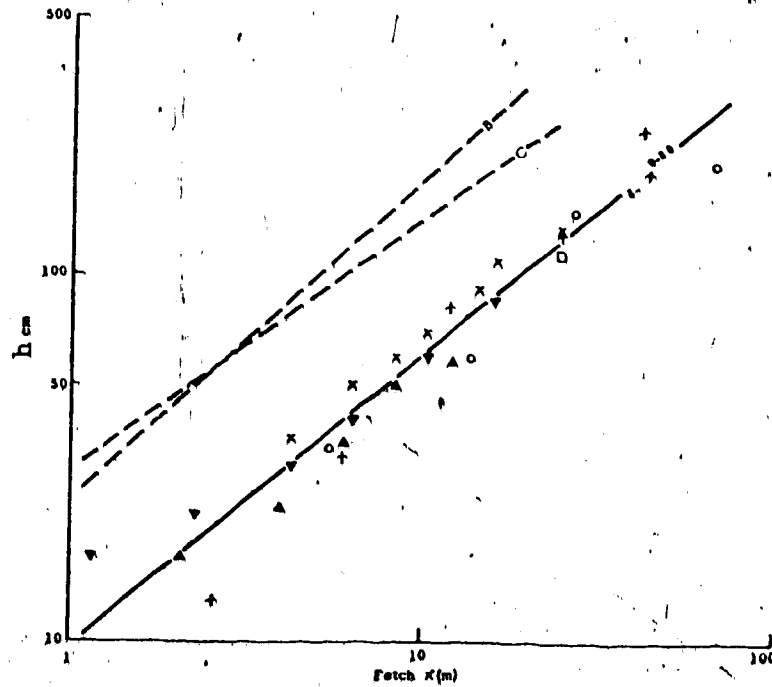
	Date	Transition
+	1 June 1964	Grass-Tarmac
O	20 June 1964	Grass-Tarmac
▲	25 August 1964	Spikes-Tarmac
□	26 August 1964	Tarmac-Spikes
×	27 August 1964	Tarmac-Spikes
▼	30 August 1964	Tarmac-Spikes

B   P-T 'd'   Tarmac-Spikes
C   P-T 'd'   Spikes-Tarmac

Figure 3-6.   The height of the modified region (from Bradley, 1968).

CHAPTER IV

NUMERICAL SOLUTIONS

4.1 A Mixing Length Model

Rather than assume a special form for the shear stress or velocity distribution, P. A. Taylor (1969a) chose to solve the governing partial differential equations by numerical means, using the mixing length relation for closure. To facilitate the computations, slightly different co-ordinates were employed, the origin of the z-axis being shifted to the local roughness length z_{ol}. The mixing length then took the form $\ell = k(z + z_{ol})$, the initial profile became $u/u_{*1} = (1/k) \ln (z + z_{ol})/z_{ol}$, and the boundary conditions were given by $u = w = 0$ at $z = 0$. Velocities were scaled with respect to u_{*1} and lengths with respect to z_{o2}. Eliminating τ the equations of motion were written as

$$U \frac{\partial U}{\partial X} + W e^{-f} \frac{\partial U}{\partial f} = 2k^2 e^{-f} \frac{\partial U}{\partial f} \frac{\partial^2 U}{\partial f^2}$$

$$\frac{\partial U}{\partial X} + e^{-f} \frac{\partial W}{\partial f} = 0$$

where $U = u/u_{*1}$, $W = w/u_{*1}$, $X = x/z_{o2}$, and $f = \ln (z + z_{o2})/z_{o2}$. Setting $Z = z/z_{o2}$ the initial conditions became

$$U = (1/k) \ln (Z z_{o2}/z_{ol} + 1)$$

Replacing the f derivatives by finite differences produced a system of ordinary differential equations for dU/dX, which were solved by the Runge-Kutta method.

The solutions were compared with the Elliot, Panofsky-Townsend, and Townsend theories as well as with a solution based on the form

$$\tau^{1/2} = u_{*2} + (u_{*1} - u_{*2}) \left[10(z/h)^3 - 15(z/h)^4 + 6(z/h)^5 \right]$$

derived by Taylor using the Pohlhausen technique (Goldstein, 1938, p. 158) of choosing the highest order polynomial that will permit reduction to a single ordinary differential equation. The results of the numerical computation were in close agreement with the Panofsky-Townsend theory, especially the velocity profiles (Fig. 4-1). The shear stress profiles were also in good agreement with the self-preservation theory of Townsend (Fig. 4-2).
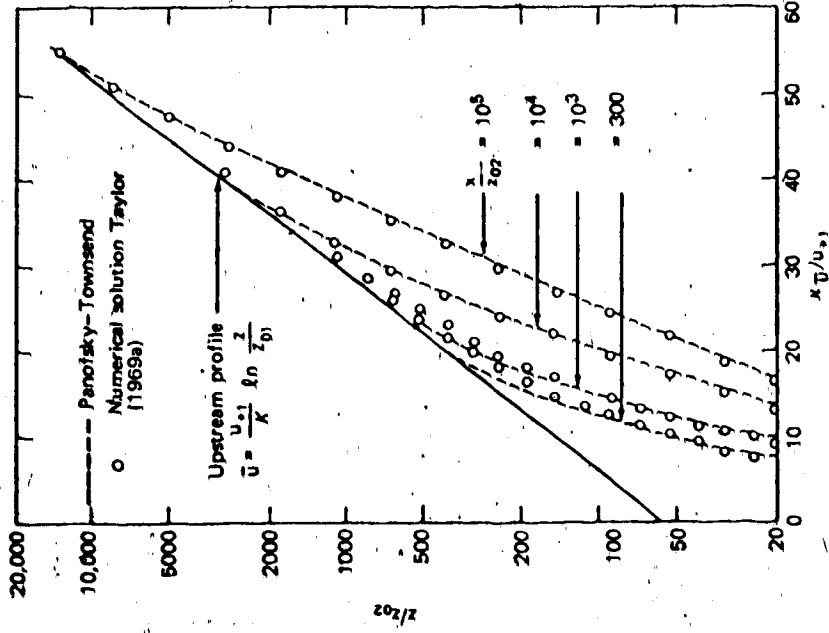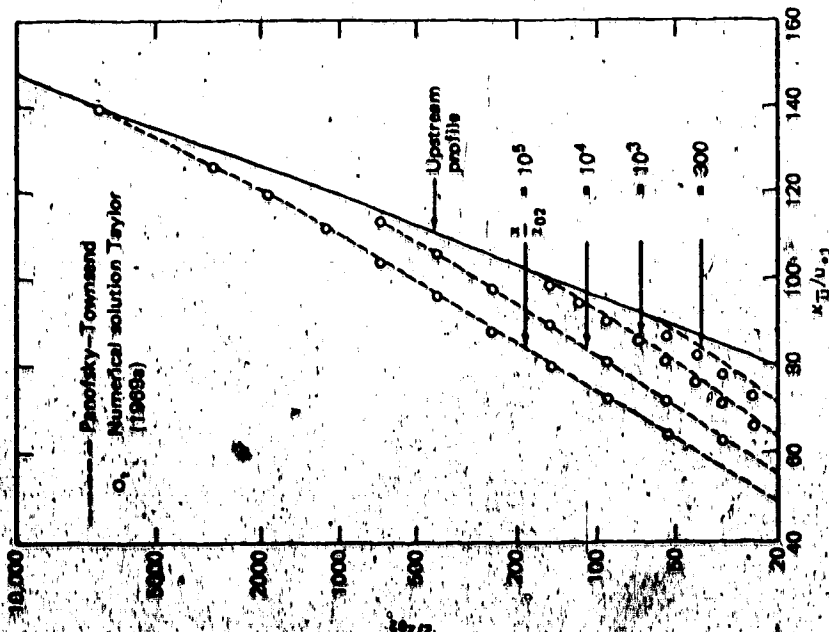
Figure 4-1. Comparison of wind profiles from mixing-length model and Panofsky-Townsend theory (from Taylor, 1969a).
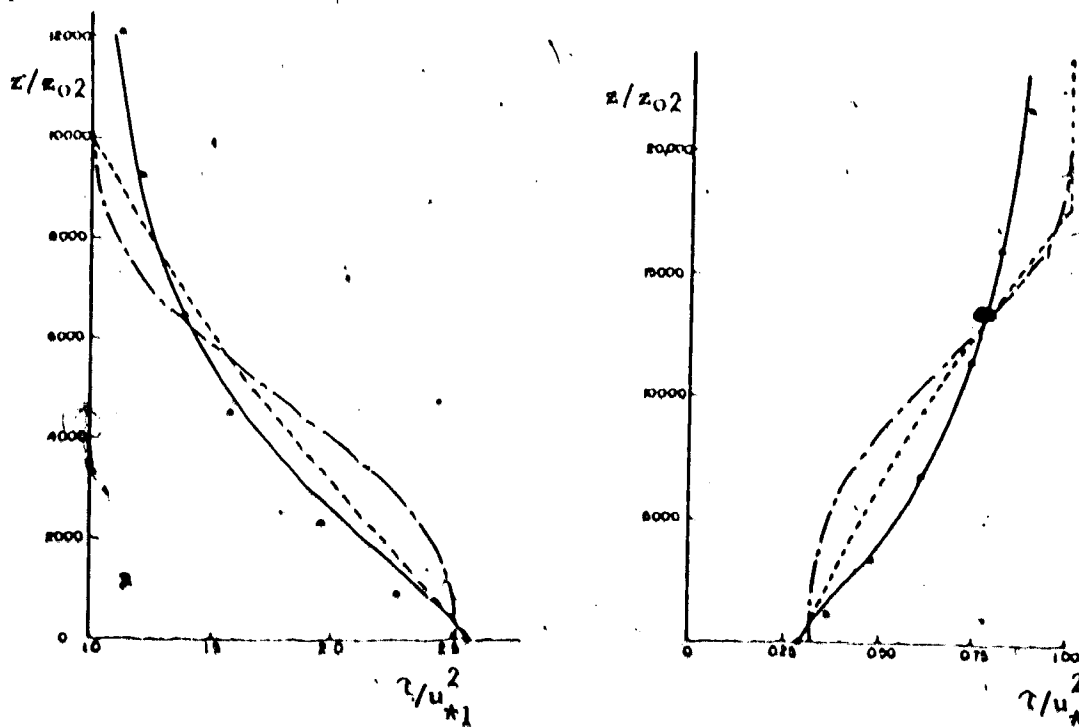
(a) $M = -5$, $x/z_{o2} = 10^5$ (b) $M = 4$, $x/z_{o2} = 10^5$

---   Panofsky-Townsend

. . .   self-preservation

—·—   polynomial

———   mixing length

Figure 4-2.   Comparison of shear stress profiles from mixing-length model with various other solutions (from Taylor, 1969a).

The turbulent energy equation then became

$$\frac{u}{q}\frac{\partial q}{\partial x} + \frac{w}{q}\frac{\partial q}{\partial z} = \tau\frac{\partial u}{\partial z} + \frac{\partial}{\partial z}\left(\frac{1}{q}\tau\frac{\partial \tau}{\partial z}\Big/\frac{\partial u}{\partial z}\right) - \frac{\tau^{1/2}}{\lambda_z}$$

The boundary condition on the shear stress was imposed in the form

$$\tau_o = \left[kz_0(du/dz)_{z_0}\right]^2$$

The numerical solution revealed several important features. The 4/5 power law for internal boundary layer growth was found to hold with the height h defined as the point where the stress reached 0.1% of the upstream value (this was about equal to the height of the interface in the Panofsky-Townsend theory). Such a definition for h meant that the velocity was essentially the upstream value above $z/h = 0.8$. The slope of the interface for large z/z_{o2} was 1/10 and the Townsend prediction of a self-preserving shear stress distribution appeared valid to first order. The stress was closer to the upstream value in the upper 75% of the transition layer. The stress and turbulent energy adjusted rather more slowly than the velocity profile; only about the bottom 10% of the layer was in equilibrium. Hence Peterson suggested a height/fetch ratio of 1/100.

There were two significant differences between the predictions of the Peterson model and the other theories. Firstly, the velocity profile contained an inflection point just below the interface (Fig. 4-5). There was a suggestion of this in Bradley's data (Fig. 3-4 and Fig. 3-5). Secondly, the non-dimensional shear $\phi = kz/\tau^{1/2}(\partial u/\partial z)$ deviated considerably from unity in the transition region. For the smooth to rough change $\phi > 1$, and for the rough to smooth change $\phi < 1$ (Fig. 4-3). Observations by Busch and Panofsky (1968), and Yeh (Peterson, 1969b) support this conclusion. Deviations from unity were also noted by Blackadar et al (1967), as mentioned in Chapter III. Peterson asserted that this was because of the slow adjustment of the turbulent energy to the new boundary conditions relative to the wind shear, and the sharp change in slope occurring in the wind profile just below the interface. An important consequence is the fallacy of exchange coefficient or mixing-length theories. Because $K = ku_*z/\phi$ and $\phi \neq 1$ is assumed
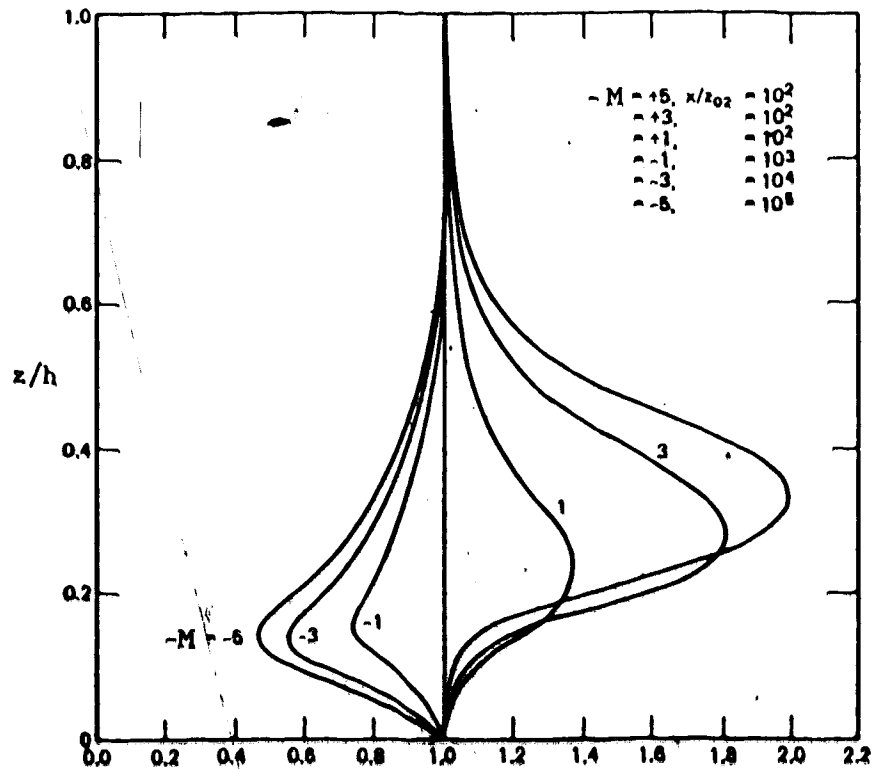
Figure 4-3. Non-dimensional wind shear in the internal boundary
layer (from Peterson, 1969a).

by these theories, calculations based on them could lead to serious errors as Peterson (1971) has demonstrated.

Peterson's basic assumption is actually an old one, advanced by Townsend (1956) and recently by Bradshaw et al (1967). Bradshaw determined the constant of proportionality to be 0.30 (which Peterson mistook for 0.15). Lumley and Panofsky (1964, p. 128) obtained values of 0.12 from Brookhaven data and 0.22 from O'Neill data. Values supplied by Hinze (1959) are in good agreement with the 0.16 used by Peterson.

As for the second assumption, Monin (1959) has argued that the relation between dissipation and shear stress is valid even in non-equilibrium conditions. Pasquill (1972) has affirmed it on empirical grounds. Bradshaw (1967) wrote the relationship in the form $\epsilon = \tau^{3/2}/L_\epsilon$ where L_ϵ is the dissipation length, and noted that the results depend significantly on the form assumed for L_ϵ. Little is known about the form of L_ϵ for atmospheric turbulent flow (Shir, 1972). When production and dissipation of turbulent energy are equal $L_\epsilon = \ell = kz$ The wind tunnel studies of Antonia and Luxton (1971, 1972) have indicated that both the dissipation length and the mixing length are altered from the value kz in the region near the roughness discontinuity (increased for rough-to-smooth, and reduced for smooth-to-rough).

The last two assumptions, Peterson has argued, are not important since the major effect of the energy divergence term is to smooth the velocity profile without modifying its basic shape. Various forms were tried with no significant differences in results. P. A. Taylor (1972) has shown that the assumption $K_E = k(z+z_{oi}) \tau^{1/2}$ simplifies computation. The results of this modified Peterson model are very close to those of the original. Details of a numerical method are presented in Appendix B.

Peterson (1972a, 1972b) has stressed the importance of diffusion of turbulent energy in the change-of-roughness problem, a feature of the flow described by the turbulent energy equation. Antonia and Luxton (1971, 1972) also found in their wind tunnel experiments that turbulent energy diffusion played an important role in the flow modification.

4.3 A Vorticity Model

The fact that Peterson's results did not agree very well with Bradley's observations for rough-to-smooth flow (Fig. 3-5) led Shir (1972) to include the pressure-gradient term and the vertical equation of motion. Neglecting the viscous and normal stress terms as before, Shir combined the two equations of motion to yield the mean vorticity equation

$$u \frac{\partial \omega}{\partial x} + w \frac{\partial \omega}{\partial z} = \frac{\partial^2 \zeta}{\partial z^2} - \frac{\partial^2 \zeta}{\partial x^2}$$

where ω is the two-dimensional vorticity. The pressure gradient does not appear because the density variations are assumed to be small. The second equation, derived from continuity, was the streamfunction equation

$$\frac{\partial^2 \gamma}{\partial x^2} + \frac{\partial^2 \gamma}{\partial z^2} = \omega$$

where γ is the streamfunction.

The third equation of the model was the turbulent energy equation as used by Peterson. Following Peterson it was assumed that:

(1) $\tau = a E$

where a was taken to be 0.22 on the recommendation of Cramer (Shir, 1972). Shir mentioned that Harsha and Lee obtained a value of 0.3 which was also used by Bradshaw (1967). Bradshaw and Ferris (1968) believed that a is a slowly varying function of the ratio of production to dissipation with a value of 0.3 in laboratory flows, but possibly smaller in the atmosphere.

(2) $\epsilon = \tau^{3/2} / L_\epsilon$

with the dissipation length L_ϵ given by

$$L_\epsilon = \lambda(z + z_{0i}) \qquad z \leq z_b$$

$$= \frac{\lambda(z + z_{0i})}{1 + \lambda(z - z_b)/\gamma} \qquad z > z_b$$

where z_b is the height of the surface boundary layer, taken as 10 m, and λ is the mixing length at the outer edge of the boundary layer, taken to be 40 m. This is a modified form of Blackadar's (1962) formula

for mixing length. Bradshaw found empirically that $L_\epsilon = kz$ near the wall and tends to a constant away from the wall. For atmospheric flow there are insufficient data to determine the exact variation with height.

$$(3) \qquad \frac{\partial}{\partial z}(\overline{w' E'}) = -\frac{\partial}{\partial z}\left(K_\epsilon \frac{\partial E}{\partial z}\right)$$

with $\qquad K_\epsilon = \tau^{1/2} L_\epsilon$

The energy flux was assumed to be of the gradient type. Once again the results were found not to be sensitive to the precise form of the flux. The boundary conditions imposed were:

$$\tau_0^{1/2} = k z \cdot \frac{\partial u}{\partial z}$$

$$u_2 = w_2 = 0 \qquad at \qquad z = 0 .$$

The results of the numerical computation were in many ways similar to Peterson's. The velocity profile had an inflection point, and the non-dimensional shear differed from unity in the transition zone. There were also several differences. For the rough-to-smooth change, the calculated stress values were a much better fit to Bradley's data (Fig. 4-4a). For the smooth-to-rough case, a local minimum appeared in the downstream surface stress (Fig. 4-4b). The latter was intimated by Bradley (1968) in the discussion of his experimental work, but not pursued because no theory at that time predicted it. The velocity profiles, however, did not fit nearly so well (Figs. 4-4c, 4-4d), and led Shir to question some of Bradley's data.

Shir also pointed to the inconsistency among authors in the definition of the internal boundary layer height h. Some chose to define it in terms of specified deviation from the upstream velocity; some, in terms of stress. Shir did both, defining a stress boundary layer height as the height where the stress is within 1% of the upstream value, and a velocity boundary layer height where the velocity is within 1% of the upstream value. The latter compared favorably with that used by Bradley, and the 4/5 power law was again upheld. The height of the interface was found to increase with roughness ratio m; but the slope remained the same. This suggested a relation of the form

$$h_u = g_1(z_{01}/z_{02}) x^{0.8} + g_2(z_{01}/z_{02})$$
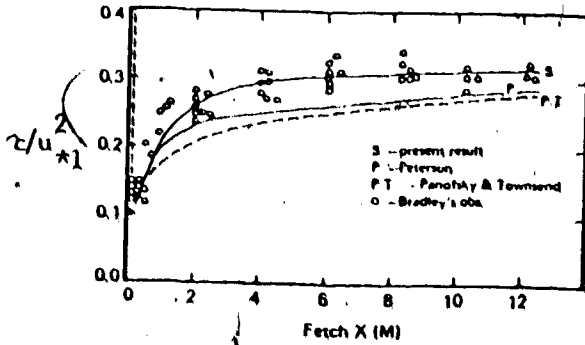
(a) Variation of surface shear stress for rough-to-smooth flow
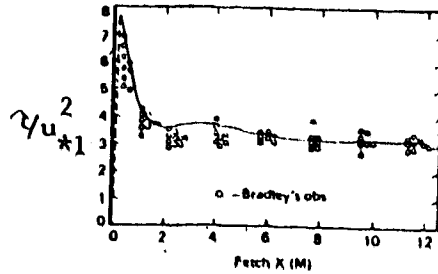
(b) Variation of surface shear stress for smooth-to-rough flow
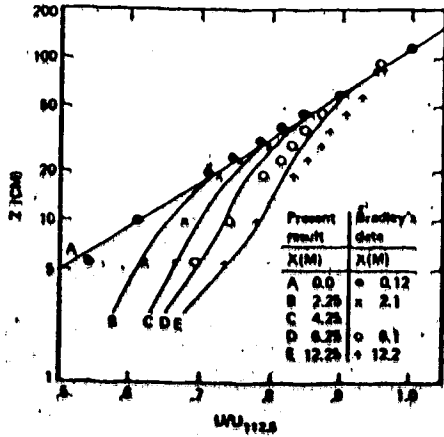
(c) Wind profiles for rough-to-smooth flow
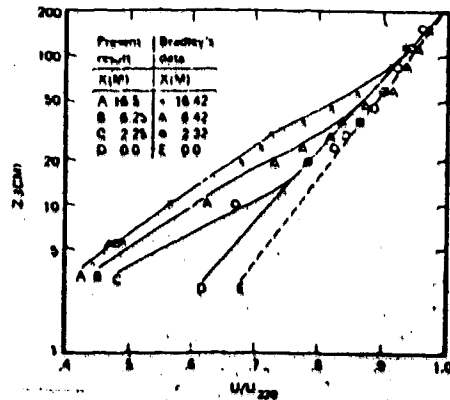
(d) Wind profiles for smooth-to-rough flow

Figure 4-4. Comparison of Bradley's observations with the model of Shir (from Shir, 1972).

The slope was larger for the smooth-to-rough transition. The height of the stress layer was about twice the height of the velocity layer, implying that the velocity adjusted more slowly than the stress. The height/fetch ratio for the stress layer was 1/10 while for the velocity layer it was 1/20.

The shear stress in the transition region was closer to the upstream value for the upper 75% of the stress layer, as pointed out by Peterson. However, if the velocity height was used, this was found to be true only for the upper 50%. The shear stress distribution was not linear, nor was it similar at different downstream distances. In the smooth-to-rough transition the shear stress was constant with height (to within 10%) for the lowest 1/10 of the layer. For the rough-to-smooth transition this was true only for the lowest 1/20 of the layer. Because the velocity profiles were logarithmic for the lowest 10% as well, this was taken as an indication of equilibrium. The height/fetch ratio was thus 1/100 for the smooth-to-rough case and 1/200 for the rough-to-smooth case, away from the discontinuity.

Peterson (1972a) has emphasized the similarities between his approach and Shir's, adding that it is difficult to judge the merits of a model using just one set of observations. In an assessment of the relative importance of the various terms in the equations Peterson (1972b) concluded that:

(a) The horizontal momentum and turbulent energy equations are essential in a physically reasonable model of the flow.

(b) The vertical momentum equation is less important.

(c) Neglect of the vertical motion terms and the continuity equation does not alter the major features of the downstream profiles.

The lack of similarity discovered by Shir has been observed in wind tunnel flow by Antonia and Luxton (1971, 1972).

4.4 An Alternative Turbulent Energy Model

The hypotheses of Glushko (Beckwith and Bushnell, 1968) have been adapted by P. A. Taylor (1972) to the atmospheric change-of-terrain problem. The mean and turbulent quantities were related by assuming:

(1)
$$\tau = K_M \frac{\partial u}{\partial z}$$

(2)
$$K_M = E^{1/2} L_G$$

where L_G is the mean scale of the turbulence given by

$$L_G = k^*(z + z_{oi})$$

and $k^* = k \, a^{1/2}$, a being the equilibrium constant stress layer value of the ratio τ/E.

(3)
$$K_E = K_M$$

(4) The dissipation is represented by

$$\epsilon = E^{3/2}/L_\epsilon$$

with the dissipation length L_ϵ given by

$$L_\epsilon = k_\epsilon^* (z + z_{oi})$$

where $k_\epsilon^* = k \, a^{-3/2}$.

The values of the constants k^* and k_ϵ^* were chosen to be consistent with a local balance of production and dissipation in the equilibrium constant stress layer where $\tau = a \, E$. Taylor used the value 0.16 for a, as suggested by Peterson. The boundary conditions on E were

$$E = u_{*1}^2 \, a^{-1} \qquad \text{at } z \geq h$$

$$\frac{\partial E}{\partial z} = 0 \qquad \text{at } z = 0$$

There is no flux of turbulent energy through the ground.

In general the results of the Glushko model were intermediate to those of the mixing-length and Peterson models. The depth of the modified region was larger than that of the Peterson model, but less than that of the mixing-length model. The inflection point in the velocity profile was present, but the change in gradient was not nearly so sharp as in the Peterson model. Figs. 4-5, 4-6, and 4-7 compare the three models (and the modified Peterson version). Details of the numerical methods are presented in Appendix B. Taylor also ran tests

with different values for a and found that larger values produced slightly more pronounced modifications, that is, larger stresses and deeper internal boundary layers.

Panofsky and Petersen (1972) found that profiles from the Risø tower in Denmark were more nearly logarithmic in the modified region than predicted by either the Peterson or Shir models. Petersen and Taylor (1972), in a later analysis of the same data, indicated that the internal boundary layer heights predicted by the Petersen model were too low. The shape of the profiles appeared to be reasonably close to that predicted by the Glushko model. Bradley's data also suggest that only a weak inflection point is present.
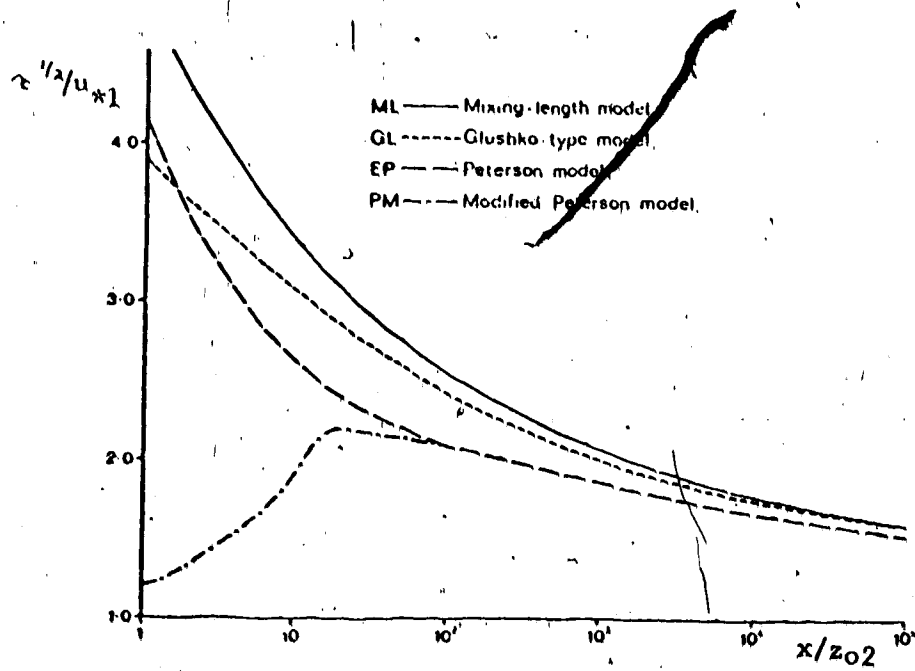
(a) Smooth-to-rough flow, $M = -5$

(b) Rough-to-smooth flow, $M = 3$

Figure 4-5. Downstream variation in friction velocity for various numerical models (from Taylor, 1972).

44

(b) Rough-to-smooth flow, $M = 3$, $x/z_{o2} = 10^4$

(a) Smooth-to-rough flow, $M = -5$

Figure 6. Comparison of velocity profiles for various numerical models (from Taylor, 1972).

z/z_{o2}

2000

1600

1200

800

400

ML

GL

PM

upstream value

τ/u_{*1}^2

(b) Rough-to-smooth, $M = 3$, $x/z_{o2} = 10^4$

τ/u_{*1}^2

z/z_{o2}

ML

GL

EP

PM
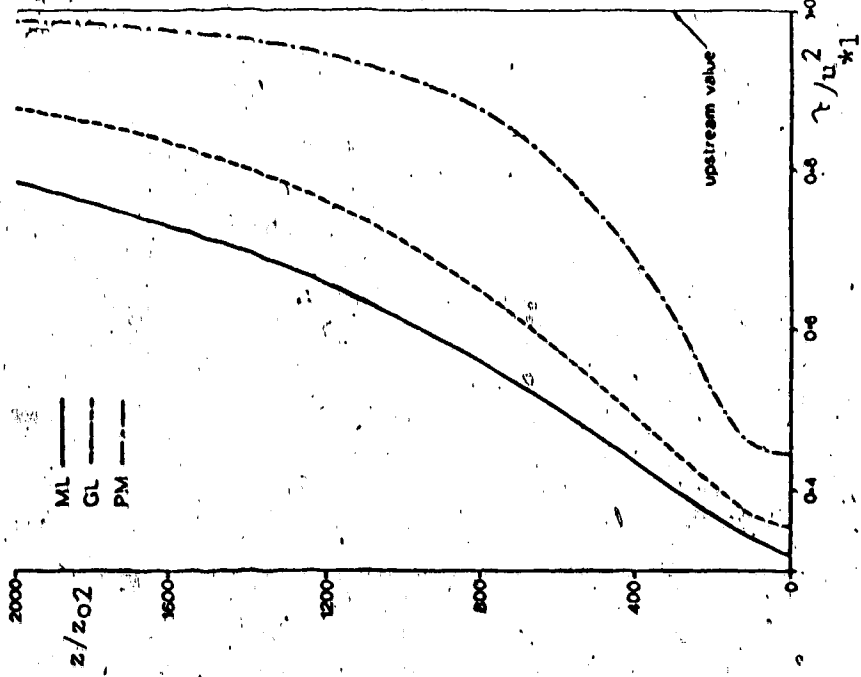
(a) Smooth-to-rough, $M = -5$, $x/z_{o2} = 10^3$
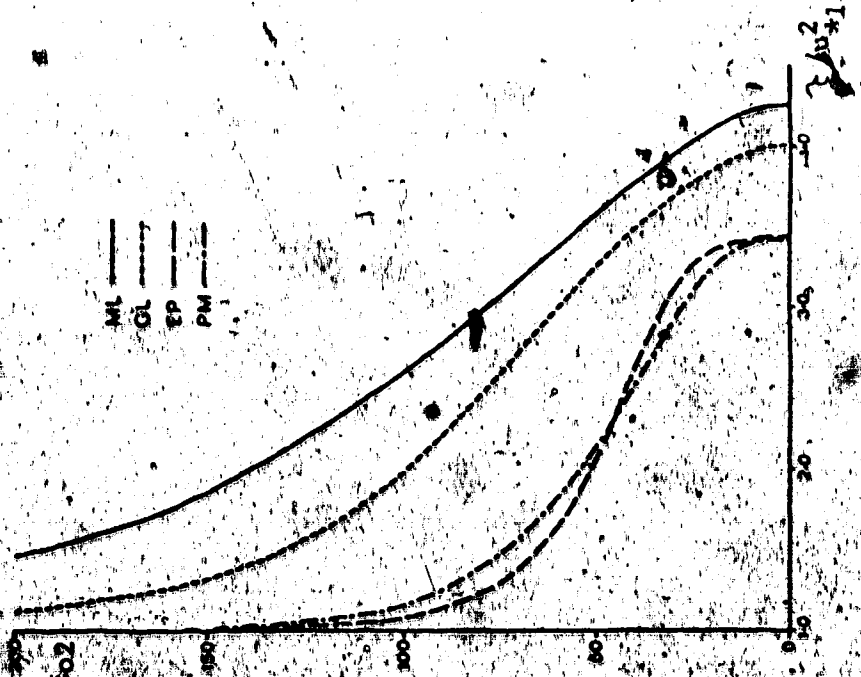
Figure 4-7. Comparison of shear stress profiles for the various models (from Taylor, 1972).

4.5 Other Numerical Work

Most other numerical investigations of the internal boundary layer problem have employed the mixing length relation and differ only in the form of the boundary conditions and equations, or in the finite difference scheme, for example Nickerson (1967). Exchange coefficient theory has been employed in numerical solutions by several Russian workers as outlined in Panchev, Donev and Godev (1971). Smith (1967) used a simple K-theory approach, neglected the terms in w, and closed the system by developing a semi-empirical equation for the rate of change of K. Since K is a measure of the turbulence, it will change because energy is fed into or removed from the mean flow during acceleration or retardation, and because the turbulence diffuses itself. Consequently, the equation proposed was of the form

$$ u \frac{\partial K}{\partial x} \qquad A K \frac{u}{u_*} \frac{\partial u_*}{\partial z} \quad + \quad K \frac{\partial^2 K}{\partial x^2} $$

where A is an empirical constant. Although the method is an over-simplification, it does serve to illustrate a different line of thought. A general technique for the calculation of all types of turbulent shear flow was presented by Nee and Kovasznay (1968). Their formulation of the equation for the rate of development of the eddy viscosity included the effects of convection, diffusion, generation of turbulence, decay of turbulence, and straining due to acceleration by pressure gradients. Such an approach could, no doubt, be used to solve the atmospheric change of terrain problem.

CHAPTER V

A MICROMETEOROLOGICAL EXPERIMENT

5.1 The Experimental Site

A site suitable for a change-of-roughness study must meet several requirements:

(1) It must be level to avoid orographically-induced vertical velocities. Such winds may have produced the anomalies described by Cameron (1970).

(2) There must be adequate fetch across a uniform surface to ensure that the flow is in equilibrium up to the maximum height of instrumentation. The appropriate height/fetch ratio is one of the things to be established in solving the change-of-terrain problem. Because it was virtually impossible to find any extensive uniform areas, estimates based on the Peterson theory were used as a guide in the selection of a site.

(3) The site must be free of large obstacles over distances several hundred times the greatest height of observation.

(4) There must be a step change to a second uniform surface in order to reproduce the two-dimensional situation for which the theories were developed.

After no little search a site which came reasonably close to fulfilling these requirements was located on the farm of Mr. Bill Perry near Chin, Alberta. A detailed map of the region is shown in Fig. 5-1. The section of land slopes downward to the north with a maximum relief of about twenty feet in a mile. The chosen site was situated at the edge of a mustard field on a fairly level area about midway down the field (east-west slope about 5 ft/mile). A uniform fetch of at least 1/6 mile (268 m) across the mustard was available in westerly (prevailing) winds. In view of the preceding theories this would be adequate for an established wind profile at the maximum anemometer height of 8 m, but it might not be sufficient for equilibrium at the 4 m height of the
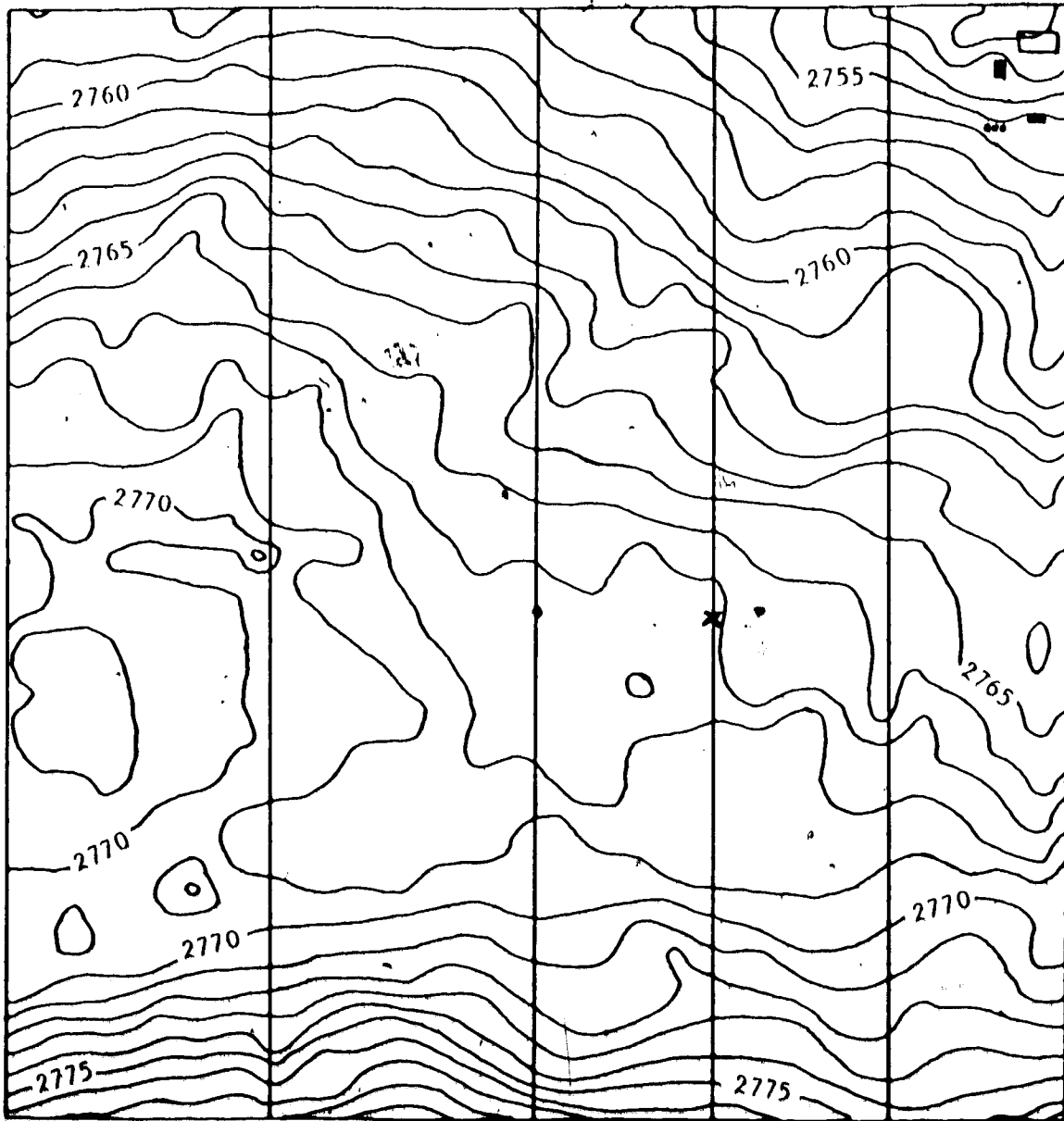
fallow   wheat   mustard   fallow   barley

■ buildings   Scale: 1 inch = 1/6 mile

▢ dugout

✕ experimental site

Figure 5-1. One-foot contours and agricultural use for the section of land on which the experimental site was located.

fast response instruments. Immediately to the west of the mustard was a wheat field extending for 1/4 mile (402 m). The crops were both about 55 cm in height, so it was expected that their roughnesses would be the same order of magnitude. Some of the empirical formulae discussed in Section 5.5 predict exactly the same values for the two roughnesses. Because the mustard was in full blossom with large flowers in addition to its rather larger leaves and stalk, it was anticipated that its roughness would be somewhat greater, as the formula of Lettau (1969) would suggest. Consequently, a small smooth-to-rough change would be present. However, with a roughness-change ratio of order one, very small modifications would occur. In fact, using a 10% criterion, the flow characteristics of the wheat and the mustard would probably be indistinguishable.

In the event of an easterly wind a uniform fetch of at least 1/6 mile (268 m) was available across the adjoining fallow. The nearest buildings were at the farmyard over 1/2 mile away, and the nearest trees were over 1 mile away.

5.2   Instrumentation

The fifty-foot main tower was erected just in from the edge of the mustard field with the booms extending outwards over the mustard (Fig. 5-2). Normally there are six such booms placed logarithmically on the tower to give instrument heights of 1/2, 1, 2, 4, 8, and 16 m. On this site the 16 m height was not employed because of inadequate fetch and the 1/2 m level could not be used because the mustard was some 55 cm high.

Mean wind speeds were measured with four RIMCO-CSIRO sensitive cup impulse anemometers. According to Sumner (1968) these 3 1/4-inch cup, low-torque anemometers have a starting speed of no more than 10 cm s^{-1} and are linear down to this speed to within 1 1/2 %. The accuracy is claimed to be ±1% and to change no more than 1/2% with extensive field use, although starting speeds may increase typically to 19 cm s^{-1}.
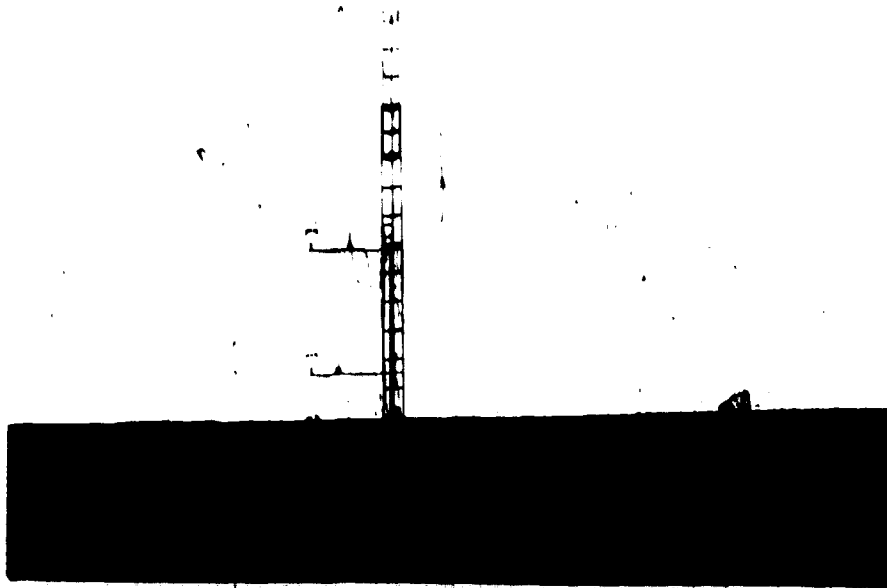
Figure 5-2. Photograph showing step change from mustard to fallow and location of main tower.

Calibrations were carried out in the University of Alberta Department of Civil Engineering Wind Tunnel, using a hot-wire anemometer and a pitot tube as standards. Similar tests were also conducted in the wind tunnel of the Defense Research Establishment at Suffield, Alberta against a secondary standard. It was found that a more realistic value for the accuracy of these particular anemometers is $\pm 5\%$ at speeds greater than 1.5 m s^{-1}. No correction was made for a possible 1% overspin in fluctuating winds (Hyson, 1972).

The vertical wind was measured with a sonic anemometer mounted on the main tower at a height of 3.66 m. Kaimal and Businger (1963) have estimated the accuracy to be $\pm 5\%$. Uncertainty in the calibration constant would raise this figure somewhat. The response time is about 0.1 s.

Heat fluxes were measured with a Fluxatron (Dyer, Hicks, and King, 1967). The propeller has a response time of about 0.4 s and the temperature sensor, 0.02 s. This instrument was mounted on a separate mast at a height of 3.66 m and was oriented to give the best exposure for the wind direction on any one test day. McBean (1972) has demonstrated that heat fluxes determined from a propeller instrument such as this could be too low by as much as 25% in near-neutral conditions.

Momentum flux was measured by the eddy correlation technique described by Hicks (1969). Random errors of about $\pm 20\%$ are expected. During the easterly winds of June 30 this vane-type shear-stress meter was mounted on a portable mast about 20 m into the fallow. During the westerly winds of July 1 it was mounted on the main tower. In both cases the height was 3.66 m. Hicks (1972) has estimated that such an instrument mounted at 5 m gives values about 8% too low. In view of the lower height used here the loss would be somewhat greater. Unfortunately the vertical propeller ceased to operate properly after the perspex retaining screw broke.

On this same mast at heights of 1 m and 2 m the two remaining RIMCO-CSIRO sensitive cup anemometers were placed. When downstream

profiles were to be taken, three of the anemomaters from the main tower were removed and mounted on this portable mast.

Data from the fast response instruments—the fluxatron, sonic anemometer, and shear stress meter— were recorded on tape by the multiplexing, digital conversion, minicomputer control system described by Honsaker, McDougall and Oracheski (1972). The mean wind was recorded by photographing electric impulse counters at 15 minute intervals.

Temperature and dewpoint sensors were also mounted on the main tower. The former failed to function properly, although this was not discovered at the time. Hourly temperatures for the test days were obtained from the nearby Lethbridge airport.

5.3 | Experimental Procedure

Two test days produced the required conditions. On the afternoon of June 30 the wind was from the northeast and complete data were obtained from 1300-1400 and 1600-2030 MDT. Near-neutral conditions prevailed on the morning of July 1 as a result of heavy overnight cloud cover and moderate westerly winds. From 0640-0805 MDT ten-minute wind profiles consisting of 5 levels up to 8 m were taken at distances of 10, 20, and 30 m downwind from the mustard-fallow boundary. Near-neutrality was confirmed by the heat flux measurements at 0800 which gave a value for the Monin-Obukhov length of -770 m. Complete fast-response data were obtained from 1300-1600 MDT. In the afternoon near-neutral conditions once again prevailed (Monin-Obukhov length $L = -900$ m). Ten-minute downstream profiles were again taken for the period 1626-1712 MDT. Unfortunately, the wind had shifted to 320-330°, so that a two-dimensional situation was no longer present; effective fetches of 22, 32, and 47 m were obtained. Uncertainty in the estimated wind direction could mean that these distances are in error by as much as ±15%.

5.4 Calculation of the Wind Profile Parameters

In neutral conditions it is generally accepted (for example, Lumley and Panofsky, 1964, p. 103) that the wind profile is given by

$$u = (u_*/k) \ln z/z_o \qquad z > z_o$$

where the symbols have the same meanings as before.

When the surface is very rough, an additional parameter, the zero-plane displacement d, is often introduced so that the equation becomes

$$u = (u_*/k) \ln (z-d)/z_o \qquad z > d + z_o$$

(for example, Munn, 1966, p. 59).

Since its introduction by Rossby and Montgomery (1935) there has been considerable controversy over the exact role of the displacement d. Munn (1966, p. 59) stated that the modification is empirical and provides a better fit for experimental data. Pasquill (1962, p. 71) claimed that it allows for the virtually stationary layer of air trapped within the roughness elements. Sutton (1953, p. 239) qualified it as applicable only for large roughness elements that are uniform in height and distribution, in which case it is to be regarded as a datum level above which normal turbulent exchange takes place. He pointed out that if both z_o and d are regarded as independent arbitrary constants, then the profile containing them cannot be derived from the first-order differential equation in the usual fashion. Sellers (1965, p. 150) asserted that because observed values are so variable and random, no real physical significance can be attached to the zero-plane displacement. He went on to say that in most cases the profile could just as well be described without the introduction of the parameter d. Lumley and Panofsky (1964, p. 103), Geiger (1965, p. 274) and others interpreted the zero-plane displacement as a shift in the origin of the z-axis because a vegetation cover produces an effective surface above the solid ground, the wind going to zero at $z = z_o + d$. Lettau (1969) identified d with the corrective height increment between the mathematically defined zero plane and the arbitrary datum level from

which an observer has measured anemometer heights. Monin and Yaglom
(1971, p. 293) derived the profile containing d formally, by treating it
as a translation of the zero level for the vertical axis. They regarded
it as being analogous to the displacement thickness in boundary layer
theory.

Given a set of wind observations at different levels under
neutral stability, the three parameters u_*, z_0, and d can be evaluated
using the method of least squares outlined by Robinson (1962). However,
steady adiabatic conditions are infrequent; neutrality is most often a
transient state occurring between night-time stability and day-time
instability of the surface boundary layer over land. Usually the
parameters must be determined from winds observed during unstable condi-
tions. A general diabatic profile is given by Lumley and Panofsky (1964,
p. 113) as

$$u = (u_*/k)\left[\ln\,(z-d)/z_0 - \gamma(f)\right]$$
()

where γ, a function representing the diabatic influence, is given by

$$\psi = \int_0^f \frac{1-\phi(f)}{f}\,df$$

where ϕ is the non-dimensional shear, and f is either z/L or z/L'
depending on whether heat flux or temperature gradient is available.
The Monin-Obukhov length is given by

$$L = -u_*^3\,c_p\,\rho T/kgH$$

where c_p is the specific heat at constant pressure, ρ is the density of
air, T is the mean air temperature, k is von Karman's constant, H is the
heat flux, and g is the acceleration due to gravity. The related length
L' was introduced by Panofsky (1963) as

$$L' = 4\,\frac{\partial u}{\partial z}\,T^{\frac{3}{2}}/g k\,\frac{\partial \theta}{\partial z}$$

where θ is potential temperature. Therefore $L' = K_H/K_M\,L$, where
K_H is the turbulent transfer coefficient for heat and K_M is the turbulent

transfer coefficient for momentum. Both parameters are related to the Richardson number,

$$Ri = \frac{g}{T} \frac{\partial \Theta}{\partial z} \Big/ \left(\frac{\partial u}{\partial z}\right)^2$$

such that $z/L' = Ri\,\phi$.

An equation which interpolates between neutral stability and free convection has been advanced by a number of authors (Lumley and Panofsky, 1964, p. 110), namely,

$$\phi^4 - \gamma \frac{z}{L'} \phi^3 = 1.$$

where γ is an empirical constant.

Substitution of $\phi = (z/L')/Ri$ yields

$$\frac{z}{L'} = \frac{Ri}{(1 - \gamma Ri)^{1/4}}$$

and elimination of z/L' gives

$$\phi = (1 - \gamma Ri)^{-1/4}$$

This is the so-called KEYPS formula. The value of γ is usually determined by numerical integration. An alternative formulation by Webb (Panofsky, 1963) involves a two-part explicit function for γ.

Paulson (1970) provided a mathematical representation for γ by integrating the analytical expression for the non-dimensional shear obtained under the Businger-Dyer hypothesis that $z/L = Ri$. This hypothesis was based on the Kerang observations (Swinbank, 1964) and has also been suggested by Pandolfo (1964). An immediate consequence is that $K_H/K_M = 1/\phi$. Hence the ratio is one in neutral conditions and increases with decreasing stability, in agreement with a suggestion by Priestley and Swinbank (1947). It also helps to account for the disparity of reported values for K_H/K_M (Lumley and Panofsky, 1964, p. 105). With

$$\phi = (1 - \gamma \frac{z}{L})^{-1/4}$$

the diabatic influence function becomes

$$\psi = 2 \ln \left[\frac{1+r}{2} \right] + \ln \left[\frac{1+r^2}{2} \right] - 2 \tan^{-1} r + \frac{\pi}{2}$$

where $r = (1 - \gamma z/L)^{1/4}$.

This implies that for $-z/L$ large u varies asymptotically as $z^{-1/4}$ in contrast to KEYPS where $u \propto z^{-1/3}$. From analysis of the Kerang data Paulson found the value for γ to be 16.

Using this representation, the wind profile parameters were computed by the method of Stearns (1970). The roughness and displacement height are determined so that the sum of error squares between the observed and calculated wind speeds is a minimum. The friction velocity is treated implicitly as a function of d and z_0. If ε_i is the error between the measured wind speed and the theoretical wind speed at height z_i then

$$\varepsilon_i = u_i - (u_*/k) \left[\ln \frac{z_i - d}{z_0} - \psi_i \right]$$

The least-squares method requires that $\sum_{i=1}^{N} \varepsilon_i^2$ be a minimum for the N measurement levels, that is,

$$\frac{\partial}{\partial z_0} \left(\sum_{i=1}^{N} \varepsilon_i^2 \right) = 0 \quad \text{and} \quad \frac{\partial}{\partial d} \left(\sum_{i=1}^{N} \varepsilon_i^2 \right) = 0$$

Setting

$$Z_i = \ln \frac{z_i - d}{z_0} - \psi_i$$

$$u_* = \frac{k}{N} \sum_{i=1}^{N} \frac{u_i}{Z_i}$$

$$\sum_{i=1}^{N} \varepsilon_i^2 = \sum_{i=1}^{N} \left[u_i - \frac{u_*}{k} Z_i \right]^2$$

the condition for a minimum with respect to z_0 requires that

$$GZ \equiv \sum_{i=1}^{N} \left[(k u_i - u_* Z_i)(Z_i \frac{\partial u_*}{\partial z_0} + u_* \frac{\partial Z_i}{\partial z_0}) \right] = 0$$

and the condition for a minimum with respect to d requires that

$$GD \equiv \sum_{i=1}^{N} \left[(k u_i - u_* Z_i)(Z_i \frac{\partial u_*}{\partial d} + u_* \frac{\partial Z_i}{\partial d}) \right] = 0$$

where

$$\frac{\partial u_*}{\partial z_0} = \frac{k}{N} \cdot \sum_{i=1}^{N} (u_i / Z_i^2) \frac{\partial Z_i}{\partial z_0}$$

$$\frac{\partial Z_i}{\partial z_0} = \frac{1}{z_0}$$

$$\frac{\partial Z_i}{\partial d} = \frac{1}{z_i - d} - \frac{\partial \psi}{\partial d}$$

$$\frac{\partial \psi_i}{\partial d} = \frac{x}{2L}\left[r^{-3}\left(1+r^{-1}\right) + r^{-2}\left(1+r^2\right)^{-1} - r^{-1}\left(1+r^2\right)^{-1} \right]$$

Successive approximations to z_o and d were obtained using the secant method. With an initial estimate for d and u_* two guesses were made for z_o and approximations were obtained from

$$z_o(n+2) = \frac{z_o(n)\, GZ(n+1) - z_o(n+1)\, GZ(n)}{GZ(n+1) - GZ(n)}$$

until the difference between successive approximations was less than 0.01 cm. This value for z_o together with d(1) and a corrected u_* were then used to compute GD(1). A second guess d(2) was made, and the procedure repeated to obtain a value for GD(2). Successive estimates for d were then obtained from

$$d(n+2) = \frac{d(n)\, GD(n+1) - d(n+1)\, GD(n)}{GD(n+1) - GD(n)}$$

until the difference was less than 0.1 cm.

The wind-profile parameters for the mustard were computed from twenty hourly-wind averages taken at four levels on July 1. For the fallow, d was assumed to be zero and the parameters were computed from twenty hourly-wind averages recorded at the two levels on the portable mast on June 30. The data are displayed in Appendix A.

The value of u_* under neutral conditions can be related to the mean wind at some level by means of a drag coefficient, namely, $c_d = u_*/u_1$, where c_d is the drag coefficient, and u_1 is the wind at 1 m. Bradley (1972) has shown that even in unstable conditions, such a relationship still holds for low levels, in keeping with the commonly-held view that neutral conditions always prevail at sufficiently low heights.

The results of the computations appear in Table 5-1. The roughness ratio for the site is thus m = 12:1 and the roughness-change parameter is M = 2.5.

Table 5-1. Results based on twenty hourly-profiles.

Surface	Roughness		Displacement		Drag Coefficient	
	z_o	s.d.	d	s.d.	c_d	s.d.
	(cm)	(cm)	(cm)	(cm)		
mustard	12	1.6	15	3.7	0.204	0.008
fallow	1.0	0.12	0	---	0.091	0.004

Table 5-2. Some values for the zero-plane displacement of mustard 55 cm high and similar crops.

Value (cm)	Circumstances	Source
15	mustard 55 cm high	observed at Chin, Alberta
55	$d = h_c$, from models in a wind tunnel	Plate and Quraishi (1965)
27-55	$h_c/2 \leq d \leq h_c$	Monin and Yaglom (1971)
10	grass 50 cm high	Taylor (1962)
25	grass 60-70 cm high	Deacon (Geiger, 1966, p. 274)
30	grass 60-70 cm high	Calder (Sutton, 1953, p. 240)
55	$d = h_c$, for field crops	Paeshke (ibid., p. 239)

5.5 Appraisal of the Computed Parameters

Values for the displacement height are not plentiful in the literature, but some empirical formulae do exist. Sutton (1953, p. 239) quoted Paeshke's result for dense crops that d is equal to the average of the measured heights of the roughness elements. Plate and Quraishi (1965) found for model crops in a wind tunnel that to a good approximation $d = h_c$ where h_c is the height of the crop. Both experiments also indicated that the velocity profile is logarithmic only for $z > 2h_c$; so-called 'canopy flow' governed by the nature of the individual roughness elements occurs below this height. Taylor (1962) chose a value of $d = 1/5 \, h_c$ for long grass 50 cm high. Plate (1971, p. 29) stated that in general d will differ from h_c when the density of the roughness elements is sparse. In the limit the flow may not be fully rough and special investigation is necessary. Geiger (1966, p. 274) asserted that d is not equal to the average height of the vegetation surface and that only an examination of the wind profile can determine the value of d which will best satisfy the equation. Geiger also quoted some results of Deacon where a displacement of 25 cm was used for long grass 60-70 cm high, that is, $d = 2/5 \, h_c$. Monin and Yaglom (1971, p. 294) took d to be zero for low vegetation and suggested the range $h_c/2 \leq d \leq h_c$ for high vegetation.

Geiger attributed this wide range of values to the high degree of pliability of the plant stalks. Rauner (Munn, 1966, p. 161) found that as the wind speed increased over a forest the value of d decreased from $h_c/2$ to $h_c/4$.

The value obtained for the mustard was 15 cm. Even though the wind speed at 1 m was quite steady at 2-2 1/2 m s^{-1} a rather large standard deviation of 4 cm was found. The ratio d/h_c for the mustard was 3/11 or 0.28. This was lower that most estimates, but higher than that of Taylor (1962). A comparison of values computed from empirical formulae and those reported by various workers for similar crops is given in Table 5-2.

No micrometeorological studies appear to have been done over mustard; there are no published values for the roughness. There are, however, once again a number of empirical formulae. Plate and Quraishi (1965) found that for crop-like elements in a wind tunnel $z_0 = 0.15\ h_c$, in agreement with the field work of Paeshke (Plate, 1971, p. 27). According to Sellers (1965, p. 150) Tanner and Pelton, Kung, and others have used relationships of the form

$$\log r_0 = \log a + b \cdot \log h_c$$

that is $\quad r_0 = a\ h^b$

where a and b are empirical constants. Values of b between 0.99 and 1.42 have been employed and values of log a ranging from -1.4 to -0.88. Plate (1971, p. 29) objected to an equation of this form because it is not dimensionally consistent. Monin and Yaglom (1971, p. 294) recommended that $h_c/10 \le z_0 \le h_c/5$, noting that the constant of proportionality is considerably greater than the value 1/30 for Nikuradse's sand roughness. They attributed the variability of estimates for both d and z_0 to the fact that both parameters depend on fairly fine details of surface structure. Natural vegetation, even of one type, is not likely to have identical structure in different places around the world.

Lettau (1969) held that the use of only the height in a roughness formula is too restrictive and produces oversimplified results. The shape and spacing of the roughness elements must also be considered. On the basis of the bushel basket experiments he proposed the relation

$$z_0 = 0.5\ h_c\ s/S$$

where s is the silhouette area of the average obstacle, that is, the cross-sectional area 'seen' by the wind in an approach to a typical roughness element; S is the specific area or lot area, that is, the average area on the earth's surface occupied by a single roughness element. If N elements are located on a site of area A, then $S = A/N$.

The factor 0.5 corresponds to the average drag coefficient of the characteristic element. Lettau considered estimates from this formula to be within ±25%. Its validity is restricted to situations where $R < S$; otherwise serious overestimation occurs.

Table 5-3 gives a comparison of the value obtained for the mustard (12 cm) with values for similar crops reported in the literature, and with values computed from the various formulae. Table 5-4 shows values for the fallow.

5.6 The Downstream Profiles

The profiles observed during the morning and afternoon runs of July 1 are shown in Fig. 5-3. The velocities were scaled with respect to the wind at the highest observation level of 8 m, which is outside the modified region for all fetches according to the Elliot theory. The uppermost points of each profile lie on the line characteristic of the upstream flow, except the 4 m point at 10 m fetch which seems to be somewhat in error. The acceleration of the flow at increasing distances appears as a shift to higher speeds in the lower portion of the profiles. The number of points lying on the upstream profile decreases with distance. Qualitatively, these features are similar to those observed by Bradley (1968).

The height of the internal boundary layer cannot be well defined by so few points, so direct comparison with predictions from the various theories has not been attempted. The surface friction velocities scaled with respect to the upstream value were computed from the 1/2 m wind speed by means of a drag coefficient similar to that described in Section 5.5. Assuming that the 1/2 m wind is in the portion of the profile characteristic of the new surface

$$u(1/2 \text{ m}) = (u_*/k) \ln 50/1$$

$$u_{*2} = c_{d2} \, u(1/2 \text{ m})$$

Table 5-3. Some values for the roughness of mustard 55 cm high and similar crops.

Value (cm)	Circumstances	Source
12	mustard 55 cm high	observed at Chin, Alberta
8	$z_o = .15 \, h_c$, from models in a wind tunnel	Plate and Quraishi (1965)
22	wheat 60 cm high	Penman and Long (Sellers, 1965, p. 151)
11-15	grass 60-70 cm high	Deacon (ibid.)
10.5	$z_o = h_c^{1.2}/12$	Lettau (1967)
5.5-11	$h_c/10 \leq z_o \leq h_c/5$	Monin and Yaglom (1971)
6-9	long grass 60-70 cm high	Priestly (1959, p. 21)
9	thick grass up to 50 cm	Sutton (1953, p. 233)
4-5	high grass, wheat	Hess (1959, p. 277)
4-9	long grass 60 cm high	Pasquill (1962, p. 72)
14	fully grown root crops	ibid.
4-12	tall grass, grain	Geiger (1966, p. 275)
3	grass 60-70 cm high	Calder (Sutton, 1953, p. 240)
14	roughness element formula ($s \sim 20$ cm^2, $S \sim 40$ cm^2)	Lettau (1969)

Table 5-4. Some values for the roughness of fallow and similar terrain.

Value (cm)	Circumstances	Source
1.0	fallow with some trash	observed at Chin, Alberta
2.1	fallow field	Hess (1959, p. 277)
0.6-2.0	prairie grass, countryside	Geiger (1966, p. 275)
0.2-2.5	mown grass 1.5-4.5 cm high	Priestly (1959, p. 21)
0.7-2.3	downland, thick grass up to 10 cm high	Sutton (1953, p. 233)
0.5	short grass	Calder (ibid., p. 240)
1.7	grassy surface	Plate (1971, p. 27)
2.1	flat country	ibid.
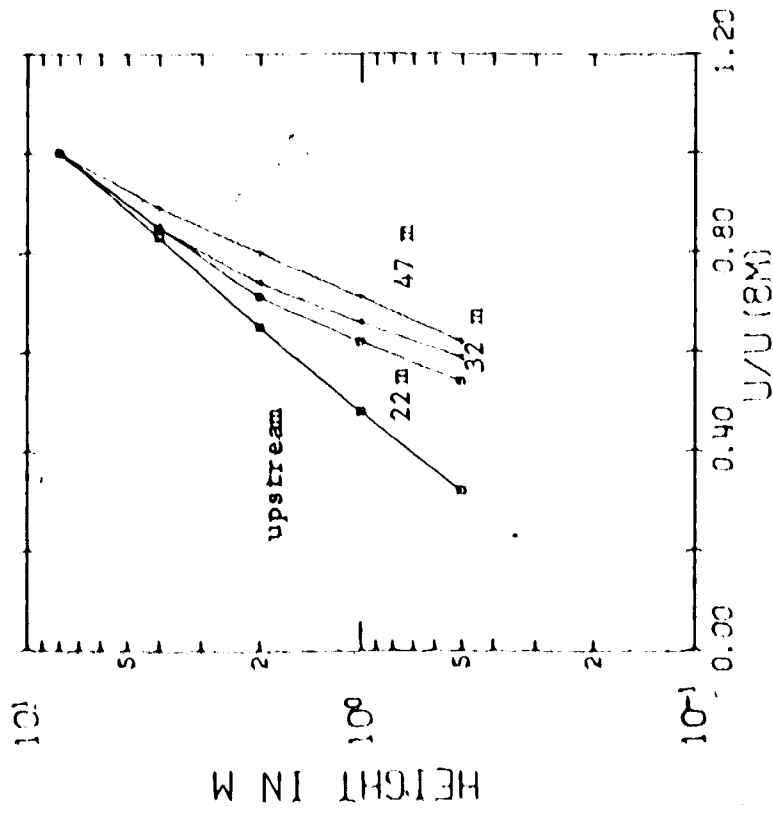
Figure 5-3. Velocity profiles observed at Chin, Alberta.

(a) Morning run

(b) Afternoon run

where $c_{d2} = k/\ln 50/1$

The wind at 8 m is characteristic of the upstream flow,

$$u(8 \text{ m}) = (u_{*1}/k) \ln (800/12)$$

assuming negligible streamline displacement.

$$u_{*1} = c_{d1} u(8 \text{ m})$$

where $c_{d1} = k/\ln (800/12)$

Hence

$$u_{*2}/u_{*1} = (c_{d2}/c_{d1})[u(1/2 \text{ m})/u(8 \text{ m})].$$

Figure 5-4 compares values of the friction velocity computed in this way
with three analytical solutions. Figure 5-5 does the same for three
numerical solutions. Details of the computational schemes are in
Appendix B. The initial overshoot was greater and the recovery was
rather more rapid than predicted by any of the theories. At larger
fetches the Glushko model seems to be in closest agreement with the data.
Extrapolation of the curve through the observed points suggests that the
Peterson model might come into closer accord at greater downwind distances.

To facilitate direct comparison of the observed velocity profiles
with the results of the various theories, a transformation was employed
to scale the speeds with respect to the upstream friction velocity,

$$u/u_{*1} = [u/u(8 \text{ m})][u(8 \text{ m})/u_{*1}]$$

The first factor is the observed value and $u(8 \text{ m})/u_{*1}$ can be calculated
because the 8 m wind is characteristic of the upstream flow, that is,

$$u(8 \text{ m})/u_{*1} = (1/k) \ln (800/12)$$

Comparisons of the observed profiles with those predicted by the various
theories are shown in Figs. 5-6 through 5-17. All of the theories
overestimate the speeds at the shorter fetches. One reason for this
lies in the zero-plane displacement associated with the mustard. No
theory takes into account the possible effects of such a displacement
on the flow modification. At 10 m downwind from the discontinuity the
flow had not yet descended fully onto the fallow; this is indicated by
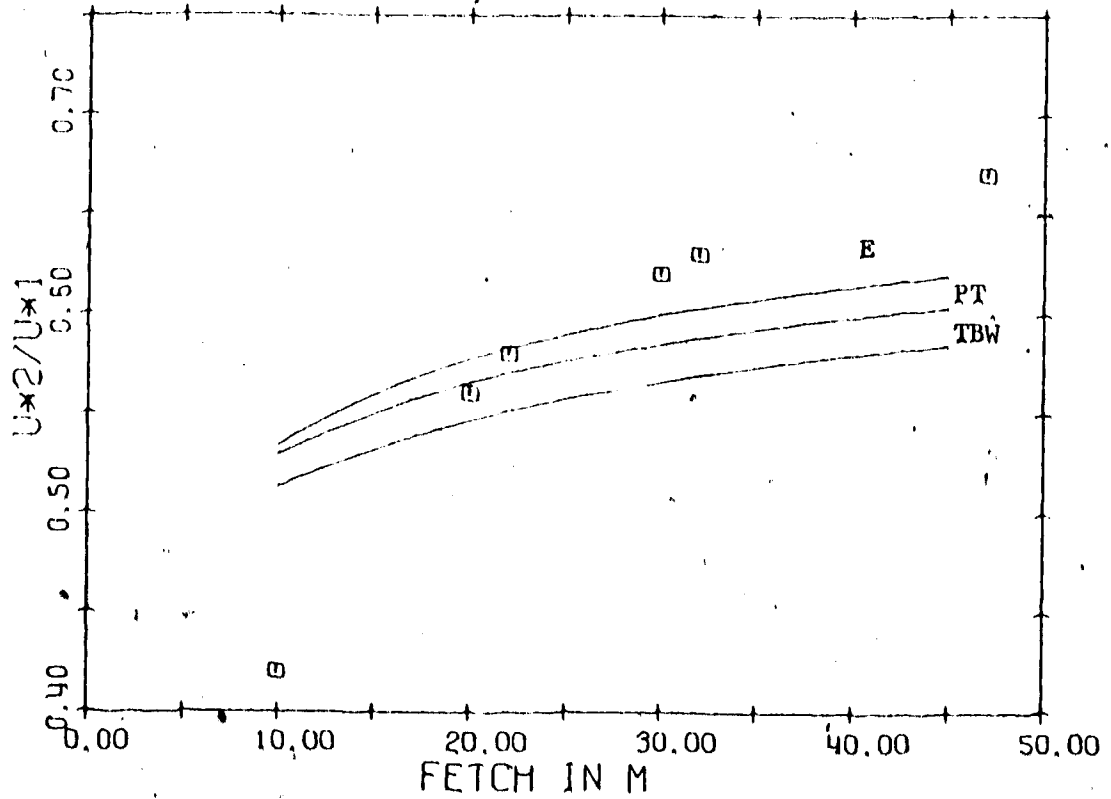
E   Elliot
PT   Panofsky-Townsend
TBW Townsend as revised by Blom and Wartena
ω   observed

Figure 5-4. Downwind variation of surface friction velocity inferred
from the wind at 1/2 m compared with three analytical
solutions.
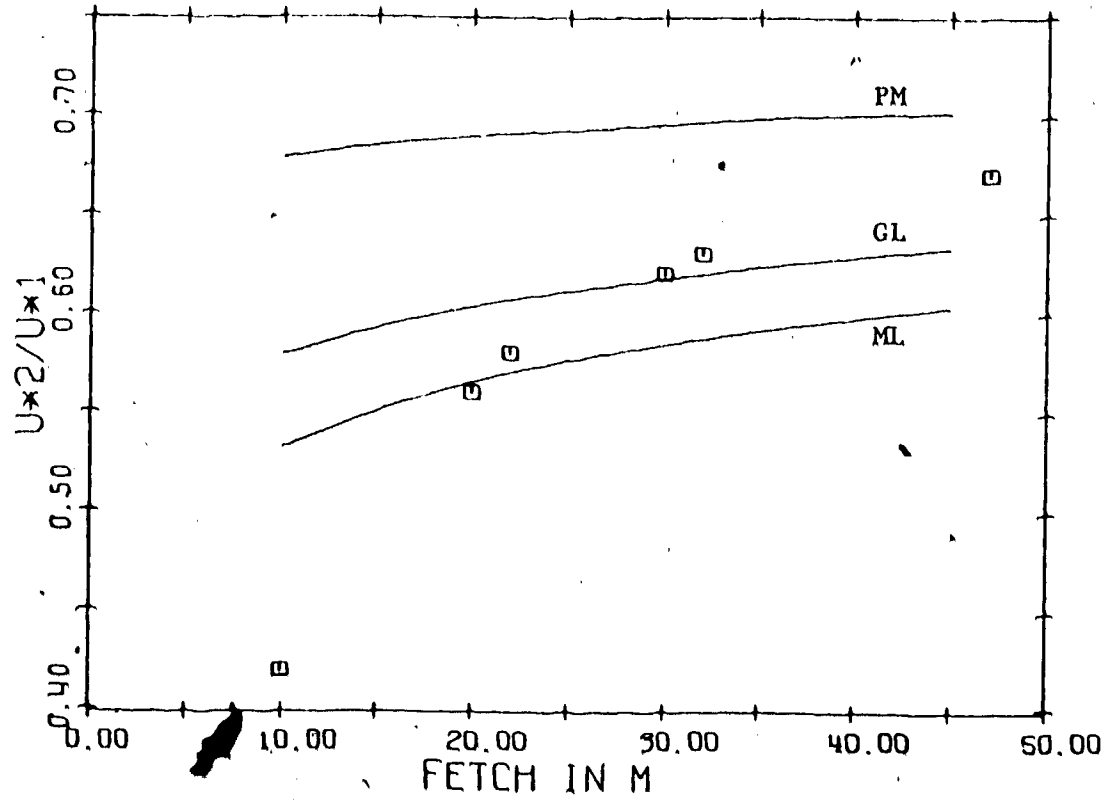
```
PM    modified Peterson
GL    Glushko.
ML    mixing-length
□     observed
```

Figure 5-5. Downwind variation of surface friction velocity inferred from the wind at 1/2 m compared with three numerical solutions.
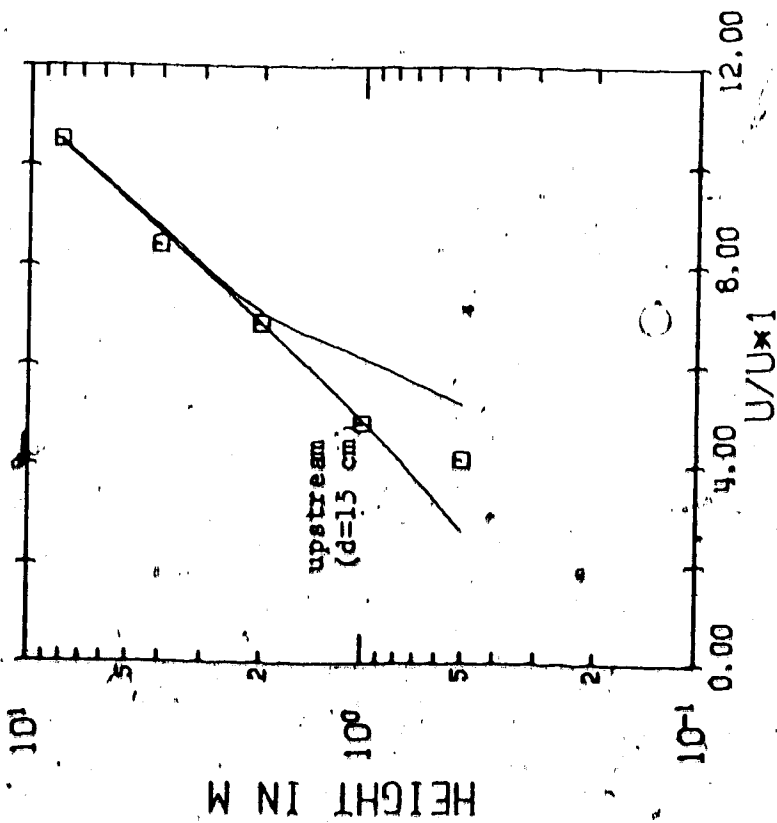
(a) Fetch 10 m, upstream profile with zero-plane displacement
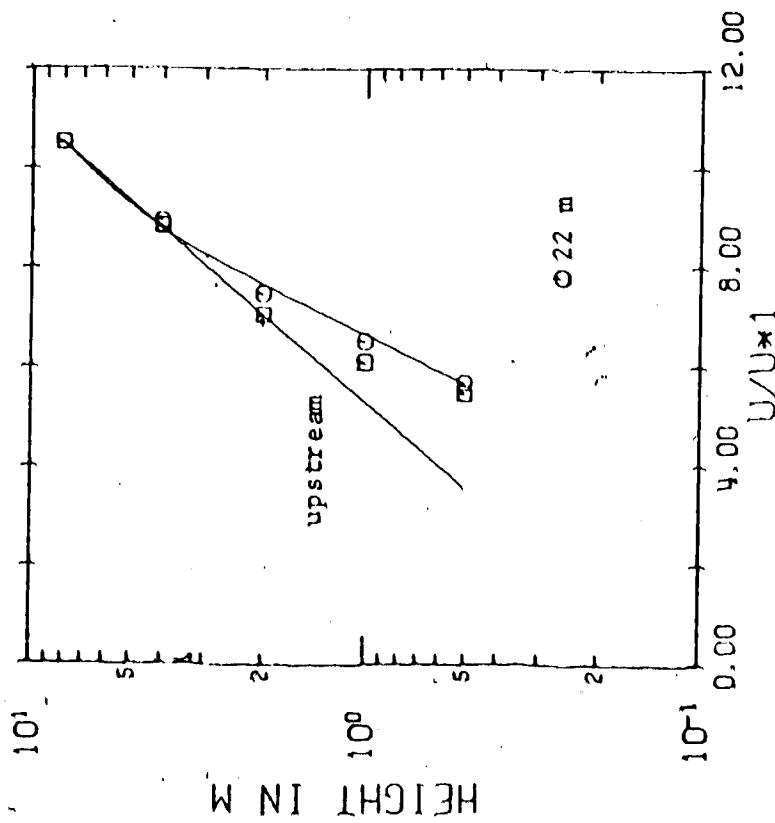
(b) Fetch 20 m

Figure 5-6. Observed wind profiles compared with theory of Elliot.
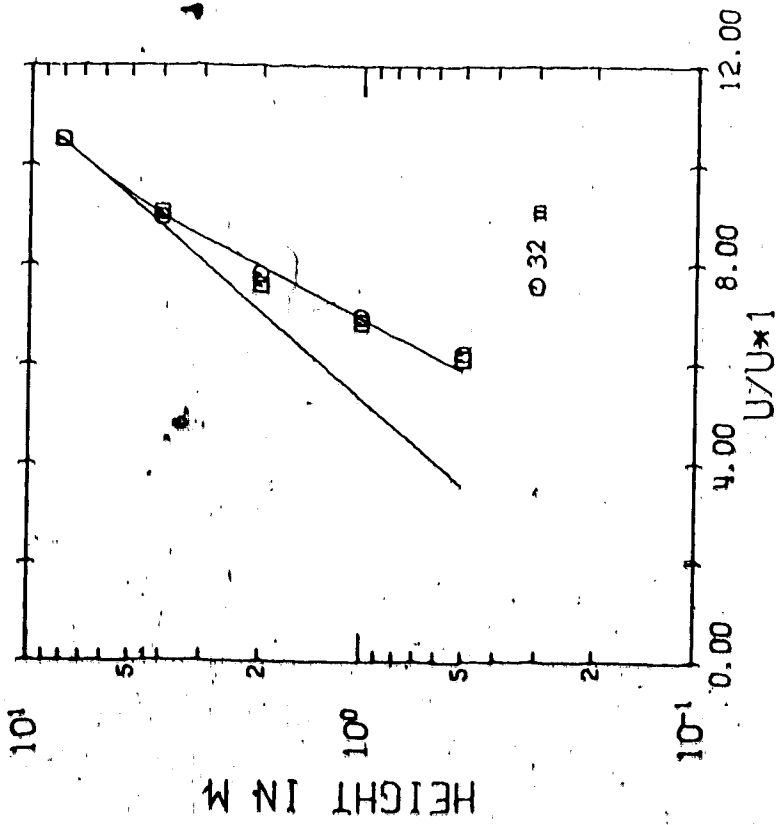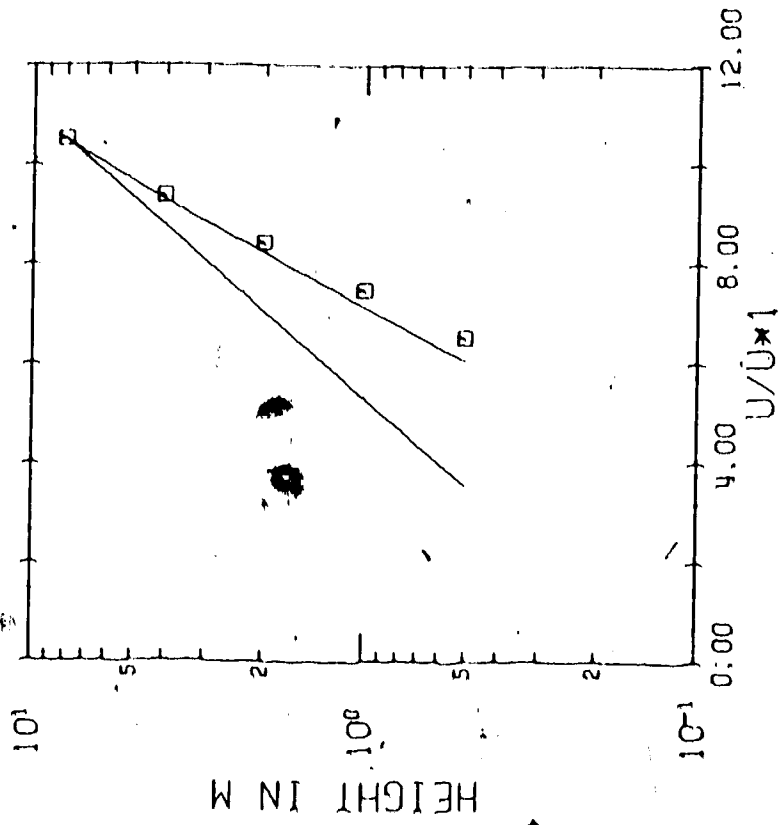
(b) Fetch 47 m

(a) Fetch 30 m

Figure 5-7. Observed wind profiles compared with theory of Elliot.

69
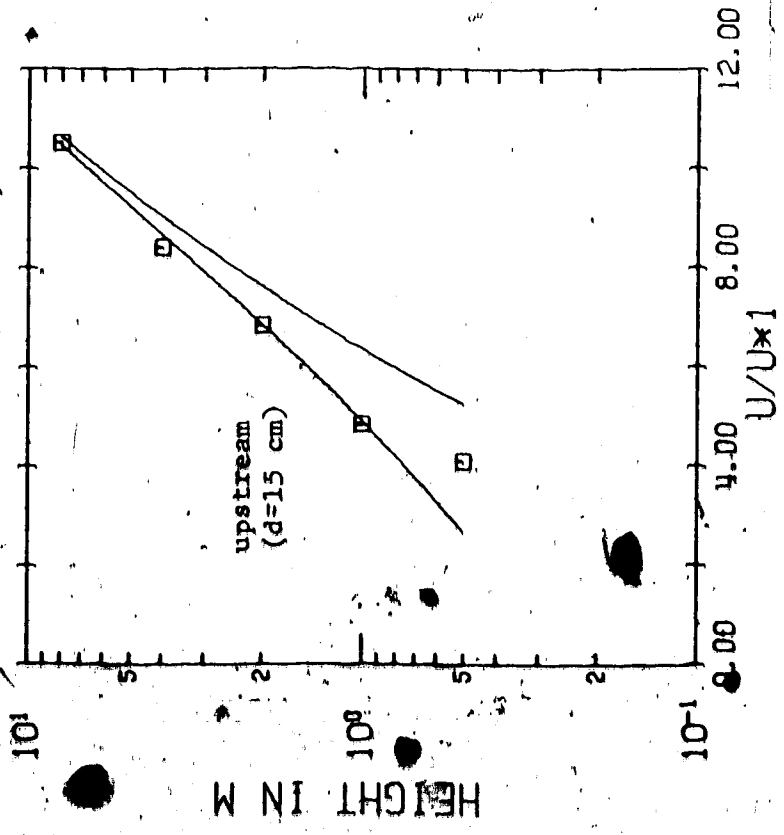
(b) Fetch 20 m

(a) Fetch 10 m, upstream profile with
zero-plane displacement
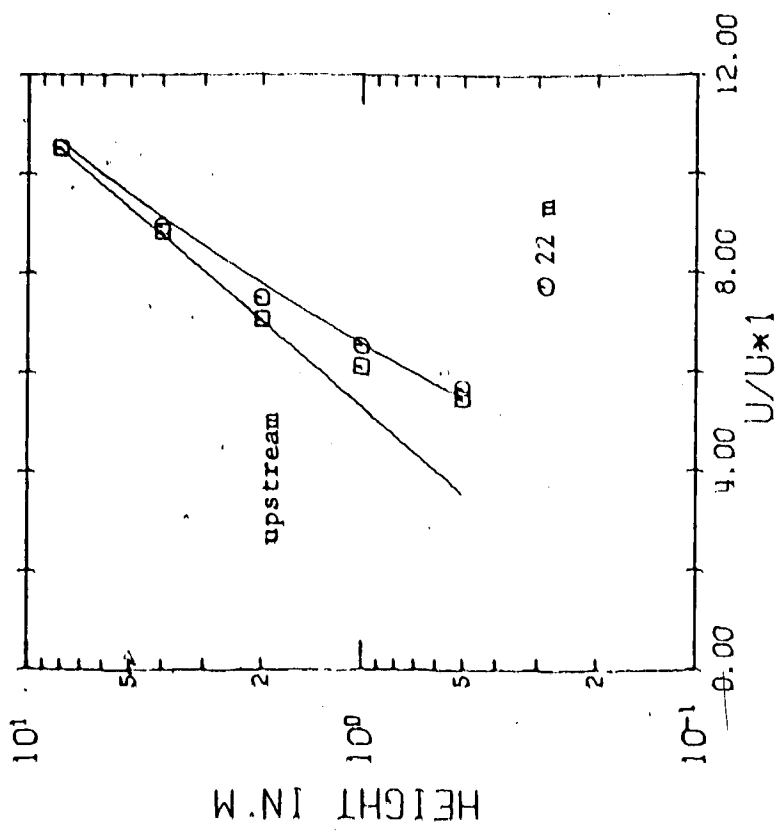
Figure 5-8. Observed wind profiles compared with the theory of Panofsky and Townsend.
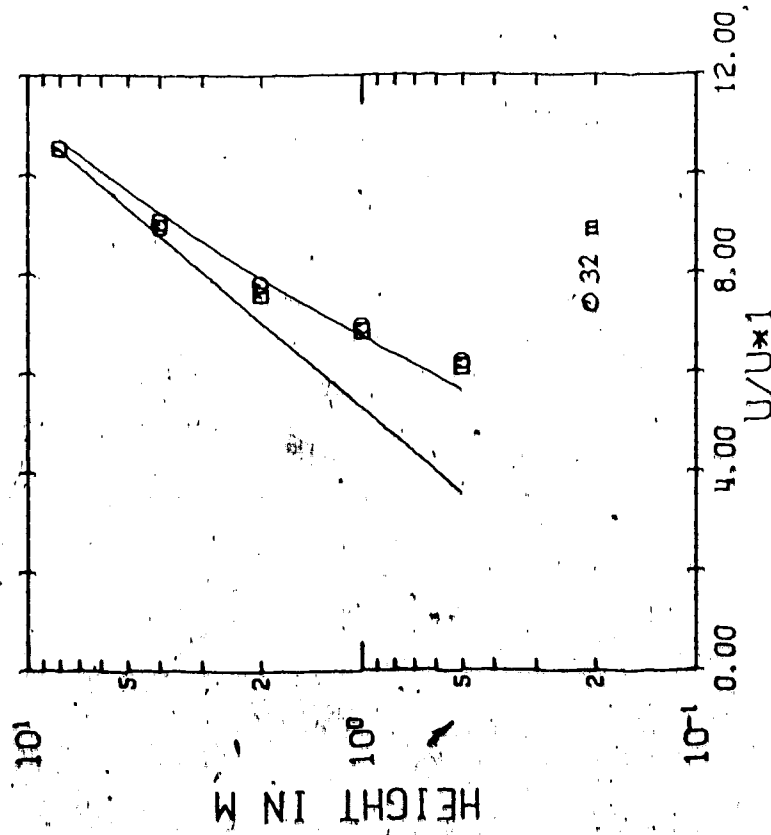
(b) Fetch 47 m

(a) Fetch 30 m

Figure 5-9. Observed wind profiles compared with the theory of Panofsky and Townsend.
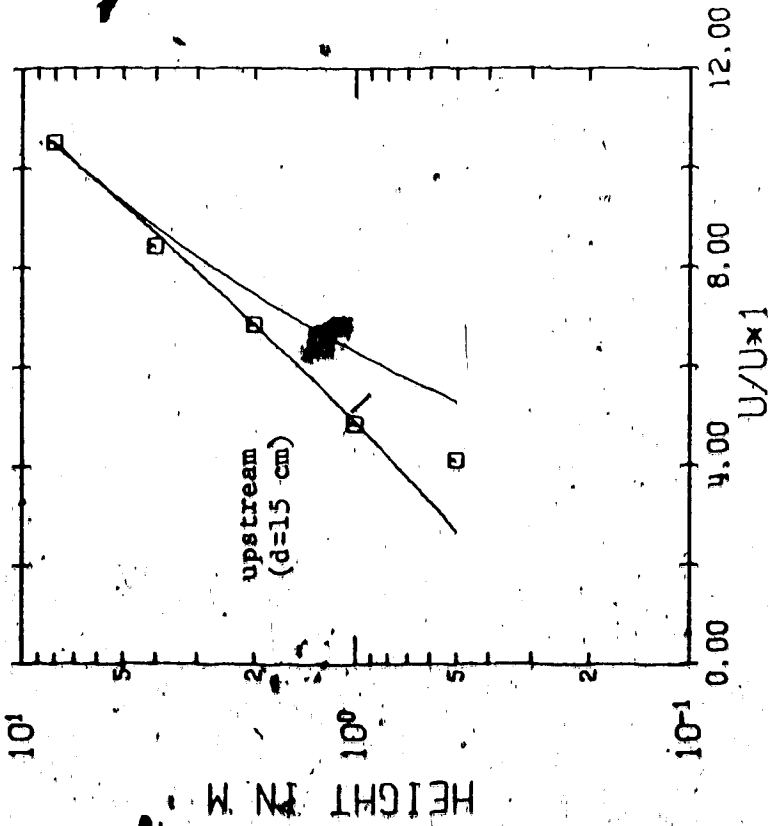
(a) Fetch 10 m, upstream profile with
zero-plane displacement
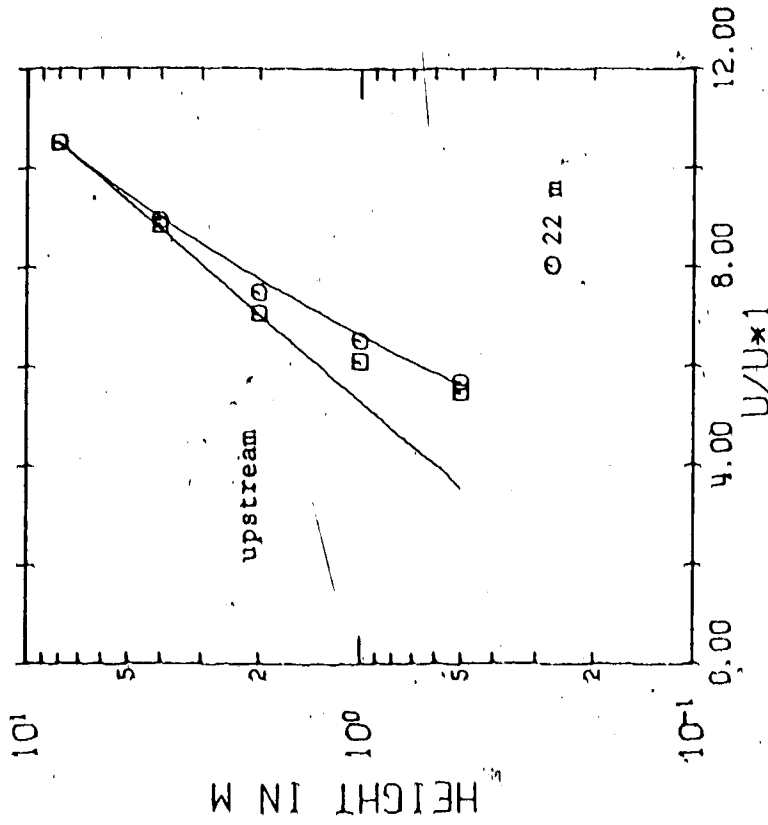
(b) Fetch 20 m

Figure 5-10. Observed wind profiles compared with theory of Townsend as revised by Blom and Wartena.
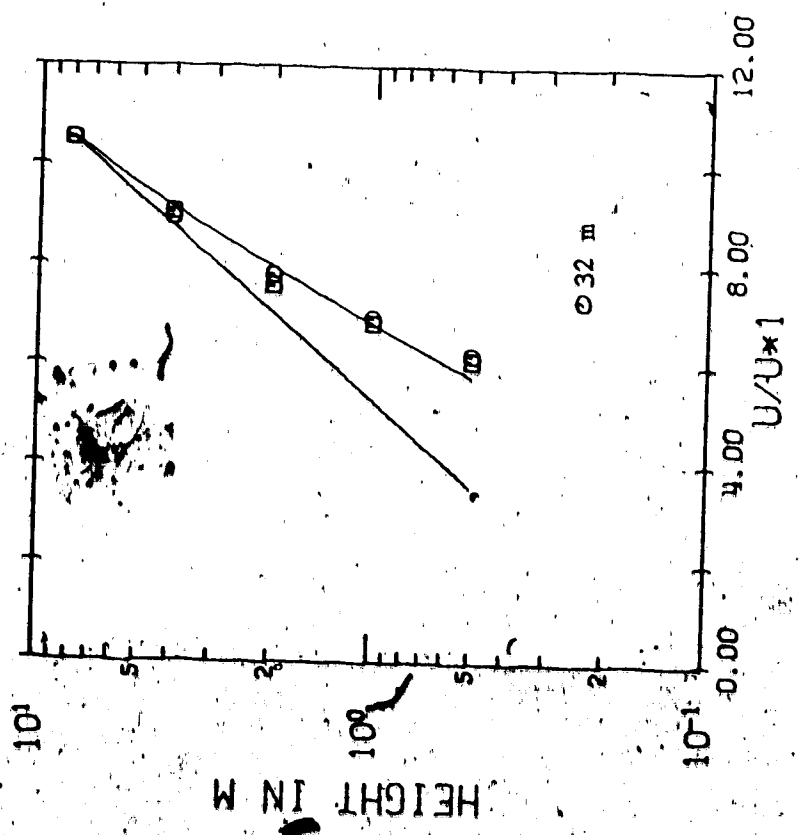
(b) Fetch 47 m

(a) Fetch 30 m

Figure 5-11. Observed wind profiles compared with theory of Townsend as revised by Blom and Wartena.
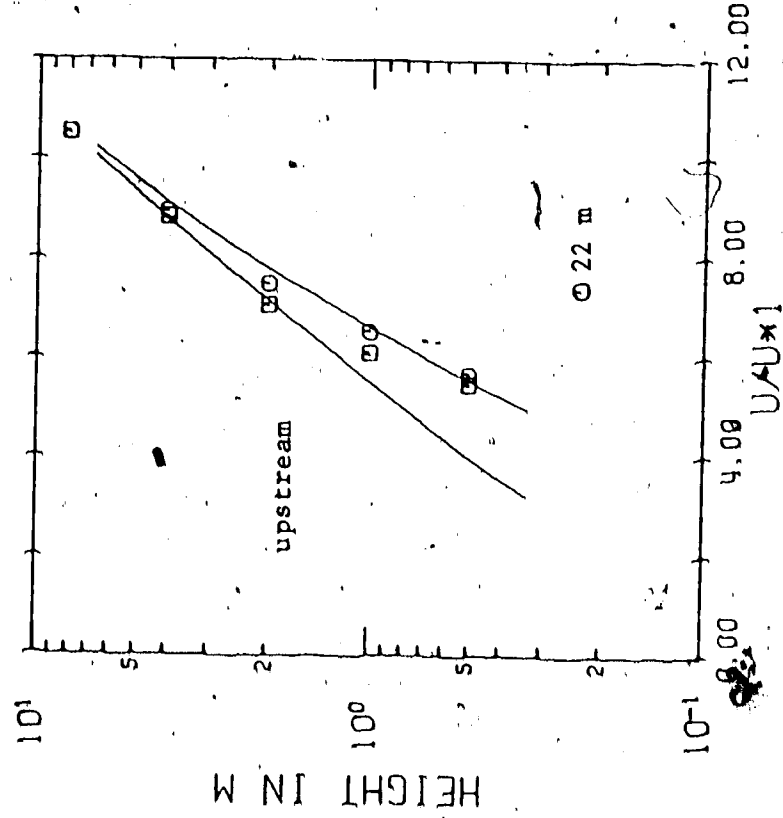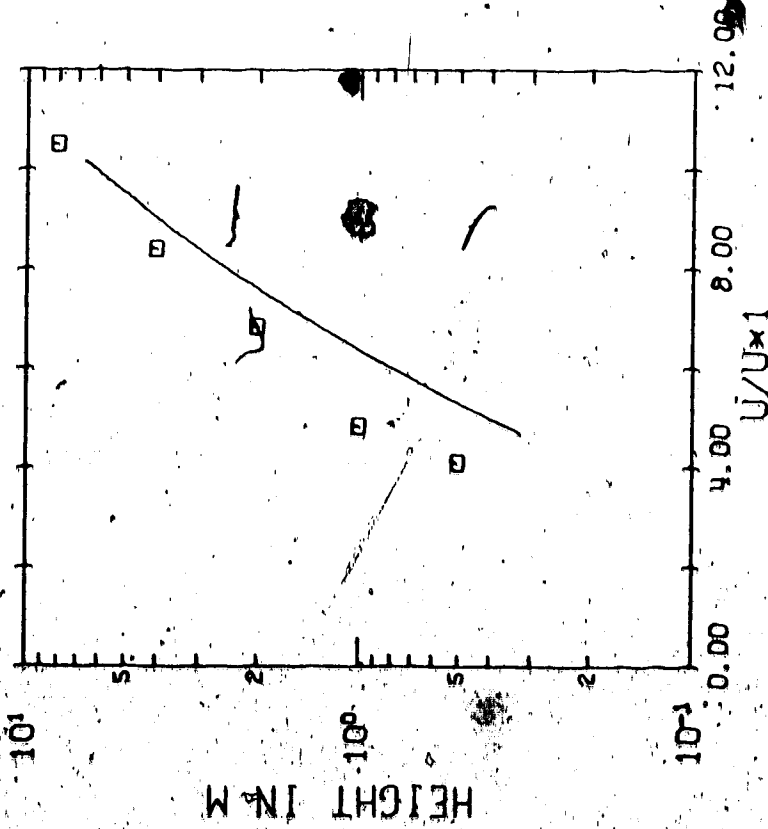
(a) Fetch 10 m.

(b) Fetch 20 m.

Figure 5-12. Observed wind profiles compared with mixing-length model.
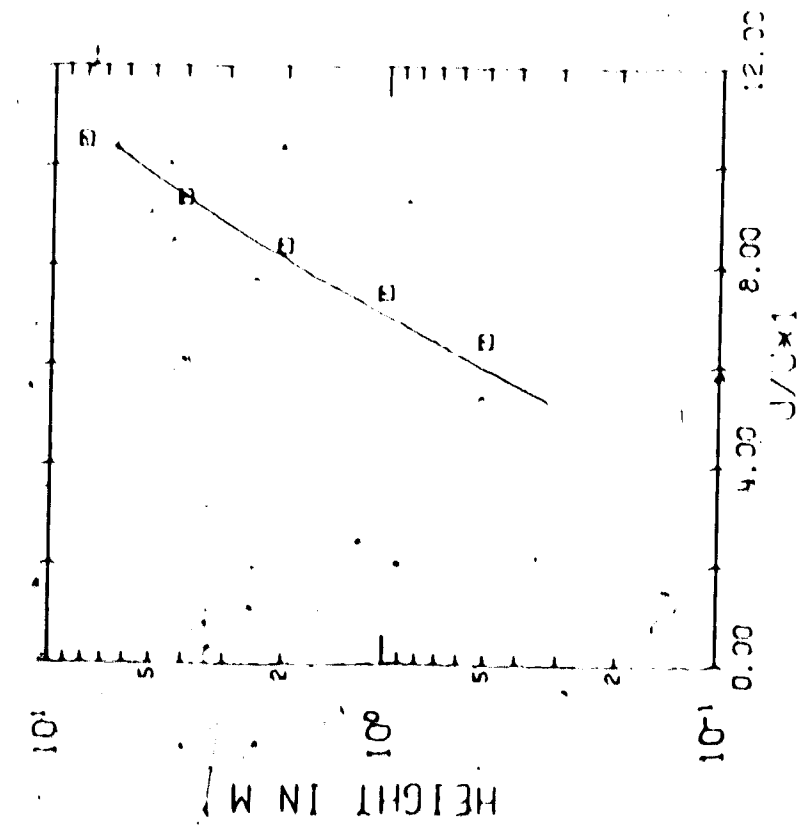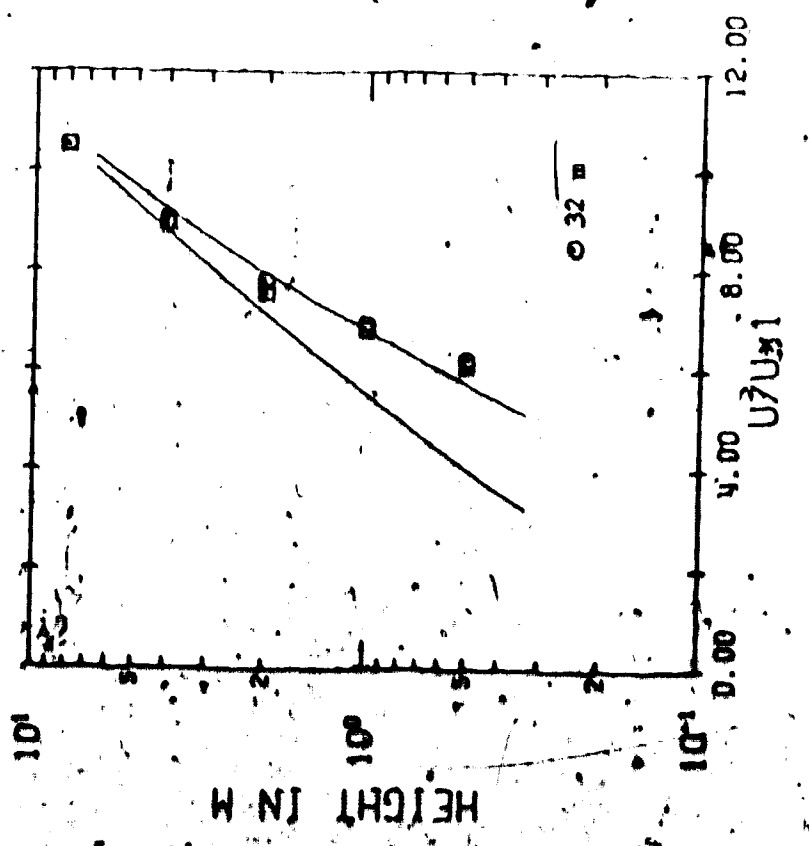
(b) Fetch 47 m

(a) Fetch 30 m

Figure 5-13. Observed wind profiles compared with mixing-length model.
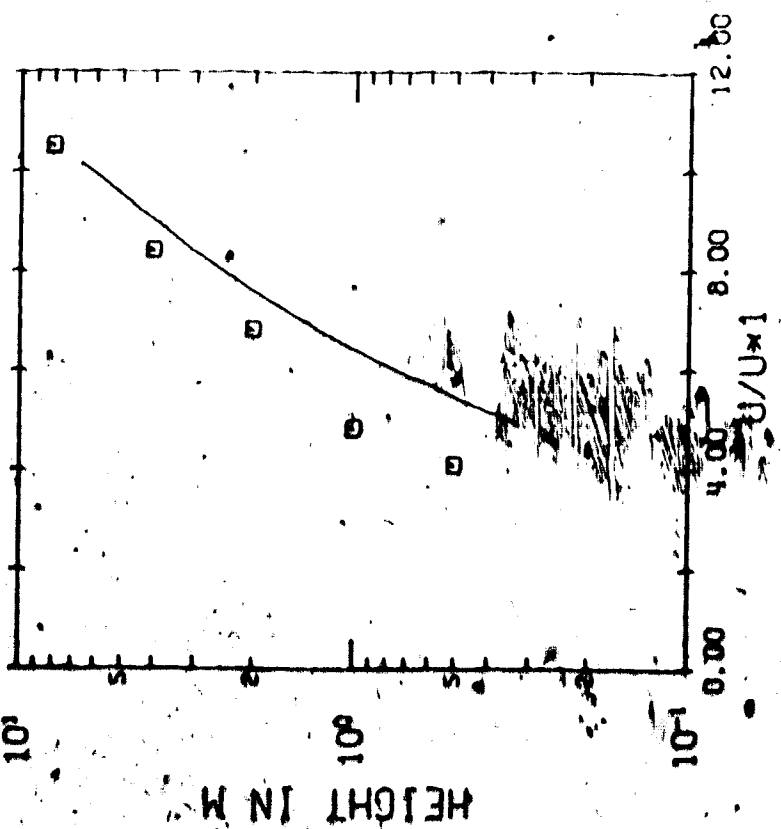
(b) Fetch 20 m

(a) Fetch 10 m

Figure 3-14. Observed wind profiles compared with the Glushko model.
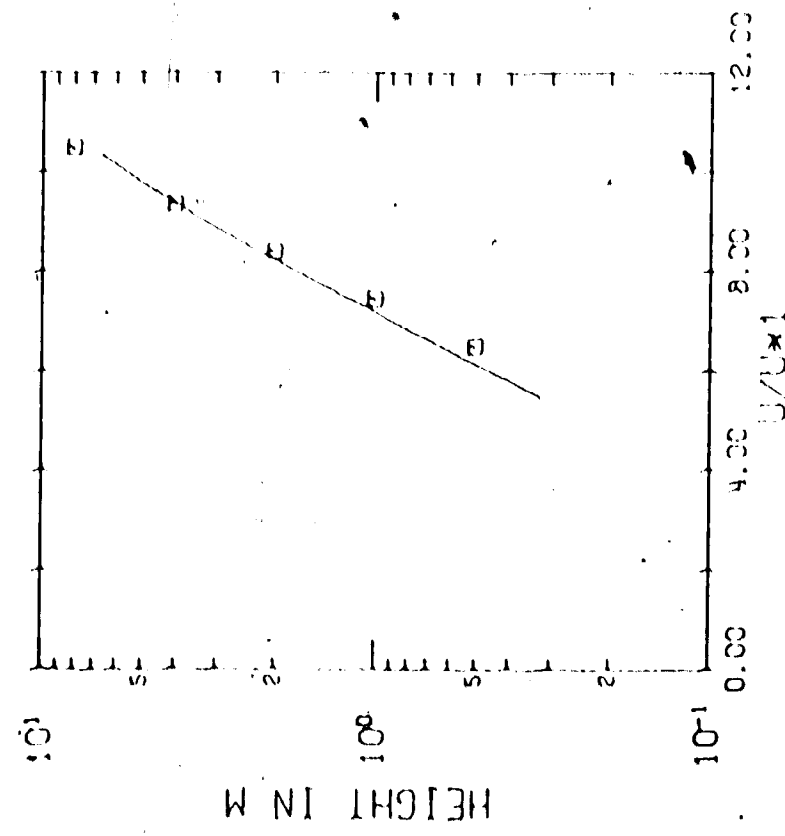
(b) Fetch 47 m
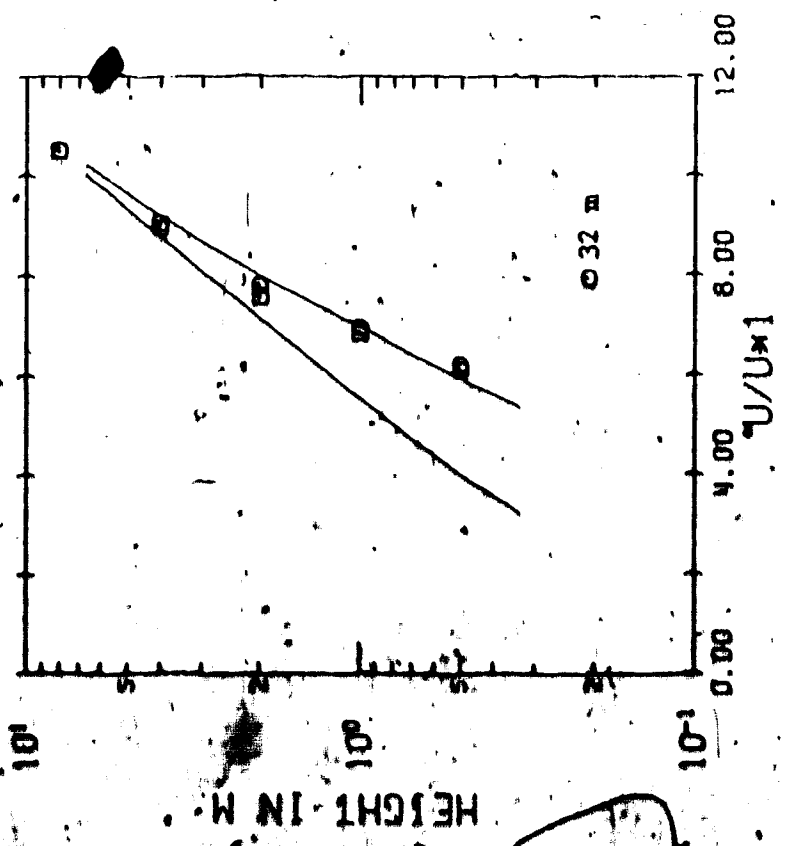
(a) Fetch 30 m

Figure 5-15. Observed wind profiles compared with Glushko model.
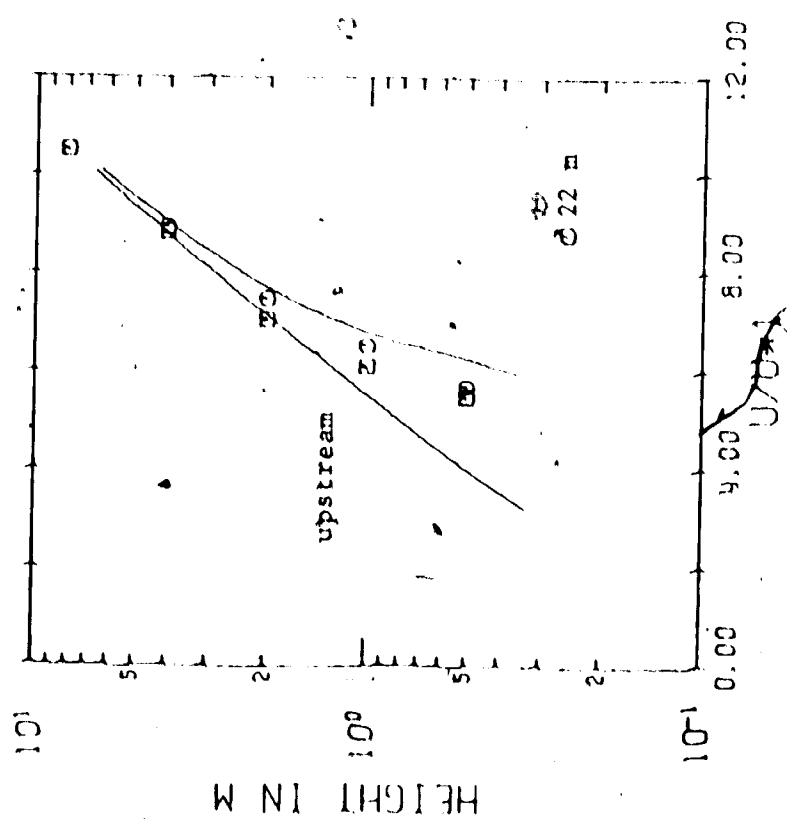
(b) Fetch 20 m

(a) Fetch 10 m

Figure 5-16. Observed wind profiles compared with modified Peterson model.
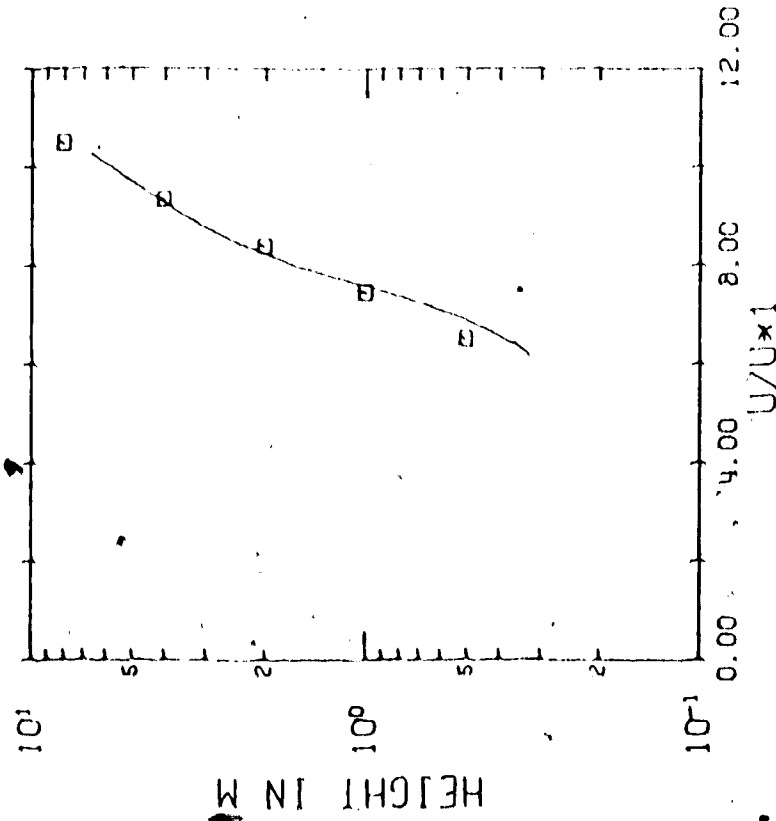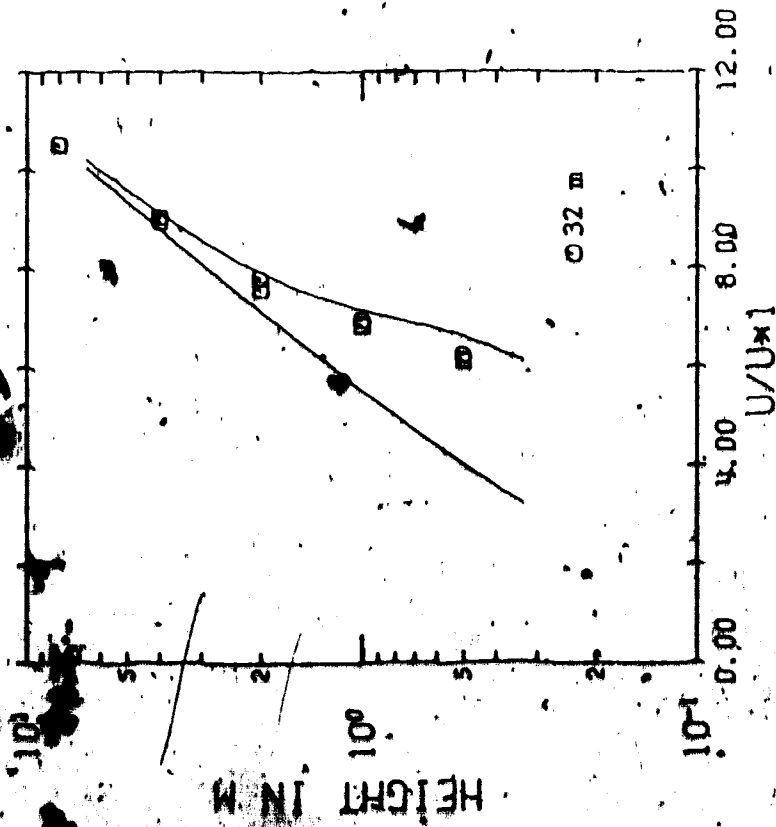
(b) Fetch 47 m

(a) Fetch 30 m

Figure 5-17. Observed wind profiles compared with the modified Peterson model.

the fact that the upper four points of the profile fit best to a line that is based on a non-zero displacement length. A 20 m a line based on the roughness length alone fit the upper three points of the observed profiles. The flow descent seemed to be complete. However, at heights greater than 2 m there is little difference in the lines. Another possible reason for the discrepancy is the proximity to the discontinuity. Elliot's theory specifically applies at distances greater than $10^3 z_{o2}$, and all other models except that of Shir exclude the region where local pressure effects may be felt.

There did not appear to be an inflection point in the observed profiles. However, no firm conclusion could be reached on the basis of so few data points; a larger number would be necessary to detect a change in curvature. The lower portions of the profiles were more nearly logarithmic than the Peterson model predicted. This is in agreement with the findings of Petersen and Taylor (1972). Both the Elliot and Glushko solutions provide a reasonable fit to the data. In view of the surface shear stress calculations the Glushko model seems to be the best overall description of the flow modification.

5.7 Some Turbulence Statistics

Existing data for the moments of the turbulent fluctuations are inexact, strongly scattered, incomplete, and do not agree well with each other. The explanation is evidently the considerable error in measurements of turbulent quantities that have quite large variability both in the vertical and the horizontal, even above a relatively homogeneous surface (Monin and Yaglom, 1971, p. 518). The fast response data obtained at Chin made possible the calculation of the standard deviations of the vertical and longitudinal wind components. The vertical wind was measured by the sonic anemometer. The wind speed was measured by the vane-mounted horizontal propeller of the shear stress meter, and the standard deviation of the longitudinal component can be obtained from this if it is assumed that the statistics of the two variables are interchangeable (Lumley and Panofsky, 1964, p. 154).

The characteristics of the vertical component near the ground are reasonably well understood; the theory is relatively simple because the proximity of the surface prevents low-frequency oscillations from forming. Furthermore, the normal roughness length serves to represent the terrain effect on the intensity of vertical turbulence (Lumley and Panofsky, 1964, p. 131). There is no doubt that large-scale features are unimportant (Monin and Yaglom, 1971, p. 518). In neutral conditions the standard deviation of the vertical velocity is proportional to the friction velocity, that is,

$$\sigma_w = A u_*$$

The value of the constant A, however, is a subject of much controversy. Estimates have ranged from 0.7 to 1.4. The mean value of all estimates from atmospheric observations lies in the range 1.2 to 1.3 (Monin and Yaglom, 1971, p. 520). A short summary of estimates is included in Table 5-5. Monin-Obukhov similarity theory predicts

$$\sigma_w / u_* = F_1 (z/L)$$

where F_1 is a universal function of the stability parameter z/L. The nature of the variation with stability is likewise a subject of debate. Recent work suggests that the ratio is not dependent on stability except at large instabilities where a slow increase is noted (Bowne and Ball, 1970; Monin and Yaglom, 1971, p. 519).

The standard deviation of the longitudinal component in neutral conditions is also proportional to the friction velocity,

$$\sigma_u = B u_*$$

Estimates of the constant B have ranged from 2.1 to 3.0. Recent atmospheric data suggest a value 2.5 (Bowne and Ball, 1970), while laboratory work suggests the value 2.3 (Monin and Yaglom, 1971, p. 280). A short summary of estimates in included in Table 5-6. There is evidence that the value varies with terrain (Lumley and Panofsky, 1964, p. 155). Large-scale factors may well be important in addition to roughness. Again similarity theory predicts

$$\sigma_u / u_* = F_2 (z/L)$$

Variations with stability tend to be small, with perhaps a slight increase with increasing instability (Monin and Yaglom, 1971, p. 518).

Table 5-5. Summary of values for ratio σ_w / u_*.

Value	Source
1.25	Panofsky and McCormick (1960)
1.33	Pasquill (1972)
0.7	Gurvich (Lumley and Panofsky, 1964, p. 135)
0.87	Perepelkina (ibid.)
1.2	Klug (1965)
1.2	Panofsky and Prasad (1965)
1.2	Mordukhovich and Tsvang (Pasquill, 1972)
1.3	Businger et al (1967)
1.29	Busch and Panofsky (1968)
1.35	Haugen et al (1971)
1.4	McBean (1971)
0.9	Laufer, Klebanoff, Comte-Bellot, Coanti (Monin and Yaglom, 1971, p. 280)
0.9	Cermak, Sandborn, Chuang (Monin and Yaglom, 1971, p. 520)

Table 5-6. Summary of values for the ratio σ_u / u_*.

Value	Site	Source
2.45	various	Davenport (1961)
2.9	O'Neill	Lumley and Panofsky (1964, p. 155)
2.5	Australia	ibid.
2.1	Brookhaven	ibid.
2.3	Tsimlyansk	Monin (ibid.)
2.2	pipe flow	ibid.
3.0	O'Neill	Klug (1965)
2.3	laboratory	Laufer, Klebanoff, Comte-Bellot, Coan (Monin and Yaglom, 1971, p. 280)

Values of σ_w and σ_u were computed using a 15 minute averaging period to coincide with the nominal 15 minute recording interval of the mean wind speeds. Four such values were then averaged to produce an hourly figure. This procedure was followed by Haugen, Kaimal, and Bradley (1971). The corresponding hourly values for u_* were then used to calculate the ratios σ_w/u_* and σ_u/u_*. Twelve ratios on June 30 gave

$$\sigma_w/u_* = 0.94 \qquad \text{s.d.} \quad 0.05$$
$$\sigma_u/u_* = 2.9 \qquad \text{s.d.} \quad 0.4$$

The stability for the period of these measurements ranged from $z/L = -0.39$ to $z/L = -0.080$. Ten ratios on July 1 gave

$$\sigma_w/u_* = 0.96 \qquad \text{s.d.} \quad 0.18$$
$$\sigma_u/u_* = 2.2 \qquad \text{s.d.} \quad 0.2$$

with stability ranging from $z/L = -0.075$ to -0.003. The ratio σ_w/u_* exhibited no significant difference for these two broad stability categories. If the indications are correct the marked difference between the values for σ_u/u_* must be attributed to the effects of terrain. Although no obvious large-scale differences were observed, a topographical map disclosed that the northeast flow of June 30 was subject to different large-scale influences from the westerly flow of July 1. The average value for the ratio σ_w/u_* is 0.95, which is in excellent agreement with the value for laboratory flows. The average value for the ratio σ_u/u_* is 2.6, in fair agreement with other recent atmospheric values.

Since $E = (1/2)(\sigma_u^2 + \sigma_v^2 + \sigma_w^2)$ a value for the constant of proportionality between shear stress and turbulent energy can be obtained, provided the ratio σ_v/u_* is known. No measurements of the standard deviation of the lateral component were made. As with the other statistics the dependence of σ_v/u_* on stability and/or terrain is an open issue. In neutral conditions Monin and Yaglom (1971, p. 518) gave the value 1.7, the same as for laboratory flows. Lumley and Panofsky (1964, p. 146) gave values ranging from 1.5 to 2.6. Takeuchi (Bowne and Ball, 1970) reported the value 4.0, while Elderkin (Bowne and Ball, 1970) obtained the value 2.4. Assuming $\sigma_v = 2.0 u_*$ together with the average observed values of $\sigma_w = 0.95 u_*$ and $\sigma_u = 2.6 u_*$, the result is $E = 0.18 u_*^2$, the constant lying between the value 0.16 used by Peterson and the value 0.22 used by Shir.

CHAPTER VI

MORE TOWARDS REALITY

Study of the change-of-roughness problem originated with the
desire to understand more fully the effects of real terrain on the
atmosphere. Substantial effort has been expended and some progress
has been made. In developing the theory certain assumptions were
necessary to render the problem tractable. The most common assumptions
were:

(1) neutral stability

(2) two-dimensional, single, abrupt change of roughness

(3) change in roughness alone, no change in other variables.

These assumptions effectively restricted the theory to somewhat
unrealistic situations. For a model to be an adequate representation
of the interaction between the Earth's surface and the atmospheric
boundary layer, other, albeit complicating, factors must also be
considered.

6.1 Non-Neutral Stability

Because the theory is restricted to adiabatic conditions,
experimental testing is quite tedious. Neutral stability, as noted in
the preceding chapter, is rather infrequent. Awaiting the time when
such conditions do present themselves is an onerous task. Onshore flow
at a coast is an approximation that has been the source of much of the
data at present. For the surface boundary layer over continental land
areas the extension of the theory to include all stabilities is
imperative.

Elliot (1958) reckoned tentatively that instability leads to
a small increase in the height of the internal boundary layer, and that
stability leads to a small decrease. The observations of Echols and
Wagner (1972) supported this idea, and suggested further that the
internal boundary layer height is dependent on wind speed. In near-
neutral conditions the height decreased with increased wind speed as
would be expected from classical theory of boundary layer growth over

a flat plate (Schlichting, 1968, p. 599). In stable night-time conditions the opposite occurred: the height increased with increased wind speed. The reason, they surmised, was a tendency toward laminar flow, which has lower boundary-layer heights according to the classical flat-plate theory (Schlichting, 1968, p. 130). Increased wind speed increases mechanically-induced turbulence and destroys the laminar character of the flow.

Blackadar, Glass and Panofsky (1967) developed a perturbation-type theory employing the log-linear wind profile for non-adiabatic lapse rates. Integration of the equations of motion across the modified region, with the constraints of continuity on the stress, wind speed, and wind shear at the top of the layer, produced an expression for $\partial h / \partial(1/L)$ as a function of the downwind distance from the discontinuity. The results were compared with the theory of Miyake as modified by Panofsky (1967) to include diabatic effects. Both theories predicted an increase in the internal boundary layer height with increasing instability, but the latter indicated a larger effect. Their experimental data was too scattered to discriminate between the two theories.

Several of the other models also lend themselves readily to extension into non-adiabatic conditions. The analysis of R. J. Taylor (1962) can be made applicable simply by using the streamfunction appropriate to the diabatic wind profile. The treatment of Dyer (1962) could be modified by making the exponents in the power laws functions of stability. Once the variation of the ratio τ/E with stability is known, the Peterson and Glushko models can also be adapted.

. Pasquill (1972) noticed that the curve for the interface height is similar in shape to the curve for the increase with distance of the mean vertical displacement of passive particles released from a crosswind line on the ground. He drew a simple analogy between mass and momentum transfer, the 'source' of passive particles being identified with the 'sink' of momentum. By using the gradient transfer approach for vertical diffusion and adopting realistic profiles of eddy diffusivity and wind speed, he was able to extend the internal boundary layer calculations to conditions of non-neutral thermal stratification. As

before, the height was found to be greatest in superadiabatic and least in stable lapse rates.

6.2 Simultaneous Changes in Other Elements

A further complication arises when there are, in addition to a change of roughness, simultaneous changes in other meteorological elements. Although the mustard-fallow transition was treated simply as a change in roughness, in reality, there were also discontinuities in surface temperature, heat flux, and humidity. The assessment of Dyer (1962) was intended to provide working estimates for the modification of these profiles and fluxes. It does not, however, allow for any interactions between the diffusing agents. Some progress along these lines has been made by P. A. Taylor (1970, 1971).

The transformation of other meteorological variables besides the wind profile has been studied by Nadejdina and Novikova (Panchev et al, 1971), using the energy balance equation and the Kolmogorov expressions for the exchange coefficient and dissipation rate. An approximate solution for the transformation of the wind profile alone as a result of a simultaneous change of roughness and temperature stratification has been obtained by Dmitriev and Sokolova (Panchev et al, 1971), using the wind profile-exchange coefficient model of Laikhtman (1964). The solution revealed that the influence of the roughness change is less than the influence of the change in intensity of turbulent exchange due to the different stratification in upstream and downstream flows. This enabled Zaitsev (Panchev et al, 1971) to simplify the equations to the case of a change in stability alone, for which he was able to obtain an exact solution in Bessel functions.

6.3 Patchy Roughness

Yet another complication is the finite lateral extent of different surfaces in real terrain. The theory needs to be extended to include the three-dimensional case. In addition, real terrain is seldom simple enough to be represented by one or even several abrupt changes from one uniform surface to another. Internal boundary layer calculations become futile. Smith (1967) represented complex terrain by allowing the drag coefficient to vary about a mean value with a specified standard deviation. The results for a periodic variation showed that the height to which flow modifications penetrate depends essentially on the period of oscillation, and to a smaller degree on the amplitude. An observer flying low over an area made up of fields of different roughness would record the oscillations, but the higher he flew, the smaller would be the variation. The effects are damped with altitude.

Pasquill (1972) applied his 'particle source-momentum sink' analogy. A particular elementary area in isolation, he reasoned, is a 'sink' which will produce a momentum deficit at any given height that will rise to a maximum at a certain distance downwind and then fall off continuously as the distance is increased further. The functional form he noted, is the same as the ground-level distribution from an elevated source. Using this it was possible to define the upwind area of ground within which the unit 'sinks' dominate the momentum deficit at any particular height. The crosswind and alongwind dimensions of these effective areas were derived from estimates of the vertical spread. The dimensions are fairly sensitive functions of height and are further affected by stability and roughness in that order. These areas are not, of course, the only roughness elements affecting the flow properties at a point. They are, however, the dominant ones. Any outstanding bigger feature outside the area may also exert an important effect. Nor is this method rigorous. In order to obtain quantitative estimates, Pasquill was forced to assume that the diffusivity field is horizontally uniform, which it patently is not. It must reflect the spatial variations of the very patchiness in question. Nevertheless, he felt that the results would be useful as a first estimate in evaluating single point measurements.

Accordingly, measurements made at some position will be representative of the underlying patchy terrain only if the patchiness is on a scale small compared with the effective source area. As a concrete example, in flat rural England the scale within which most of the major roughness elements are repeated is about 100 m. Pasquill's calculations indicated that measurements at a height of 50 m would probably be representative, except perhaps in unstable conditions. In areas containing cities with tall buildings the scale of the variation would be some kilometers, and the height required for representative measurements, some hundreds of meters. Attention is again focussed on the use of low-flying aircraft as an approach to direct spatial averaging. Fiedler and Panofsky (1972) deduced that the effective roughness of the Pennsylvania plains is about 40 cm, considerably larger than the 1 cm figure usually ascribed to grassland. The importance of individual obstacles ranging from bushes and hedges to woods and buildings is thereby confirmed.

The roughness formula of Lettau (1969) permits the objective determination of the dominant contributor to the effective roughness among such a variety of roughness elements. The significance of the natural topography of the landscape is still largely unknown. If Lettau's formula can be applied on the continental scale, the effect on the aerodynamic roughness can be assessed. Another possibility is spectral analysis of the total variance given by a topographical profile curve. Such a technique would numerically express the relative importance of various topographical features—knolls, ridges, mountains etc.— qualified, of course, by their geographical frequency. It would therefore be possible to extend the roughness change theory into the realm of the planetary boundary layer. The effect of the whole spectrum of roughness on the geostrophic drag coefficient could have important repercussions on the atmosphere as a whole. Some work in this area has been done by P. A. Taylor (1969b).

CHAPTER VII

CONCLUSION

7.1 Summary

The zero-plane displacement for mustard 55 cm high was found to be 15 cm and to exhibit rather large variations (standard deviation 4 cm). This value was lower than might be expected from most empirical formulae. The roughness of the mustard was determined to be 12 cm, in close agreement with several estimates, most notably, the roughness element description formula of Lettau. (1969) and the power law quoted by Sellers (1965, p. 150). The fallow was found to have a roughness of 1 cm.

Analysis of the downwind profiles revealed several things. The surface friction velocity inferred from the wind at 1/2 m overshot initially and returned slowly to equilibrium. The wind profile in the lower part of the internal boundary layer was more nearly logarithmic than predicted by the Peterson model. In other words, the height of the internal boundary layer was somewhat larger than predicted. No inflection point was present in the wind profile. Although the Elliot theory was in fair agreement with the data, overall, the Glushko model appeared to be the best description of the flow modification. The presence of a zero-plane displacement complicated the issue, especially as the theories do not take it into account.

A plausible value of 0.18 for the constant of proportionality between shear stress and turbulent energy was obtained using the observed average values of $\sigma_w/u_* = 0.95$, $\sigma_u/u_* = 2.6$, and the assumed value $\sigma_v/u_* = 2.0$. The two test days represented two broad stability categories. No variation of σ_w/u_* with stability was found. However, there were significant differences in the values of σ_u/u_*. This could have been the effect of stability, or, because the wind blew from different directions on the two test days, this could be attributed to the effect of large-scale properties of the terrain.

7.2 Recommendations

In weighing current knowledge a few general facts may be stated in addition to those directly disclosed by the experiment. The height of the internal boundary layer, regardless of its definition, grows with the 4/5 power of distance from the discontinuity. For representative wind profiles a height/fetch ratio of 1/20 seems to be adequate. For the turbulence statistics to be representative it appears that a height/fetch ratio of 1/100 to 1/200 is necessary, depending, perhaps, on the sense of the change. The turbulence adjusts rather more slowly than the mean wind.

Even for the simple two-dimensional change-of-roughness several practical difficulties remain. The solutions are fairly sensitive functions of the roughness ratio. In most applications the downstream roughness is not easy to obtain. At Chin, reversal of the wind direction made it possible to calculate the fallow roughness from observations at the same site as for the mustard. In many instances, however, the instrumentation may well have to be moved in order to obtain representative profiles of the second surface from which to derive the downwind roughness. The roughness formula of Lettau (1969) furnishes a means of estimating the second roughness, though with poor accuracy. An improved method of roughness estimation based on roughness element description would be most desirable. The zero-plane displacement is another issue. None of the theories have included this parameter despite its obvious importance when dealing with forested or urban areas. Existing models will have to be revised in some way to deal with this aspect of the flow situation. New models ought to contain it from the outset. A further difficulty is the possible dependence of both the roughness and displacement lengths on the wind speed.

No definitive final solution is yet available, even for the simple change-of-roughness problem. One obstacle has been the paucity of high quality data. Future experiments should employ as many anemometer heights as possible, particularly in the controversial blending region, to detect any change of curvature. Some effort should also be made to measure vertical profiles of shear stress as well as the downstream variation of the surface value. Other research needs

lie in the extension of the theory to the various 'real-life' situations discussed in Chapter VI. This would also assist the experimentalist in testing the different alternatives. The behaviour of the turbulence statistics is an important question to be answered. The hypothesis relating shear stress to turbulent energy is in need of verification, for it is a powerful tool in studying flow development.

REFERENCES

Antonia, R.A., and R.E. Luxton, 1971: The response of a turbulent boundary layer to a step change in surface roughness. part 1. smooth to rough. J. Fluid Mech., 48, 721-761.

Antonia, R.A., and R.E. Luxton, 1972: The response of a turbulent boundary layer to a step change in surface roughness. part 2. rough to smooth. J. Fluid Mech., 53, 737-757.

Beckwith, I.E., and D.M. Bushnell, 1968: Calculation of mean and fluctuating properties of the incompressible turbulent boundary layer. Proc. AFOSR-IFP-Stanford Conference on Computation of Turbulent Boundary Layers, vol. 1, Stanford University.

Blackadar, A.K., 1962: The vertical distribution of wind and turbulent exchange in a neutral atmosphere. J. Geophys. Res., 67, 3095-3102.

Blackadar, A.K., P.E. Glass, and H.A. Panofsky, 1967: A theory of the effects of stability upon the wind profile under conditions of inhomogeneous terrain roughness. Proc. USAEC Meteorological Information Meeting, Chalk River Laboratories of Ontario, C.A. Mawson (ed,), Canadian Report AECL-2787, pp. 453-461.

Blackadar, A.K., H.A. Panofsky, P.E. Glass, and J.F. Boogaard, 1967: Determination of the effect of roughness change on the wind profile. Boundary Layers and Turbulence, Phys. Fluids Suppl., pp. 209-211.

Blom, J., and L. Wartena, 1969: The influence of changes of surface roughness on the development of the turbulent boundary layer in the lower layers of the atmosphere. J. Atmos. Sci., 26, 255-265.

Bowne, N.E., and J.T. Ball, 1970: Observational comparison of rural and urban boundary layer turbulence. J. Appl. Meteor., 9, 862-873.

Bradley, E.F., 1968: A micrometeorological study of velocity profiles and surface drag in the region modified by a change in surface roughness. Quart. J. Roy. Meteor. Soc., 94, 361-379.

Bradley, E.F., 1972: The influence of thermal stability on a drag coefficient measured close to the ground. Agric. Meteor., 9, 183-190.

Bradshaw, P., D.H. Ferriss, and N.P. Atwell, 1967: Calculation of boundary layer development using the turbulent energy equation. J. Fluid Mech., 28, 593-616.

Bradshaw, P. and D.H. Ferriss, 1968: Derivation of a shear stress
         transport equation from the turbulent energy equation. Proc.
         AFOSR-IFP-Stanford Conference on Computation of Turbulent
         Boundary Layers, vol. 1, pp. 264-269.

Bradshaw, P., 1969: Comments on "on the relation between the shear stress
         and the velocity profile after a change in surface roughness".
         J. Atmos. Sci., 26, 1353-1354.

Brooks, F.A., 1961: Need for measuring horizontal gradients in determin-
         ing vertical eddy transfer of heat and moisture. J. Meteor.,
         18, 589-596.

Busch, N.E., and H.A. Panofsky, 1968: Recent spectra of atmospheric
         turbulence. Quart. J. Roy. Meteor. Soc., 94, 132-148.

Cameron, L.A., 1970: An experimental approach to the effects of a
         change of surface roughness on the wind profile. M.Sc.
         thesis, University of Alberta, Edmonton.

Dyer, A.J., 1965: Discussion on "change of terrain roughness and the
         wind profile". Quart. J. Roy. Meteor. Soc., 91, 241.

Dyer, A.J., 1967: The turbulent transport of heat and water vapour in
         an unstable atmosphere. Quart. J. Roy. Meteor. Soc., 93, 501-
         508.

Dyer, A.J., B.B. Hicks, and K.M. King, 1967: The fluxatron--a revised
         approach to the measurement of eddy fluxes in the lower
         atmosphere. J. Appl. Meteor., 6, 408-413.

Dyer, A.J., B.B. Hicks, and V. Sitaraman, 1970: Minimizing the levelling
         error in Reynolds stress measurement by filtering. J. Appl.
         Meteor., 9, 532-534.

Dyer, A.J., and B.B. Hicks, 1972: The spatial variability of eddy fluxes
         in the constant flux layer. Quart. J. Roy. Meteor. Soc., 98,
         206-212.

Echols, W.T., and N.K. Wagner, 1972: Surface roughness and internal
         boundary layer near a coastline. J. Appl. Meteor., 11, 658-
         662.

Elliot, W.P., 1958: The growth of the atmospheric internal boundary
         layer. Trans. Amer. Geophys. Union, 39, 1048-1054.

Fiedler, F., and H.A. Panofsky, 1972: The geostrophic drag coefficient
         and the 'effective' roughness length. Quart. J. Roy. Meteor.
         Soc., 98, 213-220.

Geiger, R., 1966: The Climate Near the Ground. Harvard University Press,
         revised fourth edition, 611 pp.

Goldstein, S., 1965: _Modern Developments in Fluid Dynamics_, Dover edition, Dover Publications, New York, 702 pp.

Haugen, P.A., J.C. Kaimal, and E.F. Bradley, 1971: An experimental study of Reynolds stress and heat flux in the atmospheric surface layer. _Quart. J. Roy. Meteor. Soc._, 97, 168-181.

Hess, S.L., 1959: _Introduction to Theoretical Meteorology_, Holt, Rinehart and Winston, New York, 362 pp.

Hicks, B.B., 1969: A simple instrument for the measurement of Reynolds stress by eddy correlation. _J. Appl. Meteor._, 8, 825-827.

Hicks, B.B., 1970: The measurement of atmospheric fluxes near the surface: a generalized approach. _J. Appl. Meteor._, 9, 386-388.

Hicks, B.B., 1972: Propeller anemometers as sensors of atmospheric turbulence. _Boundary Layer Meteor._, 3, 214-228.

Hinze, J.O., 1959: _Turbulence_, McGraw-Hill, New York, 586 pp.

Honsaker, J.L., F. McDougall, and D. Oracheski, 1972: Data acquisition system for eddy flux measurements. Paper presented to 6th annual congress of Canadian Meteor. Soc., University of Alberta, Edmonton.

Hsu, S.A., 1971: Measurement of shear stress and roughness length on a beach. _J. Geophys. Res._, 76, 2880-2885.

Hyson, P., 1972: Cup anemometer response to fluctuating wind speeds. _J. Appl. Meteor._, 11, 843-848.

Jacobs, W., 1939: Variation in velocity profile with change in surface roughness of boundary. _NACA Technical Memorandum No. 951._

Kaimal, J.C., and J.A. Businger, 1963: A continuous wave sonic anemometer thermometer. _J. Appl. Meteor._, 2, 156-164.

Kaimal, J.C., and Y. Izumi, 1965: Vertical velocity fluctuations in a nocturnal low-level jet. _J. Appl. Meteor._, 4, 576-584.

Kaimal, J.C., and D.A. Haugen, 1969: Some errors in the measurement of Reynolds stress. _J. Appl. Meteor._, 8, 460-462.

Kline, S.J., M.V. Morkovin, G. Sovran, and D.J. Cockrell, (eds.), 1968: _Computation of Turbulent Boundary Layers_. Proc. AFOSR-IFP-Stanford Conference, vol. 1, Stanford University, 590 pp.

Klug, W., 1965: Diabatic influence on turbulent wind fluctuations. _Quart. J. Roy. Meteor. Soc._, 91, 215-217.

Kutzbach, J.E., 1961: Investigations of the modification of wind profiles by artificially controlled surface roughnesss. University of Wisconsin, Dept. f Meteorology, Annual Report, pp. 71-113.

Laikhtman, D.L., 1964: Physics of the Boundary Layer of the Atmosphere, Israel Program for Scientific Translations, 200 pp.

Lettau, H., and B. Davidson, 1957: Exploring the Atmosphere's First Mile, Pergamon Press, New York.

Lettau, H., 1967: Problems of micrometeorological measurements. The Collection and Processing of Field Data, Interscience Publications, New York, pp. 3-40.

Lettau, H., and J. Zabransky, 1968: Interrelated changes of wind profile structure and Richardson number in airflow from land to inland lake. J. Atmos. Sci., 25, 718-728.

Lettau, H., 1969: Note on aerodynamic roughness parameter estimation on the basis of roughness element description. J. Appl. Meteor., 8, 828-832.

Logan, E., and J.B. Jones, 1963: Flow in a pipe following an abrupt increase in surface roughness. Trans. ASME, Ser. D, J. Basic Eng., 85, 35-40.

Lumley, J.L., and H.A. Panofsky, 1964: The Structure of Atmospheric Turbulence, Interscience Publications, New York, 239 pp.

McBean, G.A., 1971: The variations of the statistics of wind, temperature and humidity fluctuations with stability. Boundary Layer Meteor., 1, 438-457.

McBean, G.A., 1972: Instrument requirements for eddy correlation measurements. J. Appl. Meteor., 11, 1078-1084.

Meroney, R.N., 1968: Characteristics of wind and turbulence in and above model forests. J. Appl. Meteor., 7, 780-788.

Monin, A.S., 1959: Smoke propagation in the surface layer of the atmosphere. Adv. in Geophys., 6, Academic Press, New York, pp. 331-343.

Monin, A.S., and A.M. Yaglom, 1971: Statistical Fluid Mechanics, MIT Press, Cambridge, Mass., 769 pp.

Munn, R.E., 1966: Descriptive Micrometeorology, Academic Press, New York, 245 pp.

Nee, V.W., and L.S.G. Kovasznay, 1968: The calculation of the incompressible turbulent boundary layer by a simple theory. Computation of Turbulent Boundary Layers, Proc. AFOSR-IFP-Stanford Conference, vol. 1, pp. 300-319.

Nickerson, E.V., 1968: Boundary layer adjustment as an initial value problem. J. Atmos. Sci., 5, 207-213.

Panchev, S., E. Donev, and N. Godev, 1971: Wind profile and vertical motions above an abrupt change in surface roughness and temperature. Boundary Layer Meteor., 2, 52-63.

Pandolfo, J.P., 1966: Wind and temperature profiles for constant flux boundary layers in lapse conditions with a variable eddy conductivity to eddy viscosity ratio. J. Atmos. Sci., 89, 495-502.

Panofsky, H.A., and R.A. McCormick, 1960: The spectrum of vertical velocity near the surface. Quart. J. Roy. Meteor. Soc., 86, 495-503.

Panofsky, H.A., A.K. Blackadar, and G.E. McVehil, 1960: The diabatic wind profile. Quart. J. Roy. Meteor. Soc., 86, 390-398.

Panofsky, H.A., 1963: Determination of stress from wind and temperature measurements. Quart. J. Roy. Meteor. Soc., 89, 85-93.

Panofsky, H.A., and A.A. Townsend, 1964: Change of terrain roughness and the wind profile. Quart. J. Roy. Meteor. Soc., 90, 147-155.

Panofsky, H.A., and B. Prasad, 1965: Similarity theories and diffusion. Int. J. Air Water Poll., 9, 419-430.

Panofsky, H.A., and E.L. Petersen, 1972: Wind profiles and change of terrain roughness at Riso. Quart. J. Roy. Meteor. Soc., 98, 845-854.

Pasquill, F., 1962: Atmospheric Diffusion, D. Van Nostrand Co. Ltd., 297 pp.

Pasquill, F., 1972: Some aspects of boundary layer description. Quart. J. Roy. Meteor. Soc., 98, 469-494.

Paulson, C.A., 1970: The mathematical representation of wind speed and temperature profiles in the unstable atmospheric surface layer. J. Appl. Meteor., 9, 857-860.

Petersen, E.L., and P.A. Taylor, 1972: Some comparisons between observed wind profiles at Riso and theoretical predictions for flow over inhomogeneous terrain. To appear.

Peterson, E.W., 1969a: Modification of mean flow and turbulent energy by change in surface roughness under conditions of neutral stability. Quart. J. Roy. Meteor. Soc., 90, 561-576.

Peterson, E.W., 1969b: On the relation between the shear stress and the velocity profile after a change in surface roughness. J. Atmos. Sci., 26, 773-77.

Peterson, E.W., 1971: Predictions of the momentum exchange coefficient for flow over heterogeneous terrain. J. Appl. Meteor., 10, 958-961.

Peterson, E.W., 1972a: Comments on "A numerical computation of airflow over a sudden change of surface roughness." J. Atmos. Sci., 29, 1393-1394.

Peterson, E.W., 1972b: Relative importance of terms in the turbulent energy and momentum equations as applied to the problem of a surface roughness change. J. Atmos. Sci., 29, 1470-1476.

Philip, J.R., 1959: The theory of local advection. J. Meteor., 16, 535-547.

Plate, E.J., and A.A. Quraishi, 1965: Modelling of velocity distribution inside and above tall crops. J. Appl. Meteor., 4, 400-408.

Plate, E.J., 1971: Aerodynamic Characteristics of Atmospheric Boundary Layers, AEC critical review series, US Atomic Energy Commission, 190 pp.

Priestly, C.H.B., and W.C. Swinbank, 1947: Vertical transport of heat by turbulence in the atmosphere. Proc. Roy. Soc. London, A189, 543-561.

Priestly, C.H.B., 1959: Turbulent Transfer in the Lower Atmosphere, University of Chicago Press, 130 pp.

Rider, N.E., J.R. Philip, and E.F. Bradley, 1963: The horizontal transport of heat and moisture--a micrometeorological study. Quart. J. Roy. Meteor. Soc., 89, 506-531.

Robinson, S.M., 1962: Computing wind profile parameters, J. Atmos. Sci., 19, 189-190.

Rossby, C.G., and R.B. Montgomery, 1935: The layers of frictional influence in wind and ocean currents. Pap. Phys. Oceanogr. Meteor., 3, MIT Press, 101 pp.

Sadeh, W.Z., J.E. Cermak, and T. Kawatahi, 1971: Flow over high roughness elements. Boundary Layer Meteor., 1, 321-344.

Schlichting, H., 1968: Boundary Layer Theory, sixth edition, McGraw-Hill Book Co. Inc., New York, 747 pp.

Sellers, W.P., 1965: Physical Climatology, University of Chicago Press, 272 pp.

Shir, C.C., 1972: A numerical computation of airflow over a sudden change of surface roughness. J. Atmos. Sci., 29, 304-310.

Smith, F.B., 1967: Modification of the wind profile due to changes in surface roughness. Proc. USAEC Meteor. Information Meeting, Chalk River Nuclear Laboratories, C.A. Mawson (ed.), Canadian Report AECL-2787, pp. 463-475.

Stearns, C.R., and H.H. Lettau, 1963: Two wind profile measurement experiments in airflow over the ice of Lake Mendota. Annual Rep rt, pp. 115-149, University of Wisconsin, Dept. of Meteorology.

Stearns, C.R., 1964: Wind profile modification experiments using fields of Christmas trees on the ice of Lake Mendota. Annual Report, pp. 59-97, University of Wisconsin, Dept. of Meteorology.

Stearns, C.R., 1970: Determining surface roughness and displacement height. Boundary Layer Meteor., 1, 102-111.

Stewart, R.W., 1956: A new look at Reynolds stresses. Can. J. Phys., 34, 722-725.

Sumner, C.J., 1968: A low torque cup anemometer. Australian J. Instr. Control, Oct., pp. 39-40.

Sutton, O.G., 1953: Micrometeorology, McGraw Hill Book Co. Inc., New York, 333 pp.

Swinbank, W.C., 1964: The exponential wind profile. Quart. J. Roy. Meteor. Soc., 90, 119-135.

Swinbank, W.C., and A.J. Dyer, 1967: An experimental study in micrometeorology. Quart. J. Roy. Meteor. Soc., 93, 495-500.

Tan, H.S., and S.C. Lin, 1967: Quasi-steady micrometeorological atmospheric boundary layers over a wheat field. The Energy Budget at the Earth's Surface, E.R. Lemon (ed.), part 2, US Dept. of Agr., 49 pp.

Tani, I., 1968: Review of some experimental results on the response of a turbulent boundary layer to sudden perturbations. Proc. AFOSR-IFP-Stanford Conference on Computation of Turbulent Boundary Layers, vol. 1, pp. 483-494.

Taylor, R.J., 1962: Small-scale advection and the neutral wind profile. J. Fluid Mech., 13, 529-539.

98

Taylor, P.A., 1969a: On wind and shear stress profiles above a change
in surface roughness. Quart. J. Roy. Meteor. Soc., 95,
77-91.

Taylor, P.A., 1969b: The planetary boundary layer above a change in
surface roughness. J. Atmos. Sci., 26, 432-440.

Taylor, P.A., 1970: A numerical model of airflow above changes in
surface heat flux, temperature, and roughness for neutral
and unstable conditions. Boundary Layer Meteor., 1, 18-39.

Taylor, P.A., 1971: Airflow above changes in surface heat flux,
temperature, and roughness: an extension to include the stable
case. Boundary Layer Meteor., 1, 474-497.

Taylor, P.A., 1972: Some comparisons between mixing length and turbulent
energy equation models of flow above a change in surface
roughness. Paper presented to Third Conference on Numerical
Methods in Fluid Mechanics, Paris, July, 1972.

Townsend, A.A., 1956: The Structure of Turbulent Shear Flows, Cambridge
University Press, 315 pp.

Townsend, A.A., 1965: Discussion on "change of terrain roughness and
the wind profile". Quart. J. Roy. Meteor. Soc., 91, 241.

Townsend, A.A., 1965: The response of a turbulent boundary layer to
abrupt changes in surface conditions. J. Fluid Mech., 22,
799-892.

Townsend, A.A., 1966: The flow in a turbulent boundary layer after a
change in surface roughness. J. Fluid. Mech., 26, 255-266.

APPENDIX A

FIELD OBSERVATIONS

Table A-1. The downwind profiles.

Time (MDT)	Fetch over fallow (m)	Height in m				
		1/2	1.0	2.0	4.0	8.0
0640-0650	10	150	176	252	306	385
0700-0710	20	190	215	247	310	368
0720-0731	30	212	240	263	316	367
0755-0805	-1.6		248	348	448	536
1600-1615	-1.6		212	284	362	437
1626-1636	22	354	405	469	554	650
1644-1654	32	286	323	362	413	486
1712	47	325	372	417	464	523

At 0800. $T=48$ F, $\overline{w'T'}=0.66$ cm K s^{-1}

At 1600. $T=58$ F, $\overline{w'T'}=0.31$ cm K s^{-1}

Table A-2. Data for July 1.

Time (PDT)	u at 1m (cm/s)	u at 2m (cm/s)	u at 4m (cm/s)	u at 8m (cm/s)	$\overline{W'T'}$ (cmK/s)	T (F)	z_0 (cm)	d (cm)	u_* (cm/s)	c_d	$-L$ (m)
0900	247	346	440	527	2.07	49	12.8	14.0	52.0	.210	489
0916	234	325	416	497	2.10	49	12.9	13.0	49.3	.210	411
0930	229	317	401	482	2.10	49	13.1	10.6	47.9	.210	377
0945	208	286	365	436	2.83	49	14.7	5.2	45.0	.216	233
1000	207	285	352	418	9.21	52	13.2	9.3	44.2	.274	68.1
1015	210	283	355	416	9.23	52	13.5	6.0	44.3	.211	68.1
1030	217	293	367	429	9.80	52	12.9	7.8	45.2	.208	68.4
1041	228	309	382	441	13.06	52	9.7	19.7	44.3	.194	48.
1100	235	318	395	455	13.69	55	9.3	21.2	45.2	.192	49.2
1115	225		377	436	13.60	55	10.3	17.1	44.5	.198	47.2
1130	140		241	282	4.34	55	13.2	11.9	30.7	.219	48.5
1345	165	225	282	327	4.58	56	10.7	18.4	33.2	.202	58.5
1400	183	247	307	356	4.50	57	10.0	17.0	35.2	.192	70.0
1416	198	265	332	388	3.20	57	10.6	.3	37.9	.192	124
1431	225	316	397	468	3.32	57	9.1	27.4	43.6	.192	182
1446	243	337	426	506	2.47	57	10.9	18.0	48.3	.194	334
1505	245	340	433	515	1.68	57	11.4	16.8	49.5	.199	527
1513	250	347	443	529	1.01	57	11.8	16.0	50.9	.202	954
1530	212	295	377	431	0.51	57	12.2	14.7	43.6	.204	1190
1543	196	267	340	407	0.53	57	13.7	5.6	40.5	.207	917

Table A-3. Data for June 30.

Time (MST)	$\bar{u}$ at 1m (cm/s)	u at 2m (cm/s)	$\overline{w'T'}$ (cm℉/s)	T (F)	z_o (cm)	u_* (cm/s)	c_d	-L (m)
1300	730	831	36.00	60	0.96	63.8	.0874	53.0
1315	710	809	36.00	60	0.99	62.6	.0881	50.1
1330	662	788	35.60	60	1.01	61.2	.0884	47.4
1345	634	723	39.16	60	1.13	57.8	.0912	36.2
1400	575	653	35.64	60	1.07	52.0	.0904	29.1
1630	357	400	29.31	63	1.07	33.6	.0941	9.6
1645	366	413	26.65	63	1.18	35.0	.0956	11.9
1700	353	398	26.30	60	1.18	33.9	.0959	10.9
1715	350	392	26.11	60	1.10	33.0	.0944	10.2
1732	329	369	25.05	60	1.15	31.6	.0961	9.27
1745	340	380	24.50	60	1.03	31.7	.0933	9.59
1817	347	390	25.71	64	1.13	33.0	.0952	10.4
1830	375	423	25.18	64	1.17	35.6	.0949	13.2
1845	368	415	19.39	64	1.09	34.1	.0927	15.2
1900	382	433	15.75	63	1.13	35.4	.0926	20.8
1915	397	447	12.62	63	0.80	33.9	.0853	22.8
1930	397	446	10.62	63	0.75	33.3	.0840	25.7
1945	384	433	10.33	63	0.89	33.4	.0874	26.7
2000	336	380	8.64	62	1.00	30.1	.0896	23.3
2030	310	352	4.04	62	0.97	27.3-	.0881	37.3

APPENDIX B

DETAILS OF NUMERICAL SCHEMES OF P. A. TAYLOR (1972)

The equations of the mixing-length, Glushko, and modified
Peterson models are all essentially parabolic in nature and can be solved
with a finite difference representation moving forward in x one step at
a time. The mixing-length model gives rise to a single parabolic second
order partial differential equation, essentially in U, to be solved
simultaneously with the continuity equation, which plays a secondary
role in this context. The Glushko model gives two simultaneous parabolic
partial differential equations together with continuity. The modified
Peterson model involves a single parabolic partial differential equation,
the energy equation, to be solved simultaneously with the two first order
equations, those of momentum and continuity. To avoid discretization
errors, the transformation to a vertical coordinate $J = \ln (z+z_{o1})/z_{o1}$
is employed. All speeds are scaled with respect to u_{*1} and lengths
with respect to z_{o2}. For computational stability the 'diffusion' terms ,
that is, $/\partial J^2$, are represented implicitly. A system of equations
can then be set up with only a tridiagonal matrix to invert. The finite
difference grid is shown in Fig. B-1. The grid spacings H and STP as well
as J_N are changed in a block structure as the integration proceeds
downstream, as shown in Fig. B-2.

B.1 The Mixing-length Model

The horizontal momentum equation combined with the mixing length
hypothesis in J coordinates is

$$U, \frac{\partial U}{\partial x} + e^{-J} W \frac{\partial U}{\partial J} + e^{-J} \frac{\partial \tau}{\partial J}$$

The first and second derivatives of U with respect to J are computed
from

$$DU_j = (U_{j+1} - U_{j-1})/2H$$
$$D2U_j = (U_{j+1} - 2U_j + U_{j-1})/H^2$$

Setting $M_j = \exp(-J)$ the equation becomes
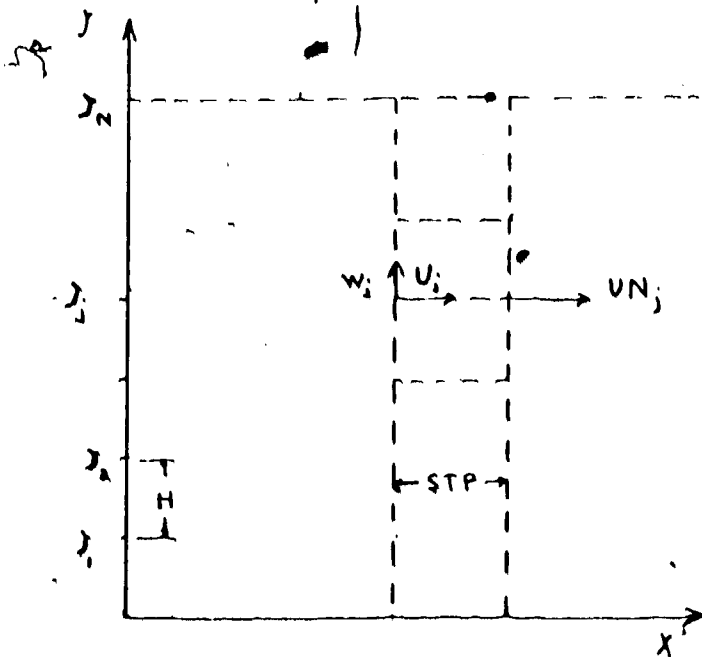
Figure B-1. The finite difference grid.
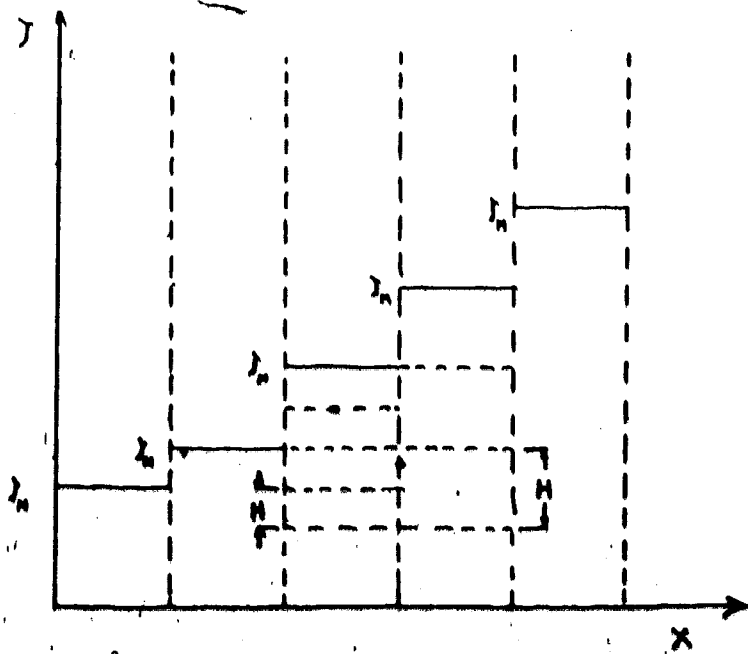
Figure B-2. Computation blocks, showing change in H and gradual
increase in f_n.

$$U_j (UN_j - U_j)/STP + M_j W_j DU_j \qquad\qquad j = 1,2 \ldots N$$

$$= k^2 M_j DU_j (D2U_j + (UN_{j+1} - 2UN_j + UN_{j-1})/H^2)$$

This equation represents N simultaneous linear equations in UN_j, the value of U at the downstream step, assuming that U and W are known. In matrix form

$$
\begin{bmatrix}
D_1 & OD_1 & & & & \\
OD_2 & D_2 & OD_2 & & & \\
& & \ddots & & & \\
& & OD_j & D_j & OD_j & \\
& & & & \ddots & \\
& & & & OD_N & D_N
\end{bmatrix}
\begin{bmatrix}
UN_1 \\
UN_2 \\
\vdots \\
UN_j \\
\vdots \\
UN_N
\end{bmatrix}
=
\begin{bmatrix}
B_1 \\
B_2 \\
\vdots \\
B_j \\
\vdots \\
B_N
\end{bmatrix}
$$

The diagonal and off-diagonal elements of the tridiagonal matrix are given by

$$D_j = U_j/STP + 2k^2 M_j DU_j/H^2$$

$$OD_j = -k^2 M_j DU_j/H^2$$

The elements of matrix B are given by

$$B_j = U_j^2/STP - M_j W_j DU_j + k^2 M_j DU_j D2U_j$$

The lower boundary condition makes no changes, but for $j = N$ the outer boundary condition requires that

$$D_N = U_N/STP + k^2 M_N DU_N/H^2$$

$$B_N = U_N^2/STP - M_N W_N DU_N + k^2 M_N DU_N (D2U_N + ALF/H^2)$$

where $ALF = U_{N+1} - U_N = UN_{N+1} - UN_N$. OD_N is unchanged.

The tridiagonal set of linear equations can then be solved using a direct 'two-pass' Gauss elimination procedure. With the values for UN_j at X+STP the values of W are computed using backward differences for

$$W_j = W_{j-1} - (H/2)(M_j^{-1}(UN_j - U_j) + M_{j-1}^{-1}(UN_{j-1} - U_{j-1}))/STP$$

This method was found by Taylor to be stable for all values of STP. The values of the control parameters and step and grid sizes used in this application are in Table B-1. Computation took about 20 s of CPU time on the University's IBM 360-67.

Table B-1. Values of the parameters used in the mixing-length program.

Range $(X = x/z_{o2})$	N	H	STP	NRAT	ITER	ITSTP	JMP	NADD	PSTP
0-4	48	0.125	0.05	1	20	4	4	0	1.0
4-10	48	0.125	0.10	1	20	3	4	0	2.0
10-40	50	0.125	0.50	1	20	3	4	2	10.0
40-200	52	0.125	1.0	1	20	8	4	2	20.0
200-500	28	0.250	5.0	2	10	6	2	2	50.0
500-1000	29	0.250	10.0	1	10	5	2	1	100.0
$10^3-4.5 \times 10^3$	32	0.250	50.0	1	10	7	2	3	500.0
$4.5 \times 10^3-10^4$	36	0.250	100.0	1	10	6	2	4	1000.0
$10^4-4.0 \times 10^4$	20	0.500	500.0	2	10	6	1	2	5000.0
$4.0 \times 10^4-10^5$	22	0.500	1000.0	1	10	6	1	2	10,000.0

B.2 The Glushko Model

With the coordinate transformation the governing equations can be written as

$$U \frac{\partial U}{\partial X} + e^{-\gamma} W \frac{\partial U}{\partial y} = e^{-\gamma} \frac{\partial}{\partial y}\left(\lambda^* E^{1/2} \frac{\partial U}{\partial y} \right)$$

$$\frac{\partial U}{\partial X} + e^{-\gamma} \frac{\partial W}{\partial y} = 0$$

$$U \frac{\partial E}{\partial X} + e^{-\gamma} W \frac{\partial E}{\partial y} = \lambda^* E^{1/2} e^{-\gamma}\left(\frac{\partial U}{\partial y}\right)^2 + e^{-\gamma} \frac{\partial}{\partial y}\left(\lambda^* E^{1/2} \frac{\partial E}{\partial y} \right) - E^{3/2} \frac{e^{-\gamma}}{\lambda^*}$$

In finite difference form, with EN_j as the value of the energy at $X+STP$, the first and third equations become

$$U_j(UN_j - U_j)/STP + M_j W_j DU_j$$
$$= (1/2)k^* M_j (E_j^{-1/2} DE_j DU_j + E_j^{1/2} D2U_j + E_j^{1/2}(UN_{j+1} - 2UN_j + UN_{j-1})/H^2)$$

$$U_j(EN_j - E_j)/STP + M_j W_j DE_j$$
$$= k^* E_j^{1/2} M_j DU_j^2 - E_j^{3/2} M_j/k^*$$
$$+ (1/2)k^* M_j (E_j^{-1/2} DE_j^2 + E_j^{1/2} D2E_j + E_j^{1/2}(EN_{j+1} - 2EN_j + EN_{j-1})/H^2)$$

where $DE_j = (E_{j+1} - E_{j-1})/2H$ and $D2E_j = (E_{j+1} - 2E_j + E_{j+1})/H^2$.

For the momentum equation the matrix elements are given by

$$D_j = U_j/STP + k^* M_j E_j^{1/2}/H^2$$

$$OD_j = -(1/2)k^* M_j E_j^{1/2}/H^2$$

$$B_j = U_j^2/STP - M_j W_j DU_j + (1/2)k^* M_j (E_j^{-1/2} DE_j DU_j + E_j^{1/2} D2U_j)$$

The lower boundary condition does not affect these expressions, but the outer boundary condition leads to

$$D_N = U_j/STP + k^* M_j E_j^{1/2}/H^2$$

$$B_N = U_N^2/STP - M_N W_N DU_N + (1/2)k^* M_N (E_N^{-1/2} DE_N DU_N + E_N^{1/2} D2U_N + E_N^{1/2} ALF/H^2)$$

with unchanged from the above.

For the turbulent energy equation the matrix elements are given by

$$D'_j = U_j/STP + k^* M_j E_j^{1/2}/H^2$$

$$OD'_j = -(1/2)k^* M_j E_j^{1/2}/H^2$$

$$B'_j = U_j E_j / STP - M_j W_j DE_j + k^* E_j^{1/2} M_j DU_j^2 - E_j^{3/2} M_j / k_\epsilon^*$$

$$+ (1/2) k^* M'_j (E_j^{-1/2} DE_j^2 + E_j^{1/2} D2E_j)$$

The boundary condition at the ground, $\frac{\partial E}{\partial \gamma} = 0$, can be imposed in the form $E_0 = E_1$, $EN_0 = EN_1$. This necessitates a change in D'_1, namely,

$$D'_1 = U_1 / STP + (1/2) k^* M_1 E_1^{1/2} / H^2$$

OD'_1 and B'_1 are calculated as before, but with $E_o = E_1$. The outer boundary condition is imposed as $E_{N+1} = 1.0/a$. This leaves D'_N and OD'_N unchanged, but B'_N has an additional term,

$$B'_N = B'_N (\text{as before}) + (1/2) k^* M_N E_N^{1/2} / aH^2$$

Both systems are solved separately for UN_j and EN_j and W_j is computed as in the mixing-length model.

Taylor found that the system was not stable for all step sizes, and shorter steps were needed than in the mixing-length case. The values used in this application are given in Table B-2. The computations required 300 s of CPU time on the IBM 360-67.

B.3 The Modified Peterson Model

In γ coordinates the governing equations can be written

$$U \frac{\partial U}{\partial x} + e^{-\gamma} W \frac{\partial U}{\partial \gamma} = e^{-\gamma} \frac{\partial \tau}{\partial \gamma}$$

$$\frac{\partial U}{\partial x} + e^{-\gamma} \frac{\partial W}{\partial \gamma} = 0$$

$$U \frac{\partial \tau}{\partial x} + e^{-\gamma} W \frac{\partial \tau}{\partial \gamma} = a\tau e^{-\gamma} \frac{\partial U}{\partial \gamma} + e^{-\gamma} \frac{\partial}{\partial \gamma} \left(k \tau^{1/2} \frac{\partial \tau}{\partial \gamma} \right) - a \frac{\tau^{3/2} e^{-\gamma}}{k}$$

In finite difference form with TN_j as the stress at $X+STP$ the turbulent energy equation becomes

$$U_j (TN_j - T_j) / STP + M_j W_j DT_j$$

$$= a T_j M_j DU_j - a T_j^{3/2} M_j / k + (1/2) M_j k (T_j^{1/2} D2T_j + T_j^{-1/2} DT_j^2)$$

$$+ (1/2) k M_j T_j^{1/2} (TN_{j+1} - 2TN_j + TN_{j-1}) / H^2$$

The matrix elements are given by

$$D_j = U_j / STP + k M_j T_j^{1/2} / H^2$$

$$OD_j = -(1/2) k M_j T_j^{1/2} / H^2$$

Table D-2. Values of the parameters used in the Glushko program.

Range $(X=x/s_{o2})$	N	H	STP	NRAT	ITER	ITSTP	JMP	NADD	PSTP
0-1	48	0.125	0.050		20	4	4	0	1.0
1-10	48	0.125	0.10	1	20	3	4	0	2.0
10-40	50	0.125	0.50	1	20	3	4	2	10.0
40-100	52	0.125	1.00	1	20	3	4	2	20.0
100-400	28	0.250	5.00	2	20	3	2	2	100.0
400-1000	29	0.250	5.00	1	20	6	2	2	100.0
10^3-4.5×10^3	32	0.250	5.00	1	50	14	2	3	250.0
4.5×10^3-10^4	36	0.250	5.00	1	80	15	2	4	400.0
10^4-4.0×10^4	20	0.500	10.00	2	100	30	1	2	1000.0
4.0×10^4-10^5	22	0.500	10.00	1	200	30		2	2000.0

$$B_j = U_j T_j / STP - M_j W_j DT_j + a\ T_j M_j DU_j - a\ T_j^{3/2} M_j / k$$
$$+ (1/2) M_j k (T_j^{1/2} D2T_j + T_j^{-1/2} DT_j^2)$$

The boundary condition at the ground, $\frac{\partial T}{\partial z} = 0$, is imposed as $T_0 = T_1$, $TN_0 = TN_1$, so

$$D_1 = U_1 / STP + (1/2) kM_1 T_1^{1/2} / H^2$$

The outer boundary condition, $T_{N+1} = 1.0$, requires that B_N be modified,

$$B_N = B_N (\text{as before}) + (1/2) kM_N T_N^{1/2} / H^2$$

With the values for TN_j the speed UN_j can be computed from the momentum equation according to

$$UN_j = U_j + (1/2) M_j STP (DT_j + DTN_j) / U_j - STP\ M_j W_j DU_j / U_j$$

where $DTN_j = (TN_{j+1} - TN_{j-1}) / 2H$.

Once again Taylor found that the scheme was not unconditionally stable, smaller step sizes being needed than either the Glushko or mixing-length models. The values used in this application are given in Table B-3. The computations required about 450 s of CPU time on the IBM 360-67.

Table B-3. Values of the parameters used in the modified Peterson program.

Range ($X = x/z_{o2}$)	N	H	STP	NRAT	ITER	ITSTP	JMP	NADD	PSTP
0-0.1	48	0.125	0.002	1	100	5	4	0	0.02
0.1-1.0	48	0.125	0.004	1	30	9	4	0	0.10
1.0-4.0	48	0.125	0.008	1	30	12	4	0	0.25
4-10	48	0.125	0.017	1	30	12	4	0	0.50
10-40	24	0.250	0.083	2	30	12	2	0	2.50
40-100	26	0.250	0.167	1	30	12	2	2	5.0
100-400	28	0.250	0.167	1	90	20	2	2	15.0
400-1000	30	0.250	0.222	1	90	30	2	2	20.0
$10^3 - 4.0 \times 10^3$	17	0.500	1.111	2	90	30	1	2	100.0
$4.0 \times 10^3 - 10^4$	21	0.500	1.333	1	150	30	1	4	200.0

```
C     INTERNAL BOUNDARY LAYER: IMPLICIT SCHEME OF P. A. TAYLOR
C
C     MIXING LENGTH MODEL
C
C     CONTROL PARAMETERS:     SSM,NTSTP,H,N
C
C          THEN NTSTP SETS OF:
C                              NRAT,ITER,ITSTP,JMP,NADD,PSTP
C
C     SSM=LN(Z0/Z1) (Z0 IS INITIAL ROUGHNESS; Z1 THE FINAL)
C     NTSTP=TOTAL NO OF BLOCKS
C     H=INITIAL GRID HEIGHT
C     N= SUBSCRIPT OF HEIGHT ABOVE WHICH OUTER B.C. CAN BE USED
C     NRAT= RATIO CONTROLLING GRID HEIGHT (AND THUS N ALSO)
C     ITER= NO OF INTERNAL STEPS WITHIN DOWNSTREAM STEP (ITERATIONS)
C     ITSTP= NO OF DOWNSTREAM STEPS TO BE TAKEN
C     JMP= SUBSCRIPT SPECIFYING HEIGHT PRINT INTERVAL
C     NADD= AMOUNT TO BE ADDED TO N FOR GRADUAL INCREASE
C     PSTP= DOWNSTREAM STEPSIZE
C
C     LENGTHS SCALED W.R.T. Z1, VELOCITIES W.R.T. U0
C     U0 IS THE INITIAL FRICTION VELOCITY; U1 THE FINAL
C
C     STP= INTERNAL STEPSIZE = PSTP/ITER
C     ALF= DIFF BETWEEN U/U0 AT LEVEL N AND LEVEL N+1
C     VK= VON KARMAN'S CONSTANT = 0.4
C     A= DISTANCE DOWNSTREAM, X/Z1
C     E     HOLDS THE RECIPROCAL OF ZETA
C     Y     HOLDS THE HORIZONTAL VELOCITY, U/U0
C     YN    HOLDS THE NEW VELOCITY AT THE DOWNSTREAM STEP
C     W     HOLDS THE VERTICAL VELOCITY, W/U0
C     Z     HOLDS THE HEIGHT, Z/Z1
C     T     HOLDS THE SHEAR STRESS, T/T0
C     D     HOLDS THE DIAGONAL ELEMENTS OF THE TRIDIAGONAL MATRIX
C     OD    HOLDS THE OFF-DIAGONAL ELEMENTS OF THE TRIDIAGONAL MATRIX
C     B     HOLDS THE ELEMENTS OF THE THIRD ARRAY IN THE EQUATION
```

```
C     SUBROUTINE HEADIN PRINTS OUT THE HEADINGS FOR EACH BLOCK
C     SUBROUTINE DSP SETS UP THE MATRICES
C     SUBROUTINE TRID SOLVES THE TRIDIAGONAL SET OF LINEAR EQUATIONS
C        USING A DIRECT TWO-PASS GAUSSIAN ELIMINATION
C
      COMMON ALF,E(100),Z(100),H,RFF,VK,VK2,H2
      DIMENSION Y(100),W(100),T(100)
      READ (5,1) SSM,NTSTP,N,R
      WRITE (6,5) SSM,NTSTP,N,M
      SP=EXP(-SSM)
      VK=0.4
      VK2=VK**2
      A=0.0
      DO 100 NOSTEP=1,NTSTP
      READ (5,2) NRAT,ITER,ITSTP,JPP,MADD,PSTP
      N=N/NRAT
      NOP1=N+1
      IF(NOSTEP.GT.1) GOTO 13
C
C     INITIAL CONDITIONS AND OUTER BOUNDARY CONDITIONS
C
      DO 11 I=1,NOP1
      W(1)=0.0
      Y(I)=2.5*ALOG(1.+SN*(EXP(FLOAT(I)*H)-1.))
      E(I)=EXP(-H*FLOAT(I))
      Z(I)=(1./E(I)-1.)
   11 IF (NOSTEP.EQ.1) GOTO 14
   13 IF(NRAT.EQ.1) GOTO 14
      H=H*FLOAT(NRAT)
      DO 15 I=1,N
      NPI=NRAT*I
      Y(I)=Y(NPI)
      E(I)=E(NPI)
      W(J)=W(NRI)
```

```
15    Z(I)=Z(NR1)
14    H2=H**2
      IF(NADD.EQ.0) GOTO 345
      N=N+NADD
      DO 17 I=NCP1,N
      E(I)=EXP(2.*FLOAT(I))
      W(I)=W(I-1)
      Z(I)=(1./E(I)-1.)
      Y(I)=Y(I-1)+2.5*ALOG((1.+SM*Z(I))/(1.+SM*Z(I-1)))
17    N11=N+1
345   Z(N11)=EXP(H*FLOAT(N11))-1.
      ALF=2.5*ALOG((1.+SM*Z(N+1))/(1.+SM*Z(N)))
      STP=PSOP/FLOAT(ITER)
      WRITE(6,4) H,ITSTP,ITER,H,STP
      CALL HEADIN(N,JMP,A,Y,Z)
      DO 101 INSTP=1,ITSTP
      CALL OSP(N,A,Y,STP,ITER,H)
      U1=VK*Y(1)/H
      WRITE(6,3) A,U1,(Y(I),I=JMP,N,JMP)
      Y(N+1)=Y(N)+ALF
      DO 102 I=2,N
      T(I)=(0.2*(Y(I+1)-Y(I-1))/H)**2
102   T(1)=(9.2*Y(2)/H)**2
      U12=U1+U1
      WRITE(6,8) U12,(T(I),I=JMP,N,JMP)
      WRITE(6,10) (H(I),I=JMP,N,JMP)
103   CONTINUE
      NFE=ITER*ITSTP
      WRITE(6,7) NFE
100   CONTINUE
1     FORMAT(F6.2,I5,F8.4,I5)
2     FORMAT(5I3,E10.2)
3     FORMAT('0',10F12.3/(' ',24X,8F12.3))
4     FORMAT('1',N=',I4,' STP=',F10.2/)
      1F8.4,' STP=',F10.2//)
5     FORMAT('1','H=',F6.2,' NO OF BLOCKS=',I4,' H=',F8.4,' N=',I4)
```

```fortran
    7   FORMAT ('-', ' NFE=',I6)
    8   FORMAT('0',3X,'T/U02 = ',9F12.3/(' ',24X,8F12.3))
   10   FORMAT ('0','VERT WIND W',12X,8F12.3/(' ',24X,8F12.3))
        STOP
        END

        SUBROUTINE HEADIN(N,JMP,B,Y,Z)
        DIMENSION Y(100),Z(100)
        WRITE(6,20)
        WRITE(6,21)(Z(I),I=JMP,N,JMP)
        WRITE(6,23)
        WRITE(6,22) B,(Y(I),I=JMP,N,JMP)
   20   FORMAT('-',7X,'X/Z1',8X,'U*/U0', 8X,'Z/Z1 THE DIMENSIONLESS HEIGHT
       1'/)
   21   FORMAT(' ',24X,8F12.3)
   22   FORMAT('0',F12.3,12X,8F12.3/(' ',24X,8F12.3))
   23   FORMAT('0',30X,'U/U0 AT THE ABOVE HEIGHTS')
        RETURN
        END
```

```fortran
      SUBROUTINE DSP(P,A,Y,STP,ITFR,W)
      DIMENSION Y(100),W(100),Z(100),D(100),B(100),YP(100)
      COMMON ALF,E(100),Z(100),H,HEF,VK,VK2,H2
      DO 801 I=1,ITFR
      UC=0.0
      UP=Y(1)
      DO 802 J=1,N
      UP=UC
      UC=UP
      IF(J.LT.N) UP=Y(J+1)
      IF(J.EQ.N) UP=UC+ALF
      EC=E(J)
      DU=(UP-UP)*0.5/H
      D(J)=UC/STP+2.*VK2+FC+DU/H2
      DD(J)=-VK2+FC+DU/H2
      B(J)=DU+EC+VK2*(UP-2.*UC+UP)/H2+(C+UC/STP-EF+H(J))*DU
C
C     MODIFICATIONS DUE TO OUTER BOUNDARY CONDITION.
C
      D(N)=D(N)-VK2+EC+DU/H2
      B(N)=B(N)+ALF+DU+FC+VK2/H2
  802 CALL TRID(D,DD,YP,W)
      A=A+STP
      W(1)=-H+0.5*(YP(2)-Y(1)-Y(1))/E(2))/STP
      DO 803 J=2,N
  803 W(J)=H(J-1)-1+0.5*(((YP(J)-Y(J))/E(J))+((YP(J-2)-Y(J-1))/E(J-2)))
     1/STP
      DO 804 J=1,N
  804 Y(J)=YP(J)
  801 CONTINUE
      RETURN
      END
```

```
C   INTERNAL BOUNDARY LAYER: IMPLICIT SCHEME OF P. A. TAYLOR
C
C   MODIFIED PTTERSON MODEL
C
C   CONTROL PARAMETERS:     SSM,NTSTP,H,N
C                     THEN NTSTP SETS OF:
C                           NPAT,ITER,ITSTP,JMP,NADD,PSTP
C
C   SSM=LN(ZO/Z1) (ZO IS INITIAL ROUGHNESS; Z1,THE FINAL)
C   NTSTP=TOTAL NO OF BLOCKS
C   H=INITIAL GRID HEIGHT
C   N= SUBSCRIPT OF HEIGHT ABOVE WHICH OUTER B.C. CAN BE USED
C   NRAT=RATIO CONTROLLING GRID HEIGHT (AND THUS N ALSO)
C   ITER= NO OF INTERNAL STEPS WITHIN DOWNSTREAM STEP (ITERATIONS)
C   ITSTP= NO OF DOWNSTREAM STEPS TO BE TAKEN
C   JMP= SUBSCRIPT SPECIFYING HEIGHT PRINT INTERVAL
C   NADD= AMOUNT TO BE ADDED TO N FOR GRADUAL INCREASE
C   PSTP= DOWNSTREAM STEPSIZE
C
C   LENGTHS SCALED W.R.T. Z1, VELOCITIES W.R.T. U0
C   U0 IS THE INITIAL FRICTION VELOCITY; U1, THE FINAL
C
C   STP= INTERNAL STEPSIZE = PSTP/ITER
C   ALF= DIFF BETWEEN U/UR AT LEVEL N AND LEVEL N+1
C   VK= VON KARMAN'S CONSTANT = 0.4
C   LBDA= THE CONSTANT OF PROPORTIONALITY BETWEEN SHEAR STRESS
C         AND TURBULENT ENERGY
C   A= DISTANCE DOWNSTREAM, X/Z1
C   E= HOLDS THE RECIPROCAL OF ZETA
C   Y= HOLDS THE HORIZONTAL VELOCITY, U/U0
C   YN= HOLDS THE NEW VELOCITY AT THE DOWNSTREAM STEP
C   W= HOLDS THE VERTICAL VELOCITY, W/U0
C   Z= HOLDS THE HEIGHT, Z/Z1
C   T= HOLDS THE SHEAR STRESS, T/T0
C   TN= HOLDS THE NEW SHEAR STRESS AT THE DOWNSTREAM STEP
```

```
C     PHI HOLDS THE NON-DIMENSIONAL SHEAR
C     D. HOLDS THE DIAGONAL ELEMENTS OF THE TRIDIAGONAL MATRIX
C     OD. HOLDS THE OFF-DIAGONAL ELEMENTS OF THE TRIDIAGONAL MATRIX
C     B HOLDS THE ELEMENTS OF THE THIRD ARRAY IN THE EQUATION
C
C     SUBROUTINE HEADIN PRINTS OUT THE HEADINGS FOR EACH BLOCK
C     SUBROUTINE DSP SETS UP THE MATRICES
C     SUBROUTINE TRID SOLVES THE TRIDIAGONAL SET OF LINEAR EQUATIONS
C           USING A DIRECT 'TWO-PASS' GAUSSIAN ELIMINATION
C
      COMMON ALF,E(100),Z(100),P,NFE,VK,VK2,P2
      DIMENSION W(100),V(100),U(100),T(100)
      DIMENSION PHI(100)
      READ (5,1) SSM,MTSTP,P,P
      WRITE (6,5) SSM,MTSTP,P,P
      SM=EXP(-SSM)
      VK=0.4
      VK2=VK**2
      A=0.0
      DO 100 NOSTEP=1,MTSTP
      READ (5,2) MRAT,ITER,ITSTP,JPP,NADD,PSTP
      N=N/MRAT
      NOP1=N+1.
      IF(NOSTEP.GT.1) GOTO 13
C
C     INITIAL CONDITIONS AND OUTER BOUNDARY CONDITIONS
C
      DO 11 I=1,NOP1
      W(I)=0.0
      T(I)=1.0
      Y(I)=2.5*ALOG(1.+SM*(EXP(FLOAT(I)*P)-1.))
      E(I)=EXP(-P*FLOAT(I))
      Z(I)=(1./E(I)-1.)
      IF (NOSTEP.EQ.1) GOTO 14
11    IF(MRAT.EQ.1) GOTO 14
13    IF(MRAT.EQ.1) GOTO 14
```

```
      H=H*FLOAT(HRAT)
      DO 15 I=1,M
      HRI=HRAT*I
      Y(I)=Y(HRI)
      E(I)=E(HRI)
      W(I)=W(HRI)
      T(I)=T(HRI)
      Z(I)=Z(HRI)
15
14    M2=M**2
      IF(MADD.EQ.0) GOTO 345
      M=M+MADD
      DO 17 I=NOP1,N
      E(I)=EXP(-M*FLOAT(I))
      W(I)=W(I-1)
      T(I)=T(I-1)
      Z(I)=(1./E(I)-1.)
      Y(I)=Y(I-1)+2.5*ALOG((1.+SM*Z(I))/(1.+SM*Z(I-1)))
17
345   N11=N+1
      Z(N11)=EXP(M*FLOAT(N11))-1.
      ALF=2.5*ALOG((1.+SM*Z(N+1))/(1.+SM*Z(N)))
      Y(N11)=Y(N)+ALF
      T(N11)=1.0
      STP=PSTP/FLOAT(ITER)
      WRITE(6,4) N,ITSTP,ITER,M,STP
      CALL HEADIN(N,JMP,A,Y,Z)
      DO 101 ITSTP=1,ITSTP
      CALL OSP(N,A,Y,STP,ITER,W,T)
      U1=VK*V(1)/4
      WRITE(6,3) A,U1,(Y(I),I=JMP,N,JMP)
      U12=U1*U1
      WRITE(6,8) U12,(T(I),I=JMP,N,JMP)
      WRITE (6,10) (W(I),I=JMP,N,JMP)
      DO 600 I=2,N
      DU=(Y(I+1)-Y(I-1))/(2.*M)
      PHI(I)=VK*DU/SQRT(T(I))
600   CONTINUE
```

119

```
101   WRITE(6,9) (PHI(I),I=JMP,N,JMP)
      CONTINUE
      NFE=ITER*ITSTP
      WRITE(6,7) NFE
100   CONTINUE
1     FORMAT(F6.2,I5,F8.4,I5)
2     FORMAT(5I3,E10.2)
3     FORMAT('0',10F12.3/(' ',24X,8F12.3))
4     FORMAT('1',' M=',I4,'   DOWNSTREAM STEPS=',I4,'  ITER=',I4,'  M=',
     1F8.4,'   STP=',F10.3//)
5     FORMAT('1',' J=',F6.2,'   NO OF BLOCKS=',I4,'  P=',F8.4,'  N=',I4)
7     FORMAT ('-3',' NFE=',I6)
8     FORMAT('0','3X,'7/UO2 = ',9F12.3/(' ',24X,8F12.3))
9     FORMAT('0',' N.D. SHEAR ',12X,8F12.3/(' ',24X,8F12.3))
10    FORMAT ('0',' VERT WIND W',12X,8F12.3/(' ',24X,8F12.3))
      STOP
      END

      SUBROUTINE TRID(D,OD,B,YN,N)
      DIMENSION D(100),OD(100),B(100),YN(100)
      DO 200 J=2,N
      D(J)=D(J)-OD(J)*OD(J-1)/D(J-1)
      B(J)=B(J)-OD(J)*B(J-1)/D(J-1)
      YN(N)=B(N)/D(N)
200   DO 201 I=2,N
      J=N+1-I
201   YN(J)=(B(J)-OD(J)*YN(J+1))/D(J)
      RETURN
      END
```

120

```
      SUBROUTINE OSP(N,A,Y,STP,ITER,W,T)
      DIMENSION Y(100),W(100),Z(100),D(100),DD(100),B(100),YP(100),TP(100)
      DIMENSION T(100)
      COMMON ALF,E(100),Z(100),H,EFE,VK,VK2,H2
      REAL LBDA
      LBDA=0.16
      DO 801 I=1,ITER
      UC=0.0
      UP=Y(1)
      IF (A.EQ.0.0) TUC=T(1)
      IF (A.GT.0.0) TUC=(VK*Y(1)/H)**2
      TUP=T(1)
      DO 802 J=1,N
      UM=UC
      UC=UP
      TUM=TUC
      TUC=TUP
      UP=Y(J+1)
      TUP=T(J+1)
      EC=E(J)
      DU=(UP-UM)*0.5/H
      DT=(TUP-TUM)/(2.*H)
      D2U=(UP-2.*UC+UM)/H2
      D2T=(TUP-2.*TUC+TUM)/H2
      D(J)=UC/STP+VK*EC*SQRT(TUC)/H2
      DB(J)=-0.5*VK*EC*SQRT(TUC)/H2
      T1=UC*TUC/STP-EC*W(J)*DT+LBDA*TUC*EC*DU
      T2=-LBDA*(TUC**1.5)*EC/VK
      T3= 0.5*EC*VK*(SQRT(TUC)*D2T+DT*DT/SQRT(TUC))
      B(J)=T1+T2+T3
  802 CONTINUE
```

C   MODIFICATIONS DUE TO THE SURFACE BOUNDARY CONDITION

```
      D(1)=D(1)-0.5*VK*E(1)*SQRT(T(1))/H2
```

C   MODIFICATIONS DUE TO OUTER BOUNDARY CONDITION

```
C
      B(N)=B(N)+0.5*VK*E(N)*SQRT(T(N))/H2
      CALL TRID(D,DD,B,TP,N)
      DO 700 J=1,N
      IF (J.EQ.1) GOTO 710
      IF (J.EQ.N) GOTO 720
      GOTO 740
710   IF (A.EQ.0.0) U12=T(1)
      IF (A.GT.0.0) U12=(VK*Y(1)/H)**2
      DT=(T(2)-U12)/(2.*H)
      DTH=(TH(2)-U12)/(2.*H)
      DU=Y(2)/(2.*H)
      GOTO 750
720   DTH=(1.-TH(N-1))/(2.*H)
      DT=(1.-T(N-1))/(2.*H)
      DU=(Y(N+1)-Y(N-1))/(2.*H)
      DT=(1.-T(J-1))/(2.*H)
      GOTO 750
740   DTH=(TH(J+1)-TH(J-1))/(2.*H)
      DT=(T(J+1)-T(J-1))/(2.*H)
      DU=(Y(J+1)-Y(J-1))/(2.*H)
750   YH(J)=Y(J)+0.5*E(J)*STP*(DT+DTH)/Y(J)-STP*E(J)*N(J)*DU/Y(J)
700   CONTINUE
      A=A+STP
      W(1)=-H*0.5*((YH(1)-Y(1))/E(1))/STP
      DO 803 J=2,N
803   W(J)=W(J-1)-H*0.5*(((YH(J)-Y(J))/E(J))+((YH(J-1)-Y(J-1))/E(J-1)))
     1/STP
      DO 804 J=1,N
      T(J)=TH(J)
804   Y(J)=YH(J)
801   CONTINUE
      RETURN
      END
```

```
C
C     INTERNAL BOUNDARY LAYER: IMPLICIT SCHEME OF P. A. TAYLOR
C
C     GLUSHKO MODEL
C
C     CONTROL PARAMETERS:      SSM,NTSTP,H,N
C
C         THEN NTSTP SETS OF:       NRAT,ITER,ITSTP,JMP,NADD,PSTP
C
C
C     SSM=LN(ZO/Z1) (ZO IS INITIAL ROUGHNESS; Z1,THE FINAL)
C     NTSTP=TOTAL NO OF BLOCKS
C     H=INITIAL GRID HEIGHT
C     N= SUBSCRIPT OF HEIGHT ABOVE WHICH OUTER B.C. CAN BE USED
C     NRAT=RATIO CONTROLLING GRID HEIGHT (AND THUS N ALSO)
C     ITER= NO OF INTERNAL STEPS WITHIN DOWNSTREAM STEP (ITERATIONS)
C     ITSTP= NO OF DOWNSTREAM STEPS TO BE TAKEN
C     JMP= SUBSCRIPT SPECIFYING HEIGHT PRINT INTERVAL
C     NADD= AMOUNT TO BE ADDED TO N FOR GRADUAL INCREASE
C     PSTP= DOWNSTREAM STEPSIZE
C
C     LENGTHS SCALED W.R.T. Z1; VELOCITIES W.R.T. UO
C     UO IS THE INITIAL FRICTION VELOCITY; U1, THE FINAL
C
C     STP= INTERNAL STEPSIZE = PSTP/ITER
C     ALF= DIFF BETWEEN U/UO AT LEVEL N AND LEVEL N+1
C     VK= VON KARMAN'S CONSTANT = 0.4
C     LBDA= THE CONSTANT OF PROPORTIONALITY BETWEEN SHEAR STRESS
C           AND TURBULENT ENERGY
C     A= DISTANCE DOWNSTREAM, X/Z1
C     E= HOLDS THE RECIPROCAL OF ZETA
C     Y= HOLDS THE HORIZONTAL VELOCITY, U/UO
C     YN= HOLDS THE NEW VELOCITY AT THE DOWNSTREAM STEP
C     W= HOLDS THE VERTICAL VELOCITY, W/UO
C     Z= HOLDS THE HEIGHT, Z/Z1
C     T= HOLDS THE SHEAR STRESS, T/TO
```

```
C     EGY  HOLDS THE TURBULENT ENERGY
C     EGYN HOLDS THE NEW TURBULENT ENERGY AT THE DOWNSTREAM STEP
C     PHI  HOLDS THE NON-DIMENSIONAL SPEAR
C     D  HOLDS THE DIAGONAL ELEMENTS OF THE TRIDIAGONAL MATRIX
C     OD HOLDS THE OFF-DIAGONAL ELEMENTS OF THE TRIDIAGONAL MATRIX
C     B  HOLDS THE ELEMENTS OF THE THIRD ARRAY IN THE EQUATION
C
C     SUBROUTINE HEADIN PRINTS OUT THE HEADINGS FOR EACH BLOCK
C     SUBROUTINE QSP SETS UP THE MATRICES
C     SUBROUTINE TRID SOLVES THE TRIDIAGONAL SET OF LINEAR EQUATIONS
C            USING A DIRECT 'TWO-PASS' GAUSSIAN ELIMINATION
C
      COMMON ALF,E(100),Z(100),W(100),P,REE,VK,VK2,F2
      DIMENSION Y(100),W(100),T(100)
      DIMENSION PHI(100)
      DIMENSION EGY(100)
      REAL LBDA,KST,KSTD
      LBDA=0.16
      VK=0.4
      VK2=VK**2
      KST=VK*SQRT(LBDA)
      READ (5,1) SSM,NTSTP,P,N
      WRITE (6,5) SSM,NTSTP,P,N
      SN=EXP(-SSM)
      A=0.0
      DO 100 MOSTEP=1,NTSTP
      READ (5,2) NRAT,ITER,ITSTP,JPP,NADD,PSTP
      N=N/PRAT
      NOP1=N+1
      IF(MOSTEP.GT.1) GOTO 13
C
C     INITIAL CONDITIONS AND OUTER BOUNDARY CONDITIONS
C
      DO 11 J=1,NOP1
      W(J)=0.0
```

```
      EGY(1)=1.0/LBDA
      Y(1)=2.5*ALOG(1.+SM*(EXP(FLOAT(1)*H)-1.))
      F(1)=EXP(-H*FLOAT(1))
11    Z(1)=(1./E(1)-1.)
      IF (NOSTEP.EQ.1) GOTO 14
13    IF(NRAT.EQ.1) GOTO 14
      H=H*FLOAT(NRAT)
      DO 15 J=1,N
      NRI=NRAT*I
      Y(I)=Y(NRI)
      E(I)=E(NRI)
      EGY(I)=FGY(NRI)
15    W(I)=W(NRI)
14    Z(I)=Z(NRI)
      H2=H**2
      IF(NADD.EQ.0) GOTO 345
      N=N+NADD
      DO 17 I=NOP1,N
      E(I)=EXP(-H*FLOAT(I))
      W(I)=W(I-1)
      EGY(I)=EGY(I-1)
17    Z(I)=(1./E(I)-1.)
345   Y(I-1)=Y(I-1)+2.5*ALOG((1.+SM*Z(I))/(1.+SM*Z(I-1)))
      N11=N+1
      Z(N11)=EXP(H*FLOAT(N11))-1.
      ALF=2.5*ALOG((1.+SM*Z(N+1))/(1.+SM*Z(N)))
      Y(N11)=Y(N)+ALF
      EGY(N11)=1.0/LBDA
      STP=PSTP/FLOAT(ITER)
      WRITE(6,4) N,ITSTP,ITER,H,STP
      CALL HEADIN(P,JKP,A,Y,Z)
      DO 101 INSTP=1,ITSTP
      CALL OSP(P,A,Y,STP,ITER,W,EGY,LBDA)
      DO 200 I=2,N
      DU=(Y(I+1)-Y(I-1))/(2.*H)
      T(I)=SQRT(EGY(I))*K.ST*DU
```

```
200   CONTINUE
      DU=Y(2)/(2.*H)
      T(1)=SQRT(EGY(1))*KST*DU
      U12=T(1)
      U1=SQRT(U12)
      WRITE(6,3) A,U1,(Y(I),I=JMP,N,JMP)
      WRITE(6,8) U12,(T(I),I=JMP,N,JMP)
      WRITE (6,10) (W(I),I=JMP,N,JMP)
      DO 600 I=2,N
      DU=(Y(I+1)-Y(I-1))/(2.*H)
      PH3(I)=VK*DU/SQRT(T(I))
600   CONTINUE
      WRITE(6,9) (PH3(I),I=JMP,N,JMP)
101   CONTINUE
      NFE=ITER*ITSTP
      WRITE(6,7) NFE
100   CONTINUE
1     FORMAT(F6.2,I5,F8.4,I5)
2     FORMAT(5I3,E10.2)
3     FORMAT('0',10F12.3/(' ',24X,8F12.3))
4     FORMAT('1',' N=',I4,' DOWNSTREAM STEPS=',I4,' ITER=',I4,' P=',
     1F8.4,' STP=',F10.3//)
5     FORMAT('1',' P=',F6.2,' NO OF BLOCKS=',I4,' P=',F8.4,' R=',I4)
7     FORMAT (' J=',' NFE=',I6)
8     FORMAT('0',3X,'T/U02 = ',9F12.3/(' ',24X,8F12.3))
9     FORMAT('0',' M.D. SHEAR ',12X,8F12.3/(' ',24X,8F12.3))
10    FORMAT ('0',' VERT WIND W ',12X,8F12.3/(' ',24X,8F12.3))
      STOP
      END
```

```fortran
      SUBROUTINE OSP(N,A,Y,STP,ITEP,W,EGY,LBDA)
      DIMENSION Y(100),R(100),F(100),P(100),OP(100),R(100),YK(100)
      DIMENSION EGY(100),EGYK(100),Z(100),DP(100),BP(100)
      COMMON ALF,E(100),KST,KSTD,H,NFE,VK,VK2,H2
      REAL LBDA,KST,KSTD
      KST=VK*SQRT(LBDA)
      KSTD=VK/(LBDA**1.5)
      DO 801 I=1,ITEP
      UC=0.0
      UP=Y(1)
      EGYUC=EGY(1)
      EGYUP=EGY(1)
      DO 802 J=1,N
      UM=UC
      UC=UP
      EGYUM=EGYUC
      EGYUC=EGYUP
      UP=Y(J+1)
      EGYUP=EGY(J+1)
      EC=E(J)
      DU=(UP-UM)*0.5/H
      DEGY=(EGYUP-EGYUM)/(2.*H)
      D2U=(UP-2.*UC+UM)/H2
      D2EGY=(EGYUP-2.*EGYUC+EGYUM)/H2
      D(J)=UC/STP+KST*EC*SQRT(EGYUC)/H2
      OD(J)=-0.5*EC*KST*SQRT(EGYUC)/H2
      T1=UC*UC/STP
      T2=-EC*W(J)*DU
      T3=0.5*KST*EC*(DEGY*DU/SQRT(EGYUC)+SQRT(EGYUC)*D2U)
      B(J)=T1+T2+T3
      DP(J)=D(J)
      TT1=UC*EGYUC/STP-EC*W(J)*DEGY+KST*SQRT(EGYUC)*EC*DU*DU
      TT2=-(EGYUC**1.5)*EC/KSTD
      TT3=0.5*KST*EC*(DEGY*DEGY/SQRT(EGYUC)+SQRT(EGYUC)*D2EGY)
      RP(J)=TT1+TT2+TT3
  802 CONTINUE
```

`802`

`C`

```
C     MODIFICATIONS DUE TO OUTER BOUNDARY CONDITION
C
      D(N)=D(N)-0.5*KST*E(N)*SQRT(EGY(N))/H2
      B(N)=B(N)+0.5*KST*E(N)*SQRT(EGY(N))*ALF/H2
      BP(N)=BP(N)+0.5*KST*E(N)*SQRT(EGY(N))/(LBDA*H2)
C
C     MODIFICATIONS DUE TO THE SURFACE BOUNDARY CONDITION
C
      DP(1)=DP(1)-0.5*KST*E(1)*SQRT(EGY(1))/H2
      CALL TRID(D,DD,B,YN,N)
      CALL TRID(DP,DD,BP,EGYN,N)
      A=A+STP
      W(1)=-H*0.5*((YN(1)-Y(1))/E(1))/STP
      DO 803 J=2,N
803   W(J)=W(J-1)-H*0.5*(((YN(J)-Y(J))/E(J))+((YN(J-1)-Y(J-1))/E(J-1)))
     1/STP
      DO 804 J=1,N
      EGY(J)=EGYN(J)
804   Y(J)=YN(J)
801   CONTINUE
      RETURN
      END
```

APPENDIX C

NOTATION

A   constant of proportionality between the standard deviation of the vertical wind and the friction velocity
also the area of a lot containing roughness elements

a   constant of proportionality between the shear stress and the mean turbulent energy

A, a, b arbitrary constants in various expressions

B   constant of proportionality between the standard deviation of the longitudinal wind component and the friction velocity

c_d drag coefficient relating the wind speed to the friction velocity

c_{d1} drag coefficient for the first surface defined in terms of the wind at 8 m

c_{d2} drag coefficient for the second surface defined in terms of the wind at 1/2 m

c_p specific heat of air at constant pressure

d   zero-plane displacement
also the depth of the modified layer in the Panofsky-Townsend theory

e   base of natural logarithms

E   mean specific turbulent kinetic energy

E' fluctuating part of the turbulent energy

Ei   exponential integral, defined at first occurrence

f_1 blending function for horizontal velocity

f_2 blending function for shear stress

f_3 blending function for vertical velocity

F_1 universal function of stability for vertical wind fluctuations

F_2 universal function of stability for longitudinal wind fluctuations

f, F universal functions of the parameter ¶ in the Townsend similarity theory

g   acceleration due to gravity

g_1
g_2 functions of the roughness ratio in the internal boundary layer growth equation proposed by Shir

G0
G2   functions used in the iteration to obtain a least-squares solution for the profile parameters

H   heat flux
also channel height in Jacobs' work

h   height of the internal boundary layer

h_1 height of the new equilibrium layer

h_c crop height

I	incomplete gamma function used in Dyer theory
i, j	indices
K	eddy diffusivity
K_H	exchange coefficient for heat
K_M	exchange coefficient for momentum
K_E	exchange coefficient for turbulent energy
k	von Karman's constant
k^*	constant of proportionality between mean scale of turbulence and height
k_ϵ^*	constant of proportionality between dissipation length and height in Glushko model
ℓ	mixing-length
l_s	length scale in Townsend similarity theory
L	Monin-Obukhov length
L'	related length ($= K_H/K_M \, L$)
L_G	mean scale of turbulence in Glushko model
L	dissipation length
m	roughness change ratio ($= z_{01}/z_{02}$)
M	roughness change parameter ($= \ln m$)
N	number of measurement levels
	also number of roughness elements in a specified area
n	index for iterations
	also exponent in one hypothesis of R.J. Taylor theory
P	parameter in Townsend similarity theory
Q	function of height only occurring in Jacobs' combined equation of motion and continuity
Ri	Richardson number
r	parameter in Businger-Dyer-Paulson diabatic profile
	as a subscript, indicates reference level
S	specific or lot area of roughness elements
s	silhouette or cross-sectional area of typical roughness element
t	time
T	mean temperature over the profile
T'	fluctuating part of temperature
u	mean horizontal wind
u'	fluctuating part of horizontal wind
u_1	mean horizontal wind over first surface
u_2	mean horizontal wind over second surface
u_*	friction velocity at surface
u_{*1}	friction velocity at first surface
u_{*2}	friction velocity at second surface
u_s	velocity scale in Townsend similarity theory
U	dimensionless horizontal velocity ($= u/u_{*1}$)
v'	fluctuating part of lateral wind
w	mean vertical wind
w'	fluctuating part of vertical wind

w_1 mean vertical wind over first surface

w_2 mean vertical wind over second surface

W dimensionless vertical wind ($\approx w/u_{*1}$)

x downwind distance from roughness discontinuity

X dimensionless downwind distance ($= x/z_{02}$)

z vertical coordinate, height

z_{o1} roughness of first surface

z_{o2} roughness of second surface

z_b height of surface boundary layer

Z dimensionless height ($= z/z_{o2}$)

Z_1 symbol introduced to shorten the expressions used in the iterative scheme for the profile parameters

γ empirical constant in diabatic profile theory

δ streamline displacement

ϵ dissipation rate

ζ transformed vertical coordinate for numerical computations ($= \ln (z+z_{02})/z_{02}$)

η parameter in Townsend similarity theory ($= z/l_s$)

θ potential temperature

also concentration of diffusing entity in Dyer theory

λ mixing-length at outer edge of boundary layer

μ viscosity

ξ dummy variable

ρ density of air

σ_u standard deviation of longitudinal wind component

σ_v standard deviation of lateral wind component

σ_w standard deviation of vertical wind component

τ kinematic shear stress

τ_1 kinematic shear stress over first surface

τ_2 kinematic shear stress over second surface

τ_{o1} value of shear stress at first surface ($= u_{*1}^2$)

τ_{o2} value of shear stress at second surface ($= u_{*2}^2$)

ϕ non-dimensional wind shear

also flux in Dyer theory

ϕ_e equilibrium flux value in Dyer theory

χ centroid of region of streamline displacement

ψ streamfunction

ψ_{cD} value of streamfunction along the streamline CD

ω two-dimensional vorticity